universität wien

DIPLOMARBEIT / DIPLOMA THESIS

Titel der Diplomarbeit / Title of the Diploma Thesis

„Bioluminescence imaging based phenotyping of transgenic mice“

verfasst von / submitted by

Michaela Albayrak

angestrebter akademischer Grad / in partial fulfilment of the requirements for the degree of

Magistra der Pharmazie (Mag.pharm.)

Wien, 2019 / Vienna, 2019

Studienkennzahl lt. Studienblatt / degree programme code as it appears on the student record sheet:	A 449
Studienrichtung lt. Studienblatt / degree programme as it appears on the student record sheet:	Diplomstudium Pharmazie
Betreut von / Supervisor:	Univ. Prof. Dipl. Ing. Dr. Manfred Ogris
Mitbetreut von / Co-Supervisor:	Dr. Haider Sami

Acknowledgement

An dieser Stelle möchte ich mich bei meinem Betreuer Professor Manfred Ogris bedanken, der mir einen Arbeitsplatz am „Laboratory of Macromolecular Cancer Therapeutics“ (MMCT) für die Erstellung dieser Diplomarbeit zur Verfügung gestellt hat.

Des Weiteren bedanke ich mich bei meinem Mitbetreuer Dr. Haider Sami, der durch seine fachliche Beratung und persönliche Unterstützung zum Gelingen dieser Diplomarbeit beigetragen hat.

Meinen Studienkollegen und inzwischen gewordenen Freunden, mit denen ich am MMCT gearbeitet habe, möchte ich ebenfalls für die angenehme Arbeitsatmosphäre und vielen heiteren Momente danken.

Ein herzliches Dankeschön geht an meine beste Freundin Thi Ngoc, die mir während der gesamten Studienzeit stets mit Rat und Tat zur Seite stand und mich immer wieder motiviert hat nicht aufzugeben.

Mein größter Dank gilt meiner Familie, insbesondere meinen Eltern, die mir mein Studium ermöglicht haben und meinen beiden Brüdern, die mich stets ermutigt und durch ihre aufmunternden Worte unterstützt haben.

Table of Contents

Bildrechte:

Ich habe mich bemüht, sämtliche Inhaber der Bildrechte ausfindig zu machen und ihre Zustimmung zur Verwendung der Bilder in dieser Arbeit eingeholt. Sollte dennoch eine Urheberrechtsverletzung bekannt werden, ersuche ich um Meldung bei mir.

Abstract

The generation of transgenic animal models has enabled the investigation of gene functions and physiological processes at the molecular level and mechanisms of diseases. Non-invasive optical imaging methods like bioluminescence imaging (2D BLI) allows the study of all these areas using animals generated to express the enzyme luciferase as a reporter of biological processes.

In this work, three firefly luciferase based transgenic mice strains named Tg Thy 1.2-Luc, Tg SpC-Luc and Tg (Luc705) Split-Luc were imaged using the 2D BLI technology in order to determine their phenotypic status. Furthermore, the organs of mice were imaged additionally after euthanasia for the validation of tissue- and / or organ-specific transgene expression.

All three transgenic models were generated in previous work by microinjection of the DNA encoding for firefly luciferase and the respective promoter. Afterwards these were mated with B6 Albino mice to obtain the next generations. The idea of these models was to use them after validation of their genotypic and phenotypic status for brain- and lung-specific transgene experiments as well as for splice-correction studies.

In this work, D-luciferin was used as luciferase substrate and injected subcutaneously into each mouse before the light signal of luciferase-expressing mice was detected by 2D bioluminescence imaging. In this way, we were able to investigate localization of luciferase expression and validate where the target genes were expressed, so that the phenotypically and genotypically positive animals can be used for other subsequent transgene-specific experiments.

In our study, we were able to detect brain-located transgene expression in Tg Thy 1.2-Luc mice both in whole-body and in the organ images. In the Tg SpC-Luc animals we have found lung specific expression, but in addition also a strong luciferase activity in the skin, which unfortunately covers the lung signal when conducting whole-body imaging. However, lung-specific expression was demonstrated by imaging explanted organs. In the third strain, Tg (luc705) Split-Luc, we also found BLI signals in some mice, although the reporter gene should be disrupted and dysfunctional. Future studies will show whether the splicing correction with splice correcting oligonucleotides would specifically change the signal intensity or not.

Zusammenfassung

Die Generierung transgener Tiermodelle hat die Erforschung von Genfunktionen, physiologischen Prozessen auf molekularer Ebene und Mechanismen von Krankheiten ermöglicht. Nicht-invasive optische Bildgebungsverfahren wie die Biolumineszenz-Bildgebung (2D BLI) erlauben die Untersuchung all dieser Bereiche unter Verwendung von Tieren, die zur Expression des Enzyms Luciferase als Reporter biologischer Prozesse erzeugt wurden.

In dieser Arbeit wurden drei auf Firefly-Luciferase basierende transgene Mäusestämme mit den Namen Tg Thy 1.2-Luc, Tg SpC-Luc und Tg (Luc705) Split-Luc unter Verwendung der 2D-BLI-Technologie abgebildet, um ihren phänotypischen Status zu bestimmen. Darüber hinaus wurden die Organe von Mäusen zusätzlich nach Euthanasie zur Validierung der gewebe- und/oder organspezifischen Transgenexpression abgebildet.

Alle drei transgenen Modelle wurden in vorhergehenden Arbeiten durch Mikroinjektion von DNA, welche das Firefly-Luciferase-Gen unter Kontrolle des jeweiligen Promotors enthält, erzeugt. Danach wurden diese mit B6-Albino-Mäusen verpaart, um die nächsten Generationen zu erhalten. Die Idee dieser Modelle war, sie nach Validierung ihres genotypischen und phänotypischen Status für gehirn- und lungenspezifische Transgenexperimente sowie für Spleißkorrekturstudien zu verwenden.

D-Luciferin wurde als Luciferase-Substrat verwendet und jeder Maus subkutan injiziert, bevor das Lichtsignal von Luciferase-exprimierenden Mäusen durch 2D-Biolumineszenz-Bildgebung detektiert wurde. Auf diese Weise konnten wir die Lokalisation der Luciferase-Expression untersuchen und validieren, wo die Zielgene exprimiert wurden, so dass die phänotypisch und genotypisch positiven Tiere für andere nachfolgende transgenspezifische Experimente verwendet werden können.

In unserer Studie konnten wir eine gehirnspezifische Transgenexpression in Tg Thy 1.2-Luc-Mäusen sowohl in den Ganzkörper- als auch in unseren Organbildern nachweisen. Bei den Tg SpC-Luc-Tieren haben wir eine lungenspezifische Luciferaseaktivität beobachtet. Es zeigte sich jedoch auch eine hohe Luciferase Aktivität in der Haut, welches leider das Lungensignal in den Ganzkörperbildern abdeckt. Eine lungenspezifische Expression konnte jedoch durch Bildgebung der Organe nachgewiesen werden. Im dritten Stamm, Tg (luc705) Split-Luc, fanden wir bei

einigen Mäusen auch BLI-Signale, obwohl das Reportergen unterbrochen sein sollte. Hier wird in zukünftigen Studien untersucht werden, ob die Spleißkorrektur mit spleißkorrigierenden Oligonukleotiden die Signalintensität verändern würde oder nicht.

1 Introduction

1.1 Transgenics background

First genetic mouse models with spontaneous mutations were developed and in the 20th century. [1] Later in 1981, Gordon and Ruddle generated the first transgenic animals [2] by pronuclear microinjection. [3] At that time, they termed animals with exogenous DNA sequence in their genome as “transgenic”. [2,3] The definition of transgenic has changed over the years and is now defined by an animal with a specific genetic modification. [2]

The generation of animal models with gene modifications has enabled the analysis of gene function and studying the mechanisms of human diseases. [1] In addition, transgenic animals are used for the expression of various proteins as well as to produce altered tissues and organs which are suitable for transplantations. [2]

Various techniques are available for the production of transgenic animals, such as pronuclear microinjection, retrovirus mediated gene transfer, embryonic stem cell technology, nuclear transfer/ ”cloning”, sperm mediated DNA transfer or producing knock-down mice with RNA interference. [2]

Pronuclear microinjection of DNA was also used for generating the mice of this study. Using a microinjection apparatus and micromanipulators [2], the cloned DNA is injected into the pronuclei of the animal zygote. [1] Here, the expression cassette (promoter, luciferase cDNA and polyadenylation signal) has been isolated from a plasmid and microinjected. In comparison to circular plasmid DNA, such linear constructs are easier integrating into the host genome. [2] The result of the microinjection is a random integration of the DNA construct, which usually occurs only at one chromosome location, into the germline. Variable numbers of transgene copies can be integrated as a head-to-tail concatemers into a single chromosomal site. [1,2] The transgene is contained in all cells of the developing embryo, as the microinjection of the DNA take place in the zygote. [2] The expression of the transgene can be affected by the availability of the integration site for transcription and by regulatory elements close to this region. [1,2] While housekeeping gene promoters are utilized for widespread expression of the transgene, tissue-specific promoters can be used to achieve targeted expression in a certain tissue. [1] The advantages of this method are a high yield of transgenic animals (20-25% for mice), hardly any restrictions on the size of the recombinant DNA and the high stability of the transgene over several generations. [2]

1.1.1 Transgenic models with brain specific expression

Transgenic models with brain specific expression are important for in vivo experiments in molecular neurobiology. These models can be generated using specific reporter genes to investigate gene expression, behaviour of cells and protein dynamics in living animals. [4]

We used bioluminescence imaging (BLI) for phenotyping of transgenic mice with a brain specific expression of firefly luciferase, i.e. the luciferase was expressed under the control of a promoter element supposed to be specific for brain tissue and neuronal cells in general (Thy 1.2-Luc strain). The mice were generated by pronuclear injection of an expression cassette containing the Thy 1.2 promoter elements and firefly cDNA at the Institute for Laboratory Animals Sciences of the University of Veterinary Medicine in Vienna. [5(p16)]

The Thy 1.2 promoter enables transgene expression exclusively in neurons of grown-up transgenic mice. The expression of the transgene starts at the postnatal day 6-12. In a period, where it can influence the neuron-glia interactions and synaptic connections during the late stages of the development of the nervous system. This has the advantages of avoiding disruptions during early development of the nervous system and the effects/consequences of the transgene during the late maturation of the nervous system and in grown-ups can be studied. In addition, it allows to analyse various combinations of neurons from different founder lines in transgenic mice. [4]

The brain specific promoter of theThy-1 gene found its usage in several studies . For example, in the articles from Feng et al. [6] or Livet et al. [7] transgenic animals were generated, which expressed fluorescent proteins of different colours selectively in neurons under control of the Thy-1 promoter.

1.1.1.1 Thy -1

The Thy-1 gene is located in mice on chromosome 9 [8] and in humans on chromosome 11 [9] and encodes for a 112 amino acid glycoprotein. [8] In mice there are two alleles, termed Thy-1.1 and Thy 1.2, which differ only by the interchange of the amino acid glutamine instead of arginine at residue 89. The distinction of these two genes can be shown by using monoclonal antibodies. [8]

Thy-1 is a cell-surface differentiation antigen and belongs to the immunoglobulin superfamily. The glycoprotein is linked to the cell membrane through a Glycosylphosphatidylinositol [10] and is expressed in neurons and T-lymphocytes and in lower amounts in other tissues like fibroblasts and muscle [4,8,10].

The Thy 1 gene contains tissue specific control elements, which have their location downstream from the transcriptional initiation site. Elements in the third intron of the murine gene controls thymus-specific expression, while sequences of the first intron direct expression in the brain. [10] Caroni [4] used because of this informations in his paper a Thy 1.2 expression cassette, where the sequences for the thymus-specific expression were deleted, to reach neuronal specific expression of transgenes. The human gene contains instead separate regions, which enhance the expression in kidney and spleen epithelium. [10]

1.1.2 Transgenic models with lung specific expression

Transgenic mouse lines with lung specific reporter gene expression are used for studying development, alteration, repair and homeostasis of lung tissue. One of the most commonly used promoters to generate transgenic mice with stable lung specific transgene expression is the promoter from the surfactant protein C gene (SFTPC-promoter). [11] In the mature lung the SFTPC-promotor activity is detected at high levels exclusively in the alveolar type II cells. [12] One of the advantages of this promoter is its high specificity in the respiratory epithelium and that it is very rare to find activity in other tissues. [11]

There are numerous studies in which SFTPC has been used as a lung-specific promoter in transgenic mouse models. The most commonly used lines according to the review from Rawlins and Perl [11] are SFTPC-rtTA and SFTPC-Cre lines. In the paper from Roper et al. [13] they generated a transgenic mouse line, which express the enhanced green fluorescence protein (EGFP), under control of surfactant protein C (SP-C) to examine type II cells.

In our study we used as lung specific transgenic model Tg SpC-Luc mice, which were generated by pronuclear injection of the firefly luciferase expression cassette containing the SFTPC promoter at the Institute for Laboratory Animals Sciences of the University of Veterinary Medicine in Vienna. [5(p14)] The cassette was isolated from the

plasmid pSPC-Luc-PGL3b, which contained the lung specific SFTPC-promoter and the firefly luciferase (Fluc) gene as reporter gene. The firefly luciferase gene was chosen for in vivo bioluminescence imaging-based monitoring of the promoter gene expression in the lung.

1.1.2.1 SFTPC

The gene SFTPC encodes for the hydrophobic surfactant protein C, [14] which is produced exclusively by the alveolar type II cells [15,16] in the mature/adult lung. [17] Several mutations of the SFTPC gene have been discovered [14,15] and are associated with interstitial lung disease. [14–16,18] Most of the reported mutations have their location in the BRICHOS domain. [14] These mutations are responsible for misfolded SPC-pro-protein, which accumulates intracellularly and causes different pathological mechanisms, like stress induction of the endoplasmic reticulum and cell apoptosis. [15]

1.1.2.2 Role of surfactant proteins

The last organ which develops during embryogenesis is the lung. Alveolar type I (ATI) and II (ATII) cells constitute the main of the lung epithelium. The large ATI cells build almost the whole alveolar surface and are responsible for the gas exchange from the alveolar spaces to the capillary lumen. [18] The pulmonary surfactant is a lipid-protein complex, which is produced by the ATII cells. It prevents alveolar collapse during breathing, by lowering the surface tension at the alveolar air-liquid interface. [17,18]

Lipids represent more than 90% of the total mass of the surfactant, while the proteins account less than 10%. [18,19] The lung surfactant contains four surfactant proteins (SP), named SP-A, SP-B, SP-C, and SP-D, each with specific characteristics. [17–19] The hydrophilic proteins SP-A and SP-D belong to the innate defence and protect the lung from various microorganisms and pathogens. [17,18] Another important task of SP-D is the surfactant homeostasis. [17,18] The hydrophobic proteins SP-B and SP-C are relevant for surface activity of the interfacial film. [17,18]

1.1.3 Split transgene based transgenic models

The third mouse strain we used for BLI based phenotyping is called Tg (Luc705) Split-Luc. These mice were generated by pronuclear injection of an expression cassette derived from the plasmid pLuc/705 into a fertilised zygote at the Institute for Laboratory Animals Sciences of the University of Veterinary Medicine in Vienna. [5(p18)] Here, the reporter gene firefly luciferase is interrupted by the mutated human ß-globin intron 2, which includes an aberrant splice site at nucleotide 705. [20] This gene was integrated into the pLuc/705 plasmid together with a Rosa26 promotor for ubiquitous and constitutive gene expression. [5]

This experimental transgenic model can be used for splice correction studies. Since the mutation at nucleotide 705 activates an aberrant splice site, the intron remains after splicing within the mRNA, and the translation into a functional luciferase protein is prevented. The aim is to block the aberrant splice site with antisense oligomer resulting in a correctly spliced mRNA and proper translation of luciferase. Therefore, splice switching oligonucleotide (SSO) treatment results in a splice correction so that functional luciferase expression can be detected by bioluminescence imaging.

A similar model was also used in the scientific work of Sazani et al. [21] which generated transgenic mice expressing the gene EGFP-654. This gene encodes for EGFP, which was disrupted by a mutated human β-globin intron 2, similar as in our study except that the mutation was at nucleotide 654 instead 705. After splice correction by chemically modified oligonucleotides, the mice expressed the protein EGFP, which can be detected by fluorescense microscopy in tissue sections. This study showed, like several others, that the sequence specific antisense-activity of these oligonucleotides is especially useful for modulation of splicing and influences gene expression. [21]

1.2 In vivo imaging - imaging biological processes in vivo

Characterization, quantification and visualization of events at cellular and subcellular stages in living subjects is enabled by molecular imaging. [22] It provides a non-invasive way of evaluating gene and protein function and studying the interplay of proteins and signal transmission of human diseases in animal models to understand the pathogenesis at molecular level. [23] Beside single photon emission computed tomography, positron emission tomography, magnetic resonance imaging, computed

tomography (CT), and ultrasound, which are applied clinically on humans, fluorescence imaging (FLI) and bioluminescence imaging are two additional preclinical methods for imaging small living animals. [22]

FLI and BLI are optical imaging techniques which detect the emission of light signals from living animals with the help of a sensitive charge coupled device (CDD) camera at a range from visible to near infrared (NIR) spectrum. [23,24] In comparison to the other methods mentioned above they are also very attractive modalities because of their low-costs, ease of use and rapidity [25].

Since both optical imaging processes, BLI and FLI, take differ in their energy sources for production of the light signal, they have different biological uses. Table 1 shows an general comparison of both optical imaging methods BLI and FLI. [24]

	Bioluminescence	Fluorescence
Imaging mechanism and energy source	Firefly luciferase enzyme metabolising D-luciferin substrate in presence of ATP and oxygen	Excitation of fluorophores by energy of an external light source
Interpretation	high sensitivity and specificity	high versatile and flexible
Biological readouts and applications	Measurement of cell location, viability and growth	1. Vascular agents for imaging of vascularity; 2. Targeted agents for binding to specific biomarkers; 3. Activatable fluorescent agents which change enzyme-mediated from non-fluorescent to fluorescent
Experimental Considerations	Requires genetic modification to obtain luciferase expression	Requires FLI of control animals, which receive same fluorophor to detect background fluorescence of the agent

Table 1. Comparison of bioluminescence and fluorescence imaging. *Source: modified from Tseng et al., 2015.* [24]

1.2.1 Fluorescence imaging for tracking biological processes

Fluorescence is based on molecules known as fluorophores, which are excited by the energy of an external light source and emit photons on another wavelength as a result. [26,27] For in vivo fluorescence based imaging there are various fluorophores with specific excitation and emission profile [24] available, which can be used to track the conjugated substance of interest. [28] There is also the possibility of using fluorescent agents as specific reporter genes, such as red fluorescent protein or green fluorescent protein (GFP) [25] which enable the investigation of molecular event. [28]

GFP, which is originally found in a jellyfish species, called Aequorea victoria, has been used extensively as a reporter gene to study protein localization and subcellular processes like gene expression. [25] Furthermore, GFP has been also used for studying processes of infections and tumour growth, its metastasis and treatment. [25]

Fluorophores that emit light in the near infrared spectrum are particularly well suited for fluorescence-based in vivo imaging, because they have low scattering effects and high tissue penetration. [27]

Filonov et al. [29] developed in 2011 a near-infrared fluorescent protein, named iRFP, which is a fluorescents mutant of the bacteriophytochrome RpBphP2. This stable and nontoxic protein has and excitation wavelength an 690nm and emits fluorescence at 713nm. [29] In comparison to fluorescent proteins emitting in the visible range, such as GFP, the signal-to-background ratio of iRFP is in mouse models much higher due to its near-infrared shifted excitation and emission spectrum. [29] Afterwards, Tran et al. [30] generated and published a transgenic iRFP mouse model with ubiquitous expression of NIR fluorescence. Recently, Kulathunga et al. [31] generated a new imagable atherosclerosis model in mice by using iRFP-expressing hematopoietic cells. This allows the generation of longitudinal data and non-invasive imaging of atherosclerotic plaques, and thus using the system to monitor the progression of the lesion. [31]

Figure 1 shows a general illustration of a 2D epifluorescence imaging, in which the camera as well as the light source are located above the animal. FLI uses in dependence of the spectral properties of the fluorophore/ imaging agent [24] a specific excitation and emission filter, [24,28] to prevent background noise [28] and to produce an optimal fluorescence signal. [24] In order to obtain a 2D image, the surface of the animal is irradiated by the excitation light and the CDD camera detects the emitted signal. [24]

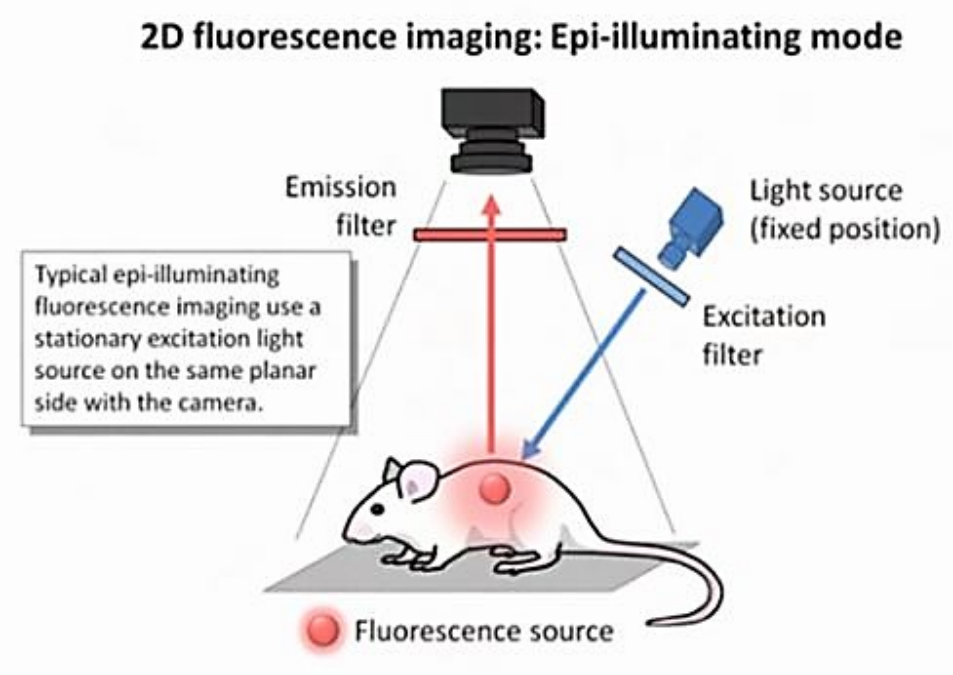

Figure 1. 2D fluorescence imaging. *Source: Tseng et al., 2015* [24]

1.2.1.1 Advantages and Disadvantages of FLI

The use of FLI has several benefits: First, fluorophores emit light after excitation without the need of additional substrates. Second, due to the large variety of different reagents with various emission and excitation ranges, numerous signals of several processes can be detected, and that in the same experimental animal. Third, it is possible to use the same emission signal of the fluorophore used to monitor a molecular event in the living animal for its subsequent ex vivo validation. Furthermore, there are fluorescent agents that do not require the generation of models expressing specific reporter genes, allowing faster evaluation preclinical research. [28]

On the other hand, FLI has some disadvantages, such as the need for an external light source to excite the fluorophore, which can be attenuated by tissue depth. [28] In addition, FLI suffers from autofluorescence and light absorption by tissue, because some parts of the body, like blood or hair, have the same excitation and emission properties like the used fluorophore and reduce so the image contrast. [27,28]

1.2.2 Bioluminescence imaging for tracking biological processes

In the recent years the number of BLI studies has increased exponentially. This noninvasive optical imaging method has been used for in vivo gene transfer and expression studies, especially in transgenic mice. BLI allows to study different biological processes by using mice or pathogens that have been generated to express the enzyme luciferase. [32]

Bioluminescence imaging is characterized by the visualization of light generated by luciferases in a living organism. [24] Luciferases are able to produce light by metabolizing their substrate. [28] Luciferase enzymes have been discovered in insects and marine species, like *Photinus pyralis* (Fluc; Firefly luciferase), *Pyrophorus plagiophthalamus* (CBR; Click beetle luciferase), *Gaussia princeps* (Gluc; Gaussia luciferase) or the *Renilla Reniformis* (Rluc; Renilla luciferase). [22] CBR and the most commonly used Luciferase FLuc emit light by catalysing the oxidation of their substrate D-luciferin to oxyluciferin [22] in the presence of oxygen and ATP [24] as shown in Figure 2. Gluc and RLuc use coelenterazine as substrate and oxygen, but do nore require ATP as a co-substrate.[22]

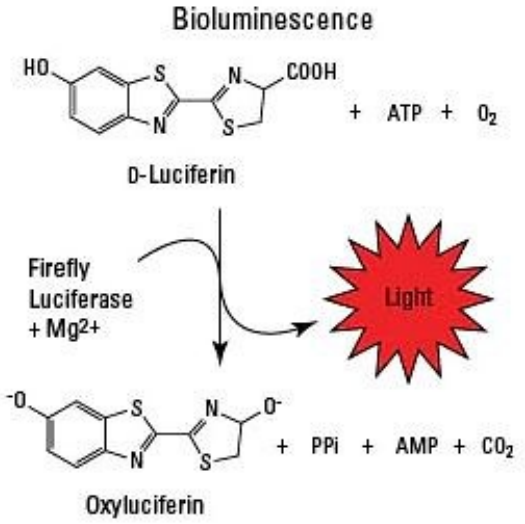

Figure 2. Chemical reaction of D-luciferin to oxyluciferin. *Source: "Luciferase Reporters," n.d.* [26]

Furthermore, there is the group of bacterial luciferases called lux. The application of these luciferases is not well suited for BLI experiments because of the low signal intensity and toxicity of the substrates. [22]

For BLI imaging investigations a luciferase expressing gene is integrated into cancer cells, viruses or the whole animal by using molecular biology techniques. [24] Here, constitutively active promoters can be used to express luciferase for monitoring growth and survival of transplanted cells, like cancer cells or stem cells, in vivo. [22]

Beside the signal intensity, the spatial distribution of the luciferase signal in the animal can be also useful, e.g. to monitor migration of neuronal stem cells or T-cell trafficking. In addition, the introduction of luciferase genes into pathogens allows the assessment of the infection pathway and the response to its treatment in the living organism. [22]

Another possibility is to use the reporter gene to monitor the activity of gene expression. For that the expression of luciferase is directed by the promoter element from the gene of interest or it is positioned downstream of the genetic elements that respond to a selected transcription factor. In case the relevant genes are actively transcribed, the reporter is also transcribed and the duration and relative amount of luciferase expression should match that gene of interest. [22]

Figure 3 illustrates the approach for 2D BLI imaging. In this mode the ultrasensitive, thermoelectrically-cooled CCD camera is placed above the mouse and detects all the emitted light coming from the surface of the animal. Due to very low background signal the 2D BLI image can also be captured without an emissions filter to maximize the imaging sensitivity and light signal capture, because mammalian tissue does not emit photons, which would lead to background noise signal. [24]

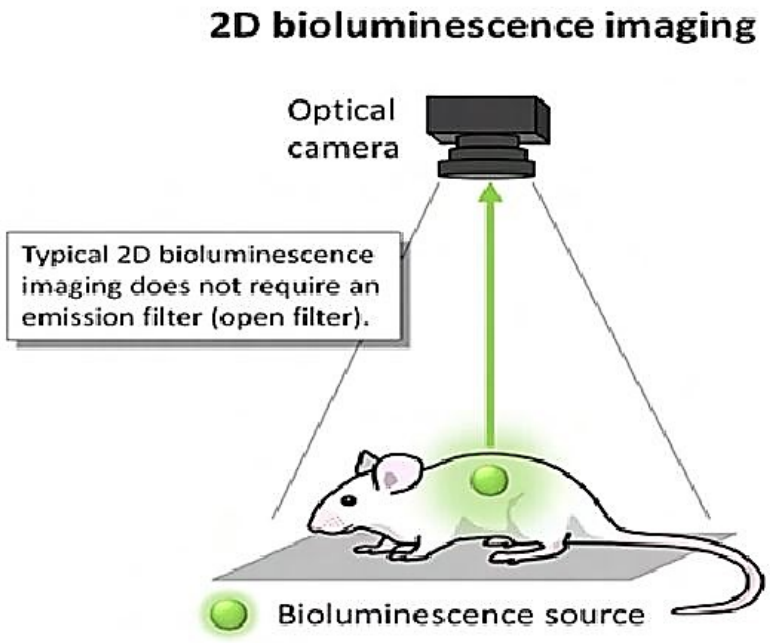

Figure 3. 2D bioluminescence imaging. *Source: Tseng et al., 2015* [24]

1.2.2.1 Advantages and Disadvantages of BLI

BLI enables to detect signals emittes from tissues in a depth of a few centimetres and allows a resolution at organ-level. In comparison other imaging methods, such as microscopy of GFP, have limited potential to detect deep seated signals. [32] Furthermore, in contrast to FLI, BLI is not dependent on excitation light [27,28] . Great advantages are the facts that luciferase-based BLI has a high signal-to-noise ratio (extremly low background signal), sensitivity and specifity since normal tissues have without luciferase no light emission. [24] Another important feature of the BLI technology is that a non-invasive, repeated and consistent study can be carried out in the same living animal at different times. [33] Thus, longitudinal studies can be performed with this technique while reducing the number of animals needed. [33,34]

Disadvantages of BLI in comparison to FLI are that it can require a longer acquisition time and administration of the substrate is necessary. [28] Furthermore, BLI suffers from low tissue penetration of photons which emit light in the visible range [27,28], so the technique is only suitable for imaging small animals. [27] Additionally, BLI requires cell engineering. [28] Moreover, it is difficult to standardize the experiments, because BLI is a semiquantitative technique and the outcomes are relative to each other. Exogenous and endogenous factors are able to alter the luciferase-substrate reaction and lead to

false interpretations since the amount of cofactors, luciferin and luciferases can also vary in different body regions and cells.[34] In case of firefly luciferase especially the cofactors ATP and oxygen (also for the other luciferases) can distort the results, if for instance the luciferase expressing cells have their location in diseased tissues, like in tumors, where the supply of ogygen and nutrient is reduced. [22]

The light signal can be also affected by the location and depth of the cells, which express luciferase. Lastly, pigmentation of skin and hair are deciding factors too, since they can dampen and scatter the BLI signal. So, the signal in mice with black fur is lower compared to those albino mice. [34]

1.2.3 The IVIS® SpectrumCT

For imaging small animals in preclinical research, the imaging platform IVIS SpectrumCT is a versatile and powerful tool. It offers the usage of X-ray computed tomography, FLI and BLI. [24]

The animals or cells are placed in a light-tight chamber. In this chamber a movable heating platform is situated. This keeps the animals warm and allows to modulate the distance to the camera to achieve different fields of view. Tumings with nose cones are also installed on the platform to deliver anaesthetic gas, like isoflurane, to sedate the animals during the imaging period. [32]

Optical components, like an ultrasensitive CCD camera to detect the emitted light, a light source with a wide excitation range, that allows surface transillumination or epi-illumination for FLI, and a complete range of emission filters to capture light from the visible to the near infrared spectral range, are included. [24]

Furthermore, the system enables a conversion of 2D optical photography, such as FLI and BLI into 3D tomography, like fluorescence imaging tomography and diffuse luminescence Imaging tomography, by combining the CT imaging with optical imaging modes. For an extensive optical imaging solution PerkinElmer's IVIS SpectrumCT is generally combined with the Living Image® software for analysis of the images and signal quantification, and together with various imaging agents this allows studying a broad range of biological processes. [24]

1.3 Transgenic models and bioimaging

Several transgenic animals have been generated with various reporters to investigate molecular processes like the metabolism of drugs, genotoxicity, and other possible toxic effects of compounds. Especially BLI-based animal models based on reporter assays as in high-throughput screenings could close the gap between biological assays in vitro and preclinical efficacy studies on animal models. The advantages of BLI reporter models is that they require fewer resources, have higher lead compound throughput, and provide quantitative data for the classification and optimization of compounds in comparison to disease animal models. Furthermore, these models allow to rank compounds quantitative in three formats, which are whole animals, tissues and primary cells. [33] Since G protein-coupled receptors (GPCRs) are important therapeutic targets, Dressler et al.[33] have created a transgenic mouse model called CRE luc with luciferase as reporter, driven by a synthetic promoter containing many cAMP response elements, to detect the activity of GPCR ligands by bioimaging in primary cells, tissues and whole animals.

Furthermore, studying the progression of diseases at the molecular level requires the investigation of biomarker activity in living animals over a longer period of time. [35] In general, biomarkers are mostly restricted to blood and urine samples. In comparison to that, BLI allows to utilize activity of the luciferase transgene in small living animals as a biomarker. [35] The study by Buckley et al.[35] describes a tissue-targeted administration of lentivirus vectors encoding for transcription factor-activated luciferase reporter to neonatal rodents. The delivery of lentivirus vectors at this age causes an immune tolerance for luciferase, because the immune system is not yet fully mature, and enables a lifelong expression of the transgene. This method allows quantification of the activity of the transcription factor (TF) in the animal. They have developed this technique to investigate TF activity during pathogenesis of diseases or to evaluate drug efficacy in preclinical studies. [35]

Recently, several transgenic reporter mouse models have been generated to visualize the growth of cancer and cancer-induced cellular behavior such as immune response, inflammation, tumor progression, and proliferation in live animals by using BLI. For example, these transgenic mice contain the reporter gene luciferase, which is driven by a promoter linked to specific processes of cancer cells in its activity, or some other of these models were developed by cDNA knock in at a site of a gene at which its

activity or expression in cancer increases. Despite tracking disease and healthy processes, these animal models can be also used to evaluate the effects of therapeutic substances. [34]

There are numerous studies about various luciferase-based transgenic mouse models which can be used to illuminate cancer or cancer-related processes via BLI. [34] For instance, Szyska et al. [36] generated in their study a transgenic mouse model by transfer of dual-luciferase transgenic T-cells to simultaneously analyze nuclear factor of activated T-cells dependent activation and T-cell migration. Another possibility is to develop a model for analyzing CD4 T-cells dynamics utilizing a human CD2 minigene that directs T-cell specific luciferase expression as described in the study by Chewning et al. [37] In another study a conditional reporter was generated to allow bioluminescent imaging of Cre / loxP-dependent genesis of tumors in mice. They showed that the reporter can be utilized to visualize and measure Kras2v12-induced tumorigenesis in the lung of an already existing non-small cell lung cancer mouse model. [38] Beside these examples there are several other reports about such genetically engineered mouse models that have been summarized in the review by Manni et al. [34].

2 Aim of the thesis

The aim of this diploma work was to determine the phenotypes of three different transgenic reporter mice strains through all breeding generations using 2D BLI technology and thereby confirm the genotype characterization.

Each transgenic mouse model was generated by pronuclear injection of a plasmid fragment with the firefly luciferase gene as reporter and the respective promoter element. Afterwards, these mice were mated with B6 Albino mice to obtain the next generations.

For phenotyping, D-luciferin was injected subcutaneously into every mouse and the light signal of luciferase expressing mice was detected by 2D bioluminescence imaging. In this way we wanted to prove if and where luciferase was expressed and in which mice they passed on to the next generations after further breeding, so that the phenotypically and genotypically positive animals can be used for subsequent studies.

Furthermore, we tried to validate tissue and/or organ specific expressions of luciferase by imaging the organs after the animals were euthanized.

3 Material and Methods

3.1 Animals

Thy 1.2-Luc, SpC-Luc and Split-Luc mice were used for 2D bioluminescence imaging based phenotyping and organ validation experiments. All three mice strains were generated by microinjection of the DNA into the pronuclei of Black 6 mice zygotes in the Institute of Laboratory Animal Science of Vetmeduni Vienna. The transgenic Black 6 mice were transferred to the animal house at the Department for Pharmaceutical Chemistry of the University of Vienna and mated with B6 Albino mice, for obtaining the next generations. Groups of two to five mice were housed in individually ventilated cages (Blue Line - SEALSAFE® NEXT IVC Sytstem, 1285L - TYPE II L, Tecniplast Deutschland GmbH, Hohenpeißenberg, Germany) under specified pathogen free conditions. Autoclaved water and food (SSniff Spezialdiäten GmbH, Soest, Germany) were provided ad libitum. To achieve optimal housing conditions the animal facility had a regulated 12-hour day-night cycle, the room temperature adjusted to 24 ± 1°C and a relative humidity of 40-55%. The animals were kept and treated according to the Austrian and European laws for animal protection. All relevant data regarding e.g. animal facility, compliance, genotyping, breeding, experiments etc. were safely documented and stored using the Animal Facility Software PyRAT (Scionics Computer Innovation GmbH, Dresden, Germany).

3.2 2D Bioluminescence imaging

2D Bioluminescence imaging was used for detecting the luciferase reporter activity in the transgenic mice.

The mice were transferred individually from their cages into an induction chamber (Rothacher Medical GmbH, Heitenried, Switzerland), which was flooded with oxygen containing 5% isoflurane (Isoflurane CP® 1ml/ml, CP Pharma, Burgdorf, Germany), by using a combi-vet® anaesthesia system (Rothacher Medical GmbH, Heitenried, Switzerland). After the mice were completely anesthetized, the animals were placed on the warming bench (combi-vet® Surgery table standard with Physitemp temperature controller unit, Rothacher Medical GmbH, Heitenried, Switzerland), and the anaesthesia was reduced to 2-2.5 % isoflurane. To prevent drying out of the eyes, eye ointment was applied (VitA POS® Augensalbe, Ursapharm, Saarbrücken, Germany). On the heated bench the fur was removed with an animal hair clipper (Isis

Aesculap®, B.Braun, Buchbach, Germany), to avoid the scattering of light caused by the hair and further to improve the imaging results. As next step the weight was determined on a scale (Model CS200, Ohaus Europe GmbH, Greifensee, Switzerland), for calculating the needed amount of D-Luciferin.

For 2D bioluminescence based phenotyping the IVIS SpectrumCT in vivo imaging system (PerkinElmer, Waltham, Massachusetts) was used. D-Luciferin (D- Luciferin potassium salt, 30mg/kg in Dulbecco's Phosphate Buffered Saline, Intrace Medical SA, Lausanne, Switzerland) was injected subcutaneously on the right abdominal side at a dosage of 120mg/kg by using a single-use insulin syringe with integrated needle (Omnican®100, B.Braun, Melsungen, Germany) under anaesthesia, prior to 2D bioluminescence imaging. The mice were placed in prone (for Thy 1.2) or supine (for SpC and SplitLuc) position and fixed with black tape (Insulating Tape, ZD Trading, Zwaagdijk, Netherlands) in the imaging chamber, which was flooded with 2-2.5 % isoflurane-mixed oxygen. The chamber includes a charge coupled device (CCD), which detects the light emission from the transgenic mice. Images were acquired with no emission filter (open filter) to maximize the sensitivity.

Following acquisition parameters were set up by using Imaging Wizard in the IVIS acquisition control panel of the Living Image Software:

Imaging mode	**Bioluminescence**
Emission filter	Stage B - for one mouse Stage C - for two or three mice next to each other
Field of View	Open Filter
Subject height	1.5 cm
Time series	Segment approx.: 12; minutes: 3

Table 2. Acquisition parameters for 2D BLI phenotyping.

After completion of the imaging session, the anaesthesia was turned off and the mice were returned to their cages upon awakening.

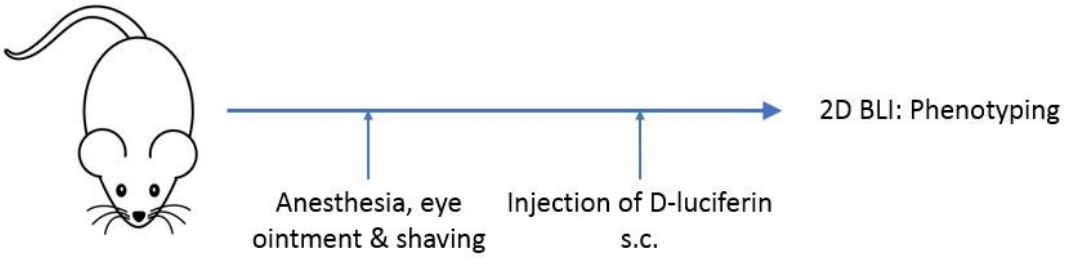

Figure 4. Timeline scheme of 2D BLI based phenotyping.

3.3 Validation of phenotyping by organ imaging

Animals, which were not needed anymore for further experiments or arrived an old age where used for validation of the 2D BLI based phenotyping. As described in "3.2 2D Bioluminescence imaging" the animals were anaesthetized, shaved and treated with D-Luciferin. After waiting 20 minutes, isoflurane was increased to 5% and the mice were euthanized by cervical dislocation. Depending on the transgenic strain the corresponding organs were removed immediately after euthanasia and transferred into the light-tight chamber of the IVIS SpectrumCT. 2D bioluminescence images were acquired to detect the bioluminescence signal in the organs.

Following acquisition parameters were set up for organ imaging:

Imaging mode	**Bioluminescence**
Emission filter	Stage B – for organs of one mouse Stage C – for organs of two mice
Field of View	Open Filter
Subject height	0.5 cm
Time series	Not used

Table 3. Acquisition parameters for 2D BLI organ imaging.

At the end of the experiment each organ was cut into 4- 5mm pieces by using a sterile surgical blade (Figur 15, BB515, Aesculap AG, Tuttlingen, Germany). The cut-up organs were transferred separately into a 1.5ml microcentrifuge tube (np Safelock-Cap, nerbe plus GmbH, Winsen, Germany) and stored for RNA analysis in the -80°C freezer of the S1 lab of the Department for Pharmaceutical Chemistry of the University

of Vienna. Information about the organs and their storage location were saved on the web-based Electronic Lab Notebook Labguru (BioData Ltd., Rosh Ha'ayin, Israel).

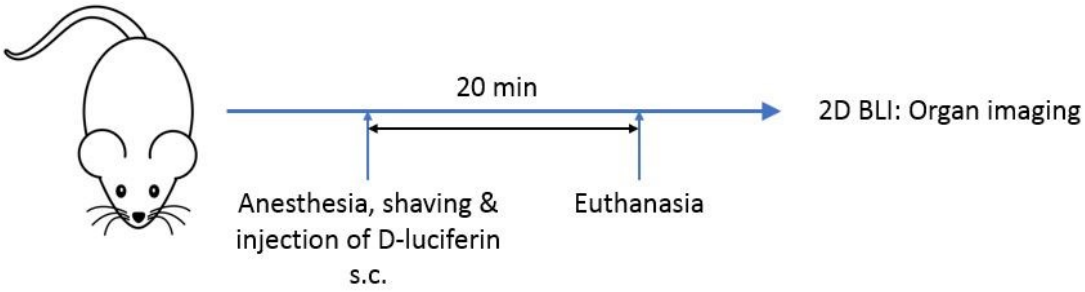

Figure 5. Timeline scheme of 2D BLI based organ validation.

3.4 Image Analysis and details of the experimental transgenic mice

The analysis of the 2D image data was done by using the Living Image software (Version 4.5.2, Perkin Elmer, Waltham, Massachusetts). Rectangular regions of interest (ROIs) were drawn for signal quantification (surface intensity). Depending on the transgenic strain, the ROIs were placed on different areas. For Tg Thy 1.2-Luc, one ROI was applied at the brain region and another one in the lower back region to be used as a background control (Figure 7). In the Tg SpC-Luc images, one ROI was drawn over the lung region for catching the lung signal and a second one over the whole body of the animal for measuring the skin signal (Figure 8). A single whole-body ROI was applied in the Tg (Luc705) Split-Luc mice data. In the organ imaging data, one ROI was drawn for each organ (Figure 9). Radiance (photons) was selected as measurement unit for quantitative comparison of signals across the images. The quantification of the signal was carried out in by measuring the total flux (photons/sec).

The analysed total photon flux data was exported and saved in Excel (Microsoft Office 365, Microsoft Corporation, Redmond, Washington) for presenting the results as graphs.

From each phenotyping session (Figure 6) the image with the highest signal within the time series was selected and saved in form of a TIFF file format.

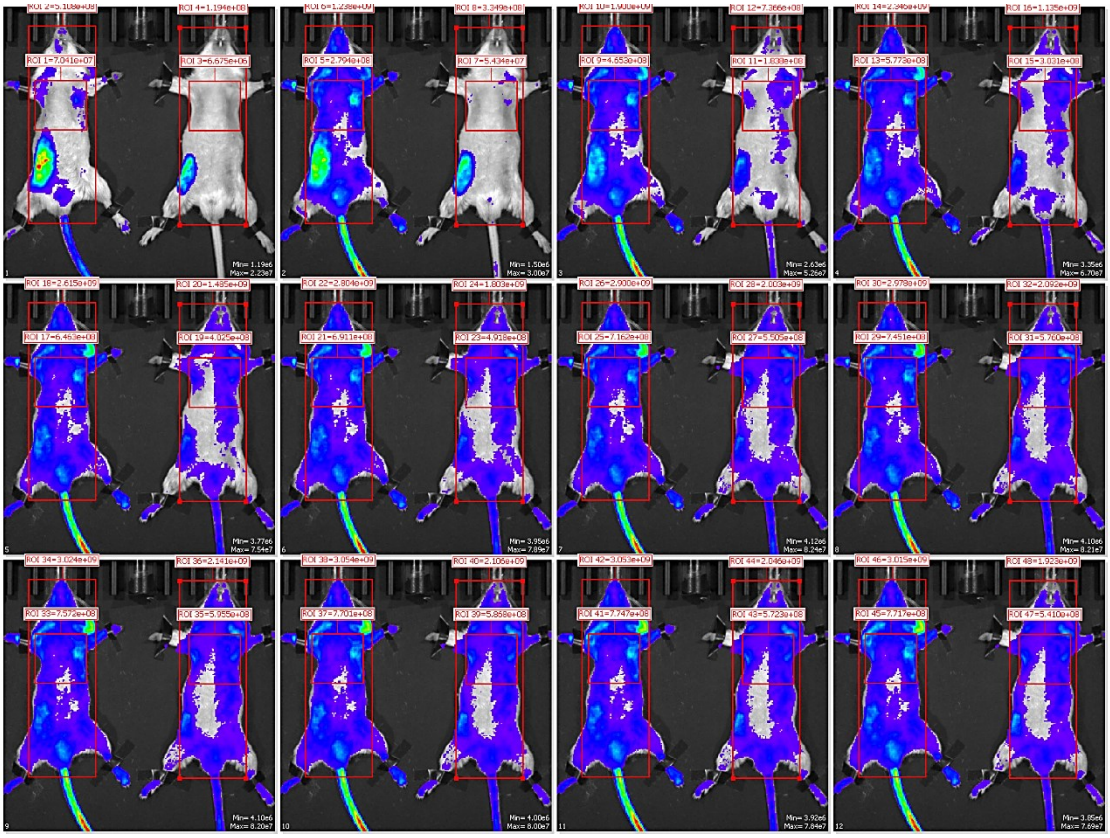

Figure 6. Representative example showing a time series by 2D bioluminescence imaging. *12 images were acquired with 3 minutes delay between each image. The session allows to track the kinetics of D-luciferin and to select the image with the highest BLI signal for analysis.*

3.4.1 Tg Thy 1.2-Luc

For understanding the following tables and chapters the possible genotypes are transgenic positive (tg+), hemizygous (hem), weak hemizygous (weak hem), which are genotypically positive or wildtype, which has a negative genotype.

Phenotyping of Tg Thy 1.2-Luc mice				
Generation	**Color**	**Genotype**	**Mouse IDs**	
G0b	black	tg +	AGE 116	
G0c	black	tg +	AGE117	
G1a	black	hem	AGE148	AGE150
			AGE151	AGE152
			AGE159	
G1b	black	hem	AGE149	AGE156
			AGE161	
G2a	black	hem	AGE249	AGE250
			AGE253	AGE254
	white	hem	AGE255	AGE256
G2b	black	wildtype	AGE266	
	white	wildtype	AGE261	
G2b	black	hem	AGE262	AGE263
			AGE265	AGE267
G2b	white	hem	AGE264	
G3a	white	hem	AGE293	
G3b	white	wildtype	AGE439	AGE443
G3b		hem	AGE442	AGE440
G4a	white	wildtype	AGE453	

Table 4. Details of phenotyped Tg Thy 1.2-Luc mice.

Organ validation of Tg Thy 1.2-Luc mice				
Generation	**Color**	**Genotype**	**Mouse IDs**	
G0b	black	tg+	AGE116	
G0c	black	tg+	AGE117	
G2a	black	hem	AGE250	
	white	hem	AGE255	AGE256
G2b	black	hem	AGE263	AGE265
			AGE267	
G3a	white	hem	AGE293	
G3b	white	wildtype	AGE439	AGE443
G3b	white	weak hem	AGE441	AGE444
G3b	white	hem	AGE440	AGE442
G4a	white	wildtype	AGE445	AGE448
			AGE453	
G4a	white	weak hem	AGE369	
G4a	white	hem	AGE374	AGE450
G5a	white	wildtype	MCT174	

Table 5. Details of Tg Thy 1.2-Luc mice used for organ validation.

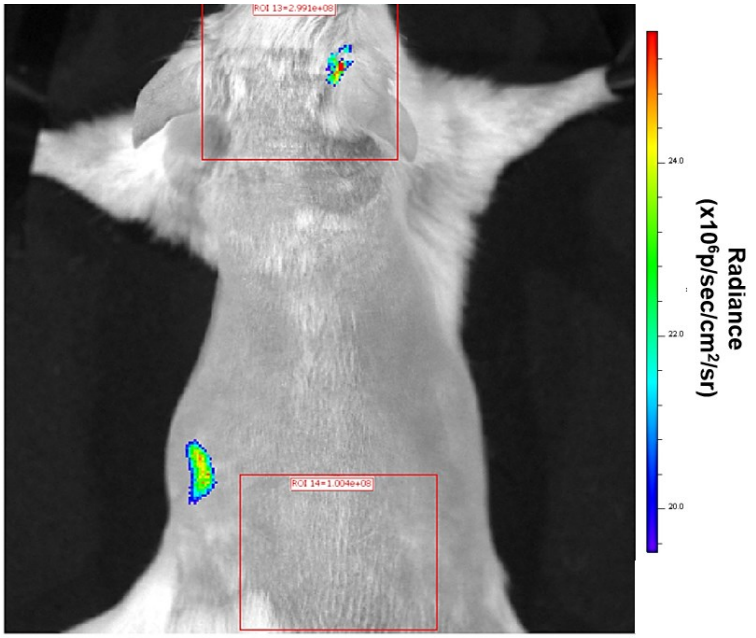

Figure 7. Representative example showing position of ROIs used for analysis of imaging data of Tg Thy 1.2-Luc mice.

3.4.2 Tg SpC-Luc

Phenotyping of Tg SpC-Luc mice				
Generation	**Color**	**Genotype**	**Mouse IDs**	
G1	black	hem	AGE312	AGE316
G2	black	weak hem	AGE342	AGE343
			AGE349	AGE350
			AGE357	AGE362
			AGE363	AGE364
G2	back	hem	AGE344	AGE348
			AGE359	
G2	white	weak hem	AGE355	
G2	white	hem	AGE345	AGE346
			AGE347	AGE360
			AGE361	
G2a	black	weak hem	AGE416	
G2a	white	wildtype	AGE413	
G3	white	wildtype	AGE457	
			AGE467	AGE476
			AGE477	AGE478
			MCT237	MCT238
			MCT240	MCT242
G3	white	weak hem	MCT239	
G3	black	weak hem	MCT241	
G3	white	hem	MCT236	
G4	white	wildtype	MCT196	
G4	white	weak hem	MCT191	MCT194
			MCT192	MCT195
G4	white	hem	MCT193	MCT197
			MCT198	

Table 6. Details of phenotyped Tg SpC-Luc mice.

Organ validation of Tg SpC-Luc mice				
Generation	**Color**	**Genotype**	**Mouse IDs**	
G2	black	weak hem	AGE357	AGE363
G2a	black	hem	AGE414	
G3	white	wildtype	AGE477	AGE478
G3	black	weak hem	MCT241	
G3	white	weak hem	AGE464	AGE468

Table 7. Details of Tg SpC-Luc mice used for organ validation.

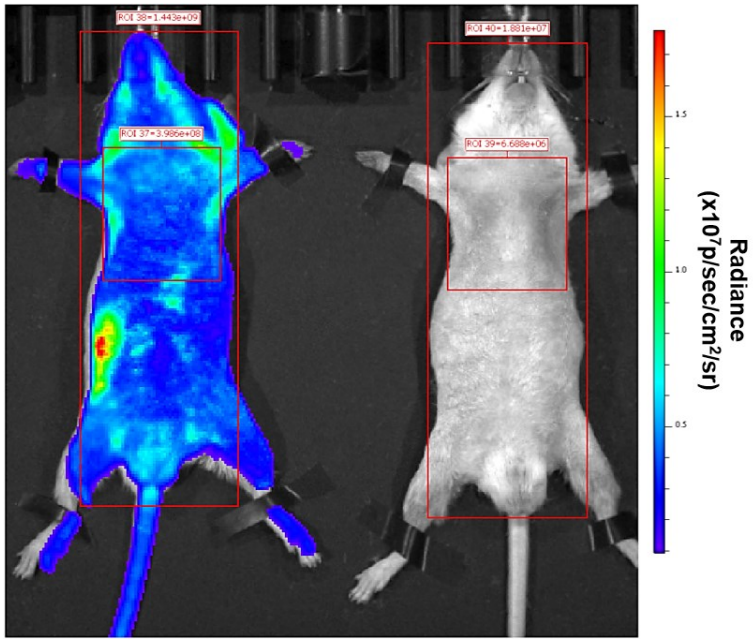

Figure 8. Representative example showing position of ROIs used for analysis of imaging data of Tg SpC-Luc mice.

3.4.3 Tg (Luc705) Split-Luc

Phenotyping of Tg (Luc705) Split-Luc mice				
Generation	**Color**	**Genotype**	**Mouse IDs**	
G2b	white	wildtype	AGE380	AGE387
			AGE404	
G3b	white	wildtype	MCT163	MCT164
			MCT167	MCT170
			MCT183	
G3b	white	weak hem	MCT169	MCT184
G3b	white	hem	MCT165	MCT166
			MCT168	MCT171
			MCT185	MCT186
			MCT187	
G2c	white	hem	AGE435	

Table 8. Details of imaged Tg (Luc705) Split-Luc mice.

Organ validation of Tg(Luc705)Split-Luc mice			
Generation	**Color**	**Genotype**	**Mouse IDs**
G2b	black	weak hem	AGE402
	black	hem	AGE389
	white	wildtype	AGE387
G3b	white	wildtype	MCT164
G2c	white	wildtype	AGE431
	black	weak hem	AGE434

Table 9. Details of Tg (Luc705) Split-Luc mice used for organ validation.

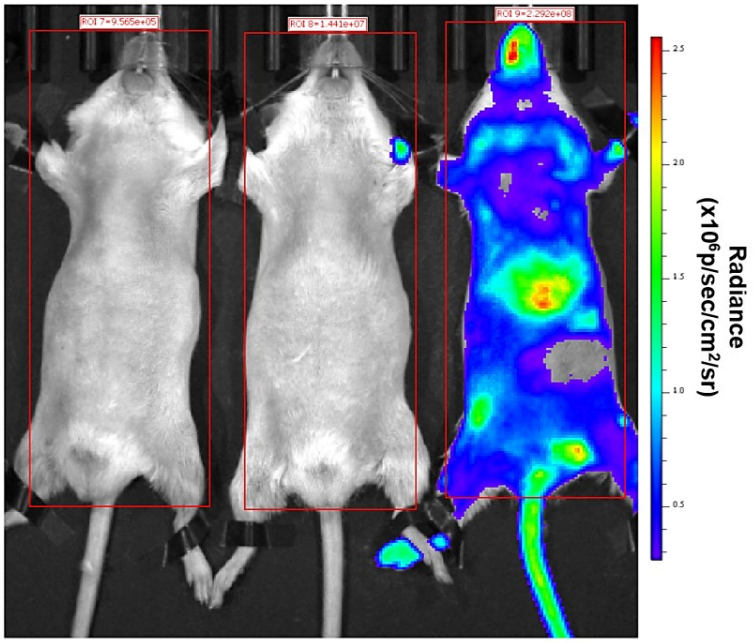

Figure 9. Representative example showing position of ROIs used for analysis of imaging data of Tg (705) Split-Luc mice.

4 Results and Discussion

4.1 Phenotyping and organ validation results of Tg Thy 1.2-Luc

For phenotyping of Tg Thy 1.2-Luc mice, one to three animals were investigated per imaging session. The anesthetized mice were placed in prone position in the imaging chamber and the 2D BLI pictures were acquired right after subcutaneous injection of D-luciferin in the right abdominal side. The picture with the highest bioluminescence signal of each session was selected for the analysis. By using the Living Image software, one ROI was applied over the brain region and a second one in the lower back region as a background control. ROIs of the brain region that provided a value of over log 6 in the signal quantification and showed higher values than in the background ROI were assessed as phenotypically positive and values below log 6 were evaluated with a negative phenotype.

The phenotyping data includes wildtype and hem mice of the generations G0b, G0c, G1a, G1b, G2a; G2b; G3a, G3b and G4a (Table 4).

For validation by organ imaging the mice were sacrificed by cervical dislocation 20 minutes after subcutaneous injection of D-Luciferin. After euthanasia brain and different other organs such as kidney, spleen, liver, heart, lung, bladder, skin and muscle were directly removed and imaged. Also here ROIs were placed around each organ and quantified. A visibly detected BLI signal of the brain in the organ image validated the positive phenotype. For this experiments wildtype, weak hem and hem mice of generation G0b, G0c, G2a; G2b; G3a, G3b, G4a and G5a were used (Table 5).

4.1.1 Generation G0b and G0c

The data of only one mouse of each generation, G0b and G0c, is available for the phenotyping results. Both mice are genotypically positive. These two mice showed a high signal between log 6 and log 7 in the brain region, which was also significantly higher in comparison to the background region (Figure 10, 11).

The organs were taken from both mice and visualized (Figure 12 – A1, B1). Also, here clear signals of the brains can be recognized in the organ images as well as in the signal quantifications (Figure 12 – A2, B2), which confirm positive phenotypes.

I. 2D BLI

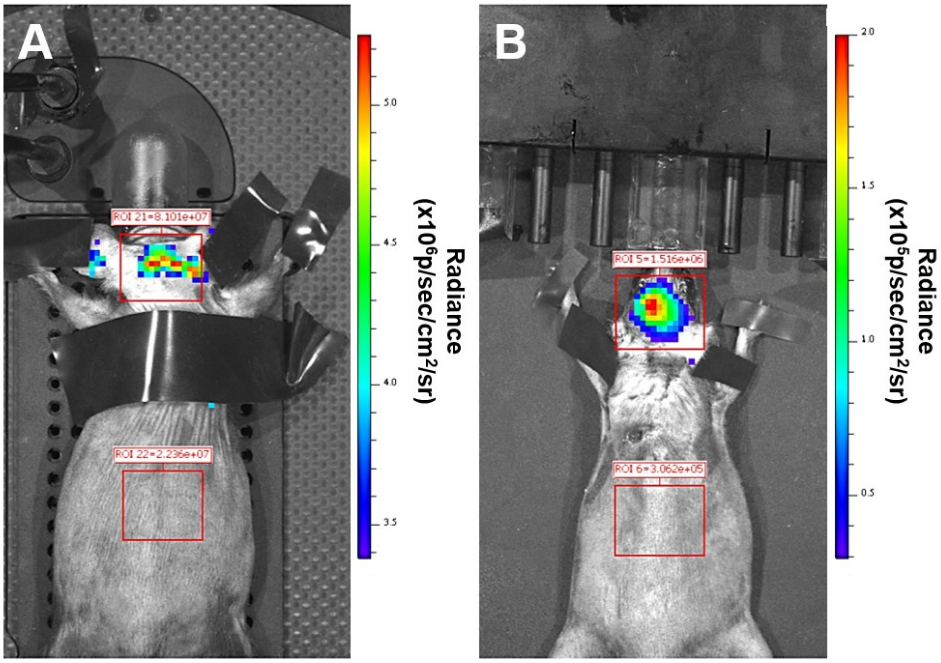

Figure 10. 2D bioluminescence images of G0b and G0c mice after s.c. injection of D-luciferin. *Both mice were tg+ and had a black coat. Imaging position: prone. A: G0b - AGE116; Color Scale: Min = 3,38e6 / Max = 5,25e6. B: G0c - AGE117; Color Scale: Min = 2,95e4 / Max = 2,00e5.*

II. Analysis

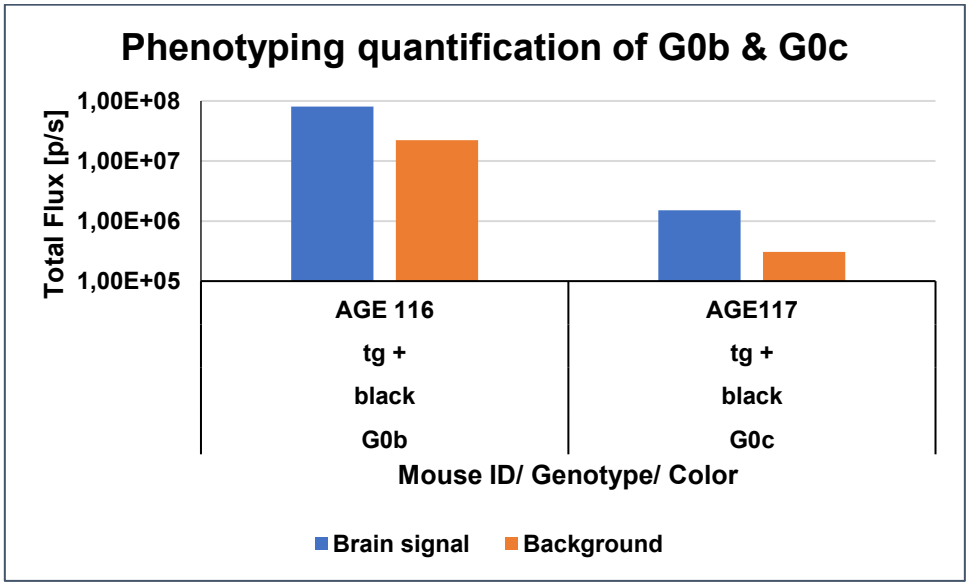

Figure 11. 2D BLI signal quantification of images of Figure 10.

III. Organ validation

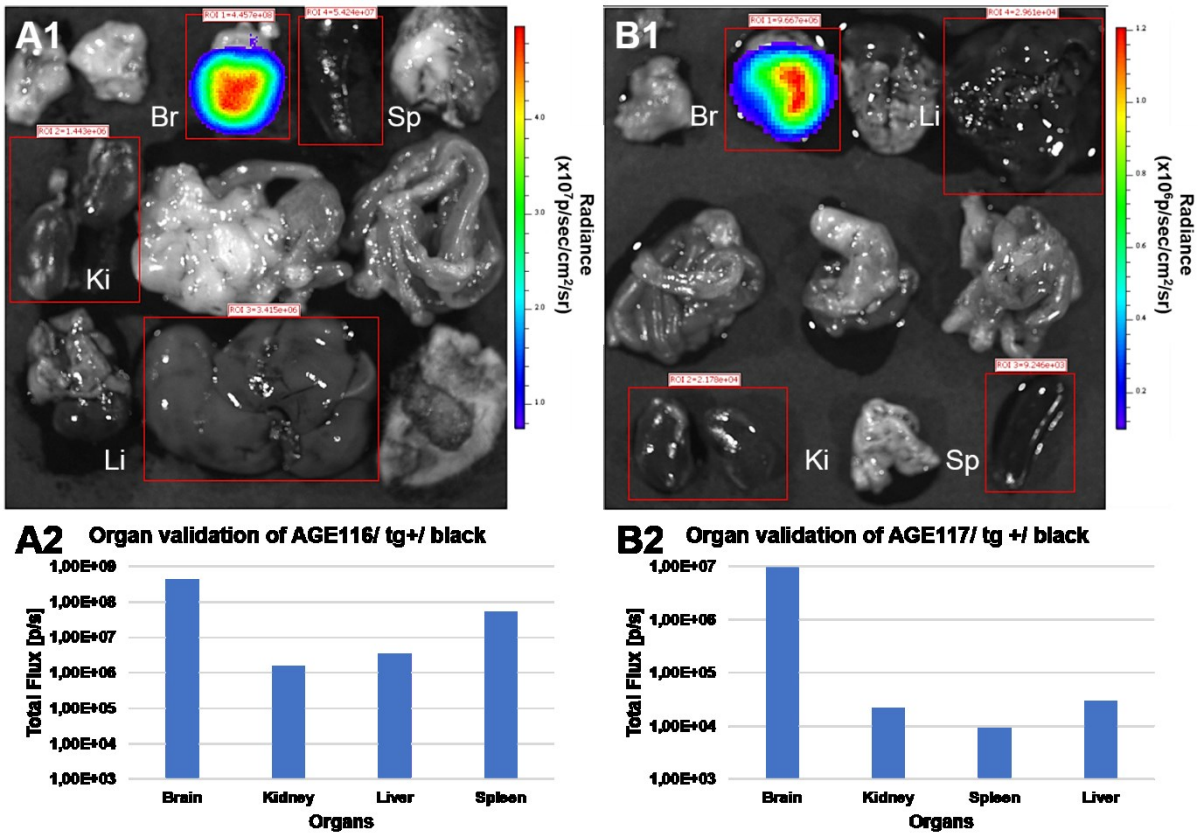

Figure 12. 2D Bioluminescence images and signal quantification of the organs of G0b and G0c mice of Figure 10. *A1: 2D BL images of the organs from AGE116 – G0b; Color Scale: Min = 7,47e6 / Max = 4,99e7. A2: Signal quantification of organ images from A1. B1: 2D BLI of organs from AGE117 – G0c. B2: Quantification of organ images from B1; Color Scale: Min = 9,97e4 / Max = 1,21e6. Br = Brain, Ki = Kidneys, Li = Liver, Sp = Spleen.*

4.1.2 Generation G1a

Five mice of generation G1a were imaged. All of them had a black coat and a hem genotype. The mouse AGE151 (M2) showed a very strong BLI signal in the picture (Figure 13 - A), which had also the highest quantified brain signal in relation to the other mice. (Figure 14) The brain signals of the other mice were slightly or not visible (Figure 13). However, the quantification of the ROIs in Figure 14 showed a value of every mouse over log 6-8 in the brain region, which is also higher than the background range. So, the phenotype of all five mice was determined as positive. No organ validation of generation G1a was carried out.

I. 2D BLI

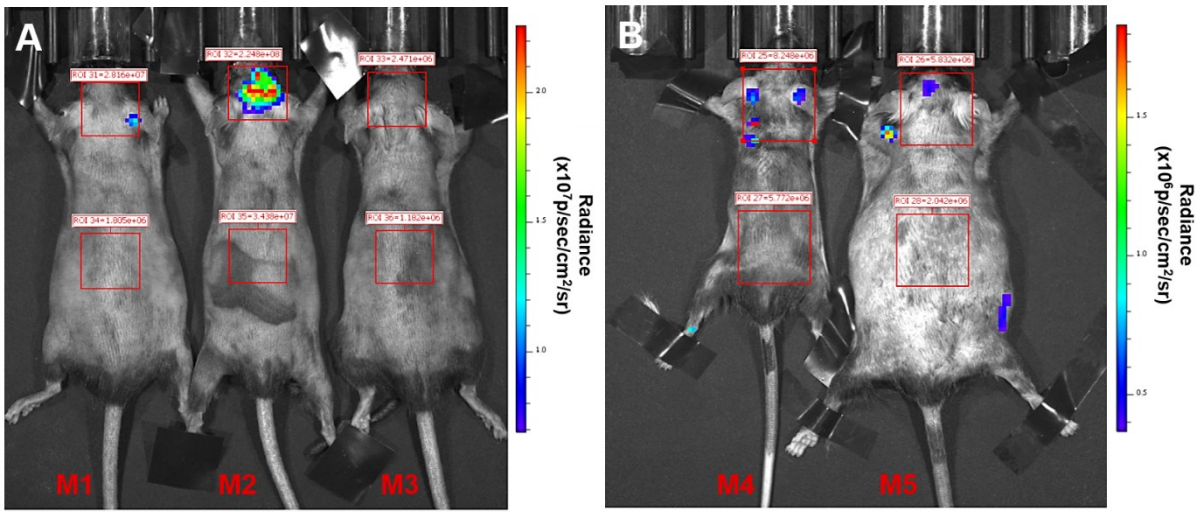

Figure 13. 2D bioluminescence images of G1a mice after s.c. injection of D-luciferin. *All mice were genotypically hem and had a black coat. Imaging position: prone. A: M1 = AGE150, M2 = AGE151, M3 = AGE152; Color Scale: Min = 6,90e6 / Max = 2,26e7. B: M4 = AGE159, M5 = AGE148; Color Scale: Min = 3,60e5 / Max = 1,83e6.*

II. Analysis

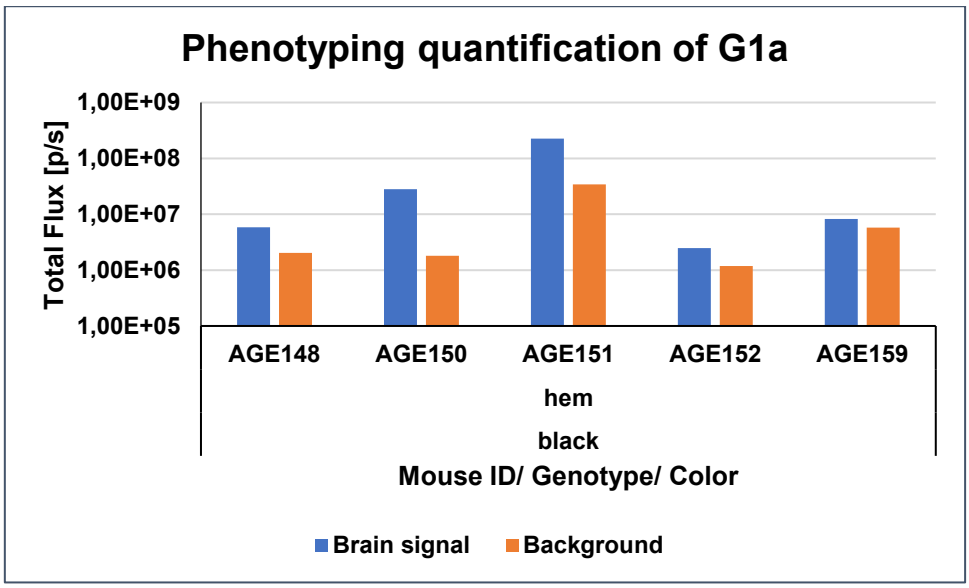

Figure 14. 2D BLI signal quantification of images of Figure 13.

4.1.3 Generation G1b

Three mice of generation G1b were phenotyped. All of them had like the mice from G1a a black coat and a hem genotype. In Figure 15 only the light signal of AGE156

(M1) is significant visible, but all three mice had brain signals between log 6 and log 8, which were also higher than the background area (Figure 16). Thus, the phenotype determination here also agrees with the genotype. However, it is striking that AGE149 shows in Figure 16 a significant lower signal than the mice AGE156 and AGE161 although all three are hem mice and from the same generation. No organ validation of generation G1b was carried out.

I. 2D BLI

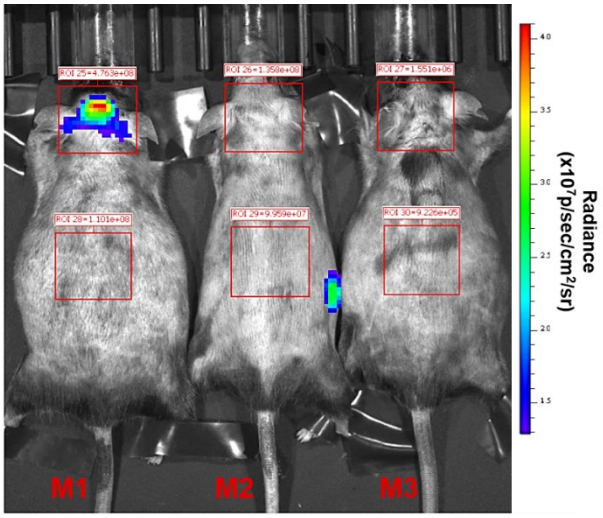

Figure 15. 2D bioluminescence images of G1b mice after s.c. injection of D-luciferin. *All mice were genotypically hem and had a black coat. Imaging position: prone. M1 = AGE156, M2 = AGE161, M3 = AGE149; Color Scale: Min = 1,29e7 / Max = 4,10e7.*

II. Analysis

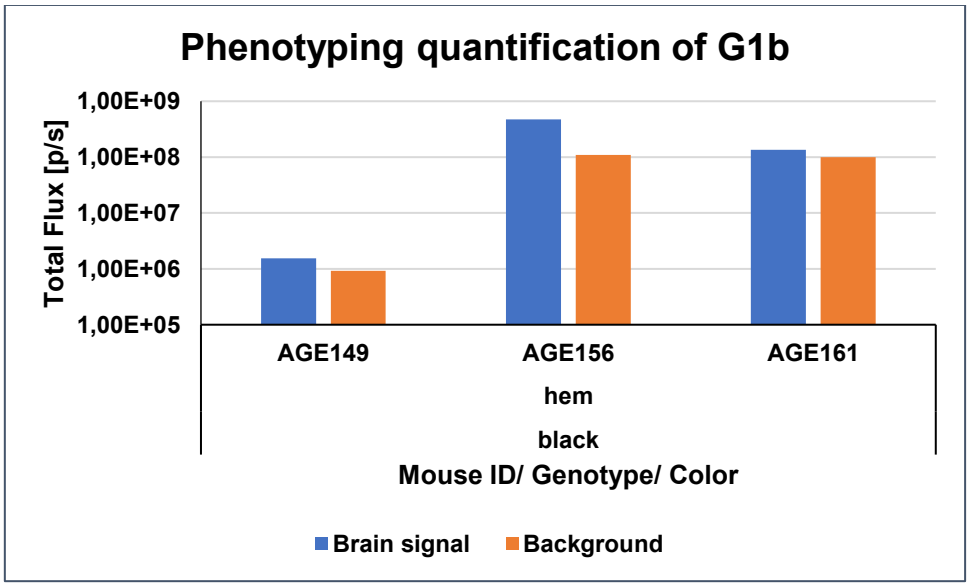

Figure 16. 2D BLI signal quantification of images of Figure 15.

4.1.4 Generation G2a

The number of 2D BLI based phenotyped mice of generation G2a is six. All mice were hem and two of them had a white coat, while the others had a black fur. All animals, except AGE256 (M3), appear positive, as seen in the graph in Figure 18, as the brain ROI gives a higher values than the background ROI. Although, due to the intense spots in Figure 17, the brain signal cannot be clearly seen in the phenotyping images. These visible spots are probably skin lesions, which are able to activate the Thy-1 promotor during wound healing. [39] However, the ex vivo imaging of two of these mice AGE255 and AGE250 confirm the positive phenotypic status by significant visible and measureble brain signals (Figure 19). Only, AGE256 is definitely negative, since the explanted brain showed also no signal (Figure 20).

I. 2D BLI

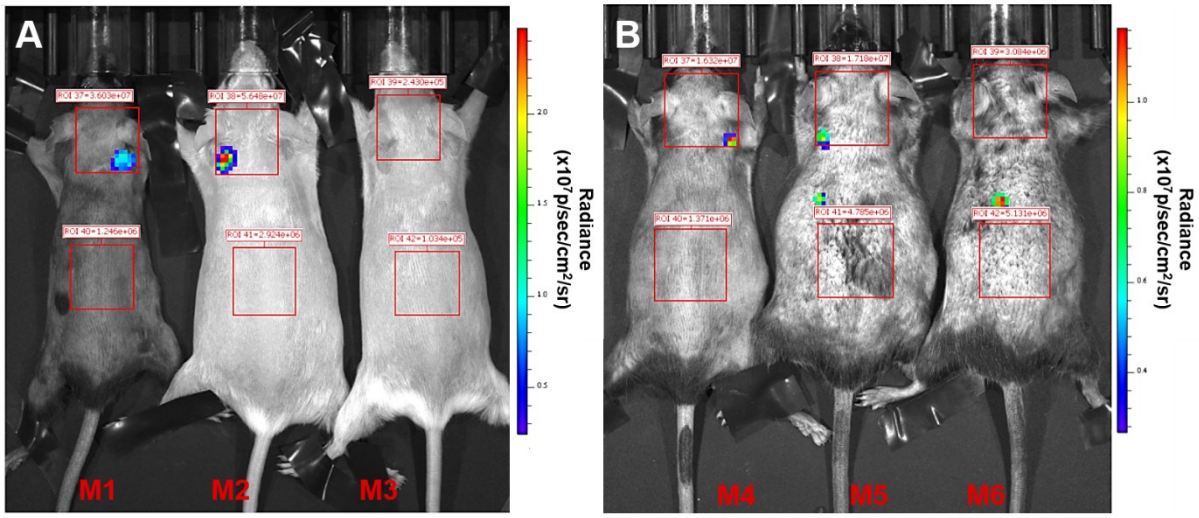

Figure 17. 2D bioluminescence images of G2a mice after s.c. injection of D-luciferin. *All mice were genotypically hem. M2 and M3 had a white coat and all the other a black coat. Imaging position: prone. A: M1 = AGE253, M2 = AGE255, M3 = AGE256; Color Scale: Min = 2,44e6 / Max = 2,47e7. B: M4 = AGE254, M5 = AGE249, M6 = AGE250; Color Scale: Min = 2,60e6 / Max = 1,17e7.*

II. Analysis

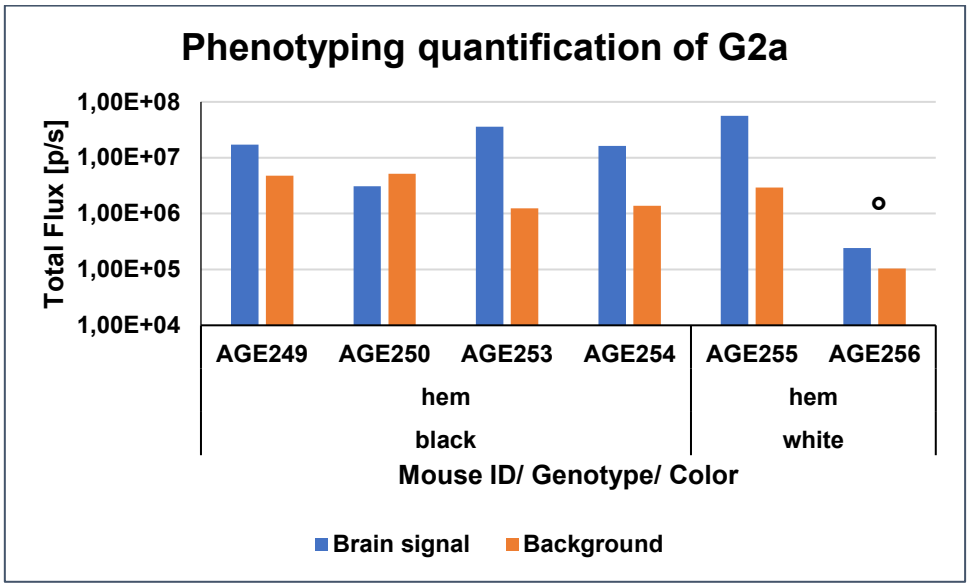

Figure 18. 2D BLI signal quantification of images of Figure 17. *Genotypically positive mouse AGE256 with negative phenotypic status marked with a circle (°) as outlier.*

III. Organ validation

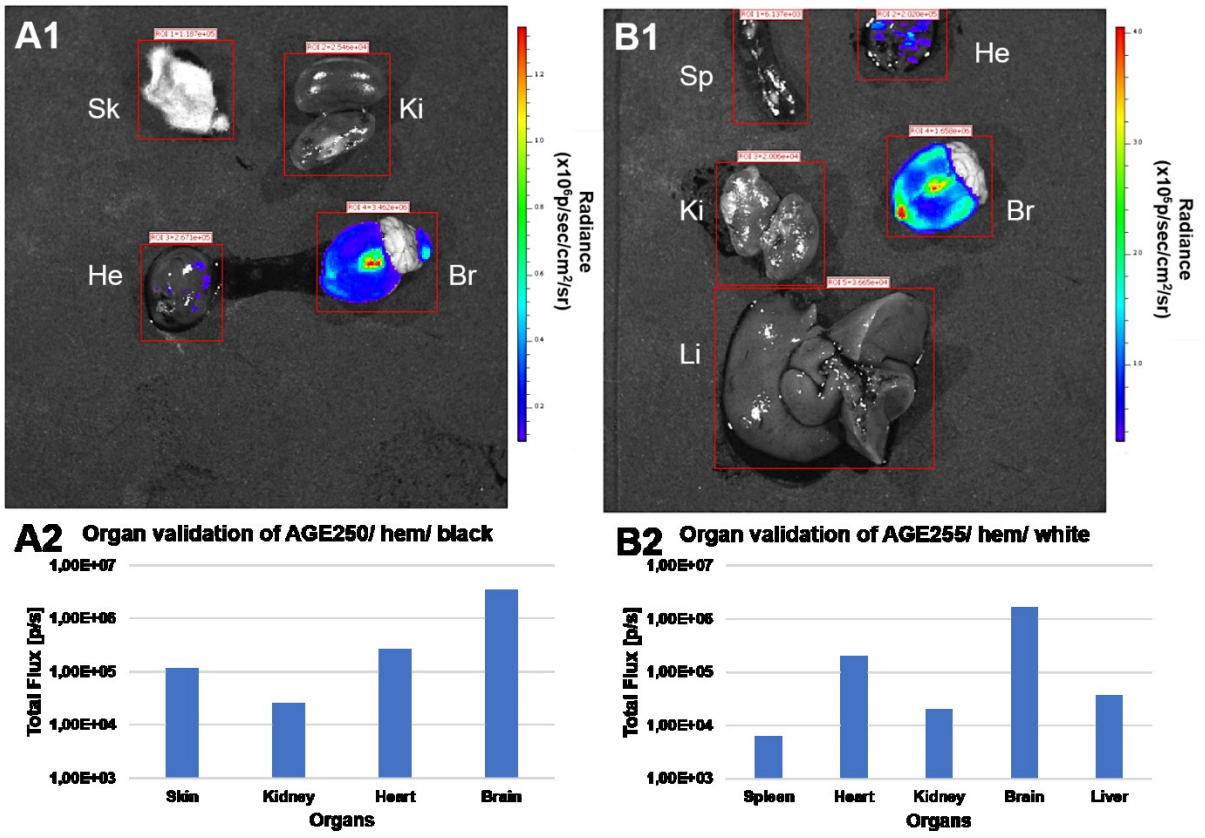

Figure 19. 2D Bioluminescence images and signal quantification of the organs of G2a mice. *A1: 2D BL images of the organs from AGE250; Color Scale: Min = 1,00e5 / Max = 1,35e6. A2: Signal quantification of organ images from A1. B1: 2D BLI of organs from AGE255; Color Scale: Min = 3,11e4 / Max = 4,06e5. B2: Signal quantification of organ images from B1. Br = Brain, He = Heart, Ki = Kidneys, Li = Liver, Sp = Spleen.*

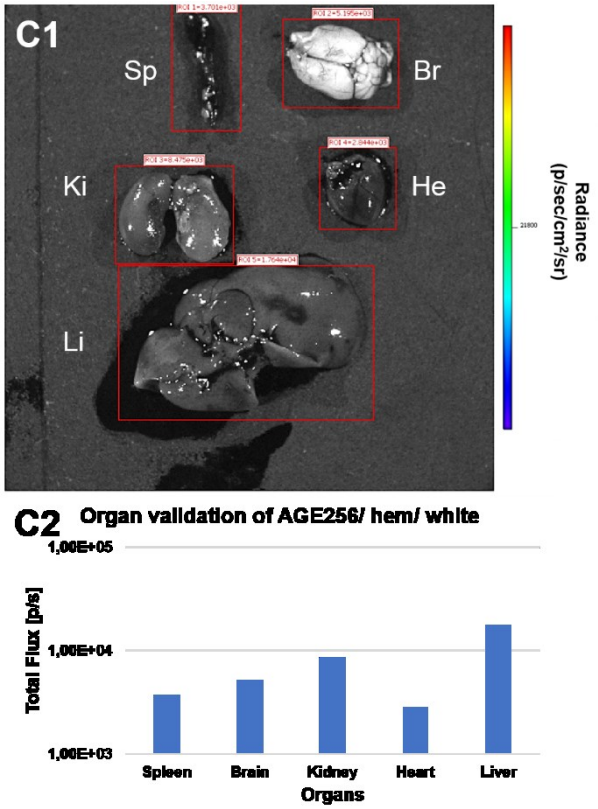

Figure 20. 2D Bioluminescence images and signal quantification of the organs of the G2a mouse AGE256. *C1: 2D BL images of the organs from AGE256; Color Scale: Min = 2,18e4 / Max = 2,18e4. C2: Signal quantification of organ images from C1. Br = Brain, He = Heart, Ki = Kidneys, Li = Liver, Sp = Spleen.*

4.1.5 Generation G2b

Two genotypically wildtype and five hem mice of generation G2b were imaged (Figure 21). All had values between log 6 and log 8 in the brain region (Figure 22), which can be considered as positive phenotype, except AGE265 (M6) which had the same value in the brain ROI as in the background ROI. Also here intense spots are visible, which are able to cover the brain signal in the whole-body images (Figure 21) as mentioned in 4.1.4. However, two of the imaged mice were determined as wildtype after genotyping, and therefore did not match with their phenotypes.

Furthermore, the hem mouse AGE265 was used for organ validation because of its low phenotyping value compared to the other mice. In Figure 23 – B1, it can be shown that no brain signal was detected in the organ image, which thus explains the low value from whole body imaging compared to the others (Figure 22) and is therefore determined as phenotypically negative. An explanation for the nevertheless high value of the brain could be that the positive signal of the mouse next to it may have covered

the negative value. In addition, two other hem mice, AGE263 (M3) and AGE267 (M4), were chosen for organ imaging. As shown in Figure 23 – A1, B1 both had significant BLI signals in their brains and confirm the results of 2D phenotyping. Additionally, in both mice a slightly signal of the spleen were detected, which can be explained by the fact that Thy-1 also plays an important role in adhesion of monozytes and leukozytes to endothelial cells. [39]

I. 2D BLI

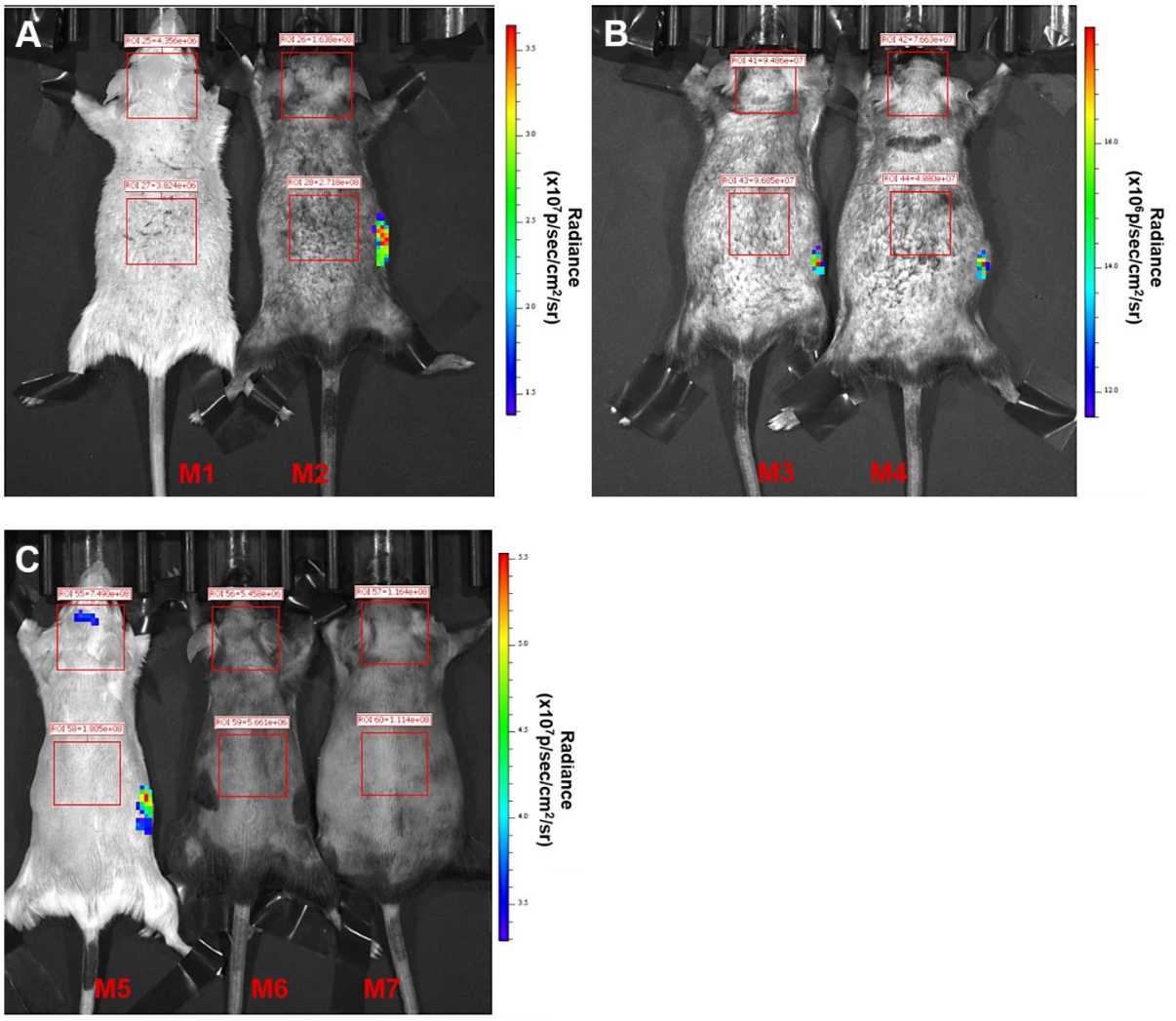

Figure 21. 2D bioluminescence images of G2b mice after s.c. injection of D-luciferin. *M1 and M2 were genotypically wildtype and all the other animals hem. M1 and M5 had a white coat, the rest a black coat. Imaging position: prone. A: M1 = AGE261, M2 = AGE262; Color Scale: Min = 1,38e7 / Max = 3,65e7. B: M3 = AGE263, M4 = AGE267; Color Scale: Min = 1,16e7 / Max = 1,79e7. C: M5 = AGE264, M6 = AGE265, M7 = AGE266; Color Scale: Min = 3,29e7 / Max = 5,53e7.*

II. Analysis

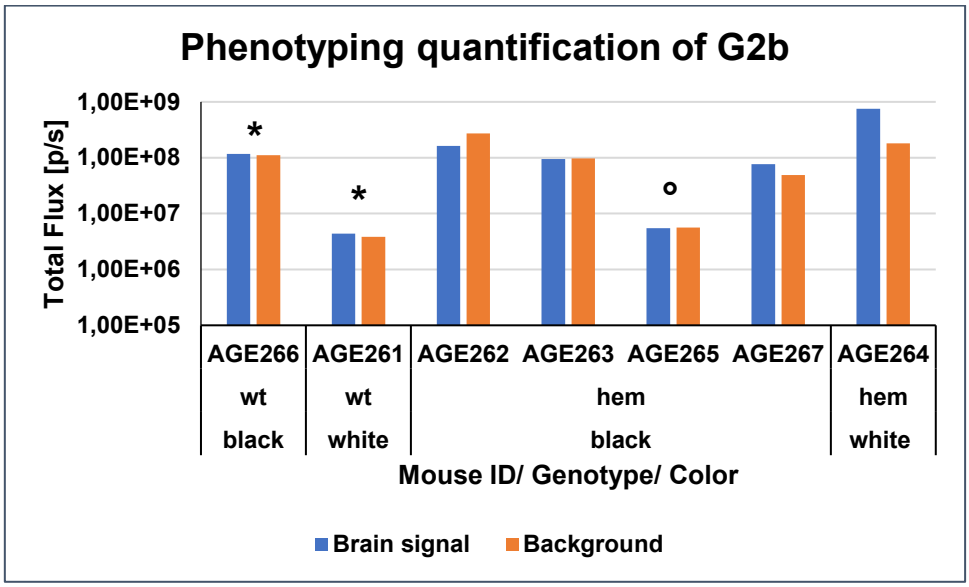

Figure 22. 2D BLI signal quantification of images of Figure 21.*Genotypically positive mouse AGE265 with negative phenotypic status marked with a circle (°). Genotypically negative mice AGE266 and AGE261 with positive phenotypic status marked with an asterisk (*) marked as outliers. wt = wildtype.*

III. Organ validation

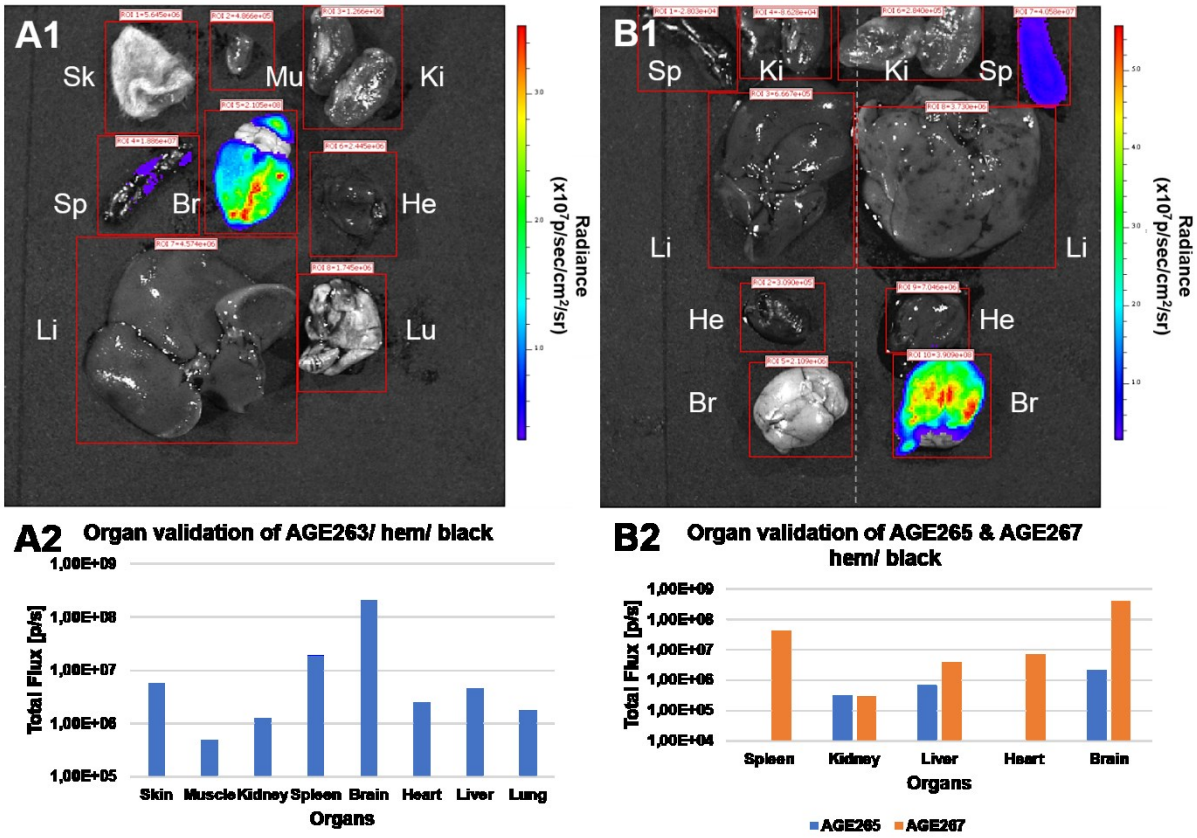

Figure 23. 2D Bioluminescence images and signal quantification of the organs of G2b mice. *A1: 2D BL images of the organs from AGE263; Color Scale: Min = 2,97e6 / Max = 3,54e7. A2: Signal quantification of organ images from A1. B1: 2D BLI of organs from AGE265 (left) and AGE267 (right); Color Scale: Min = 2,87e6 / Max = 5,58e7. B2: Signal quantification of organ images from B2. Br = Brain, He = Heart, Ki = Kidneys, Lu = Lung, Li = Liver, Mu = Muscle, Sk = Skin, Sp = Spleen.*

4.1.6 Generation G3a

Only one mouse of generation G3a was visualized by 2D BLI. This is AGE293, which was genotypically hem and had a white coat. As there was no signal in the whole body image (Figure 24) or quantification (Figure 25), the mouse was used for organ imaging. Again, there was no signal in the brain (Figure 26). Therefore, the phenotype does match the genotype here.

I. 2D BLI

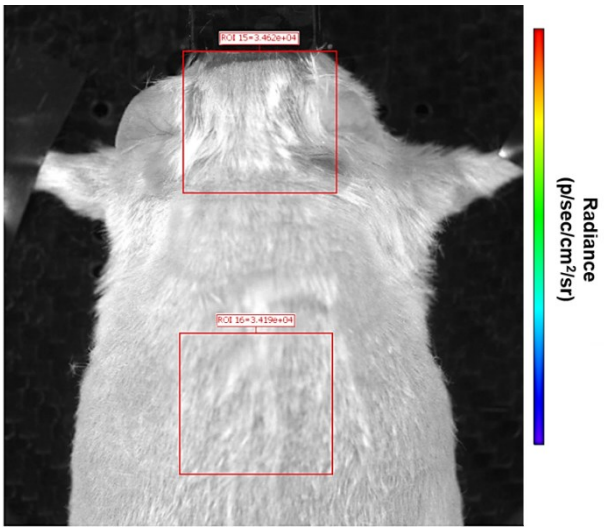

Figure 24. 2D bioluminescence image of the G3a mouse AGE293 after s.c. injection of D-luciferin. *The animal had a white coat and was genotypically hem. Imaging position: prone; Color Scale: Min = 2,77e3 / Max = 2,77e3.*

II. Analysis

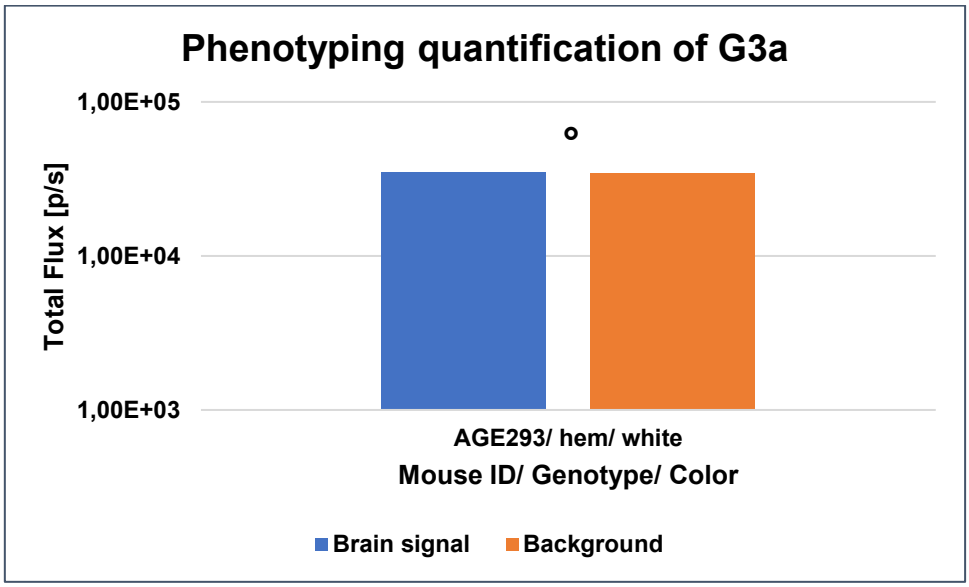

Figure 25. 2D BLI signal quantification of image of Figure 24. *Genotypically positive mouse AGE293 with negative phenotypic status marked with a circle (°) as outlier.*

III. Organ validation

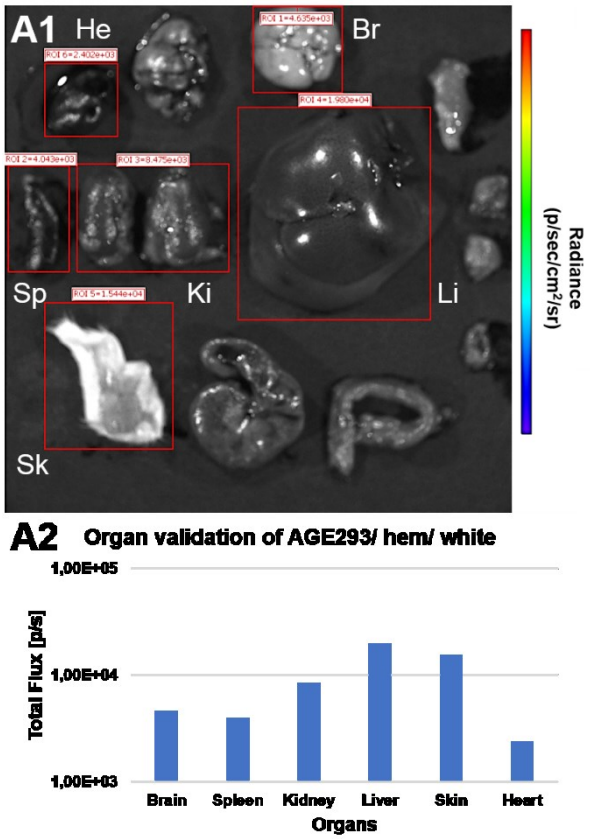

Figure 26. 2D Bioluminescence images and signal quantification of the organs of G3a mouse AGE293. *A1: 2D BL images of the organs from AGE293; Color Scale: Min = 2,96e3 / Max = 2,96e3. A2: Signal quantification of organ images from A1. Br = Brain, He = Heart, Ki = Kidneys,, Li = Liver, Sk = Skin, Sp = Spleen.*

4.1.7 Generation G3b

Four white mice of generation G3b were imaged. Two of them were genotypically wildtype and the other two hem. All of them were also chosen for organ validation (Figure 29, 30). The wildtype mouse AGE439 shows no signal in both figures (Figure 27 -C, Figure 29 – A1), which thus agrees phenotypically with its genotype. AGE442 also match with its genotype, as it shows a clear brain signal in both whole body and organ images (Figure 27 – A, Figure 29 – B1). The other two mice AGE443 and AGE440 had a different phenotype than expected, because the wildtype mouse AGE443 had a positive signal in the brain region (Figure 27 - B, Figure 30 – C1) and the hem mouse AGE440 (Figure 27 – D, Figure 30 – D1) no BLI signal. The images and quantifications of the organs confirmed this (Figure 30).

In addition, two weak hem mice were euthanized, and their organs were imaged (Figure 31 – E1). Here also only one of the two animals showed a brain signal and the other one did not match with its genotype, due to the missing signal.

I. 2D BLI

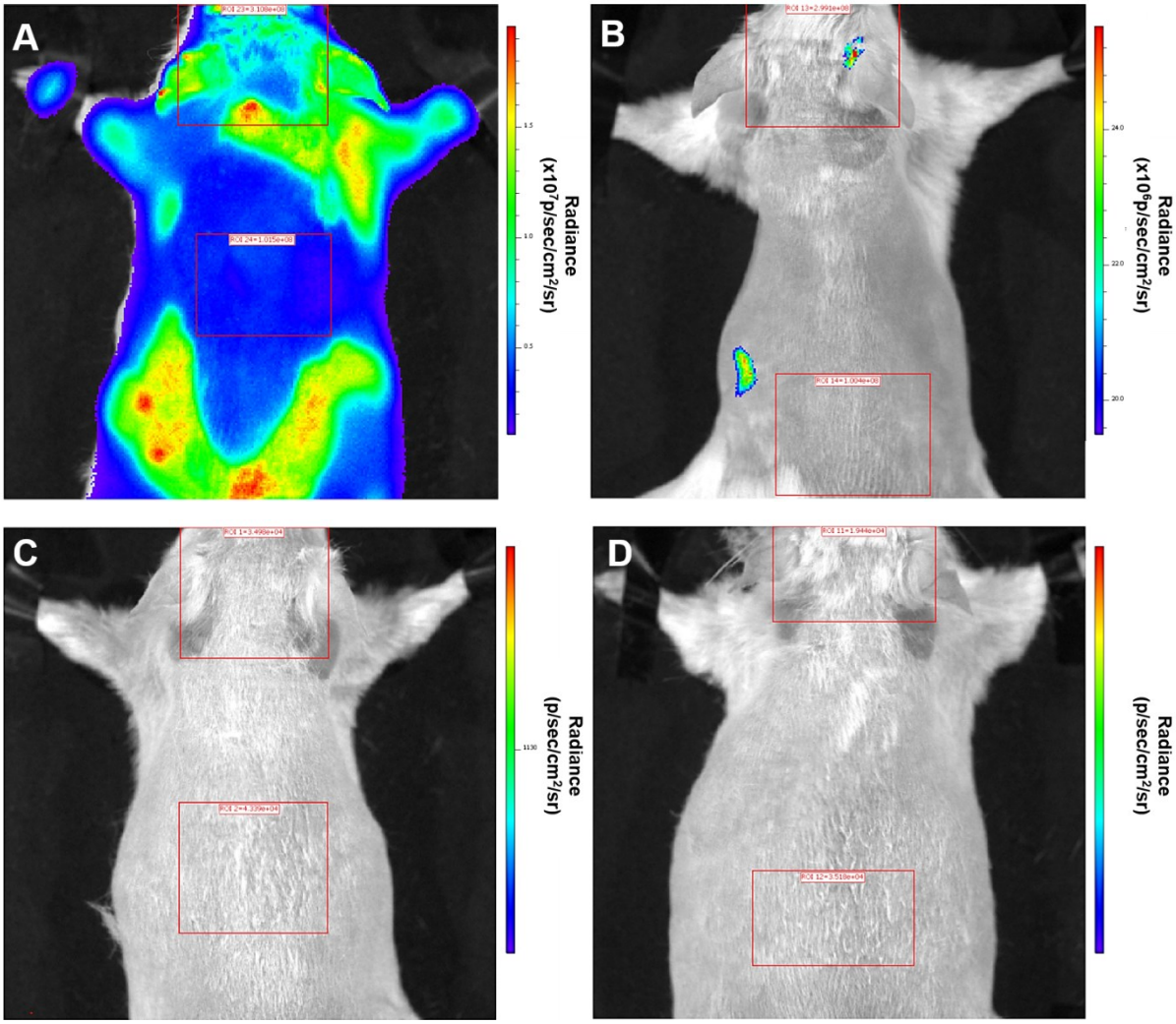

Figure 27. 2D bioluminescence images of G3b mice after s.c. injection of D-luciferin. *AGE439 and AGE443 were genotypically wildtype and all the two other mice hem. All of them had a white coat. Imaging position: prone. A: AGE442; Color Scale: Min = 1,09e6 / Max = 1,96e7. B: AGE443; Color Scale: Min = 1,95e7 / Max = 2,55e7. C: AGE439; Color Scale: Min = 1,13e4 / Max = 1,13e4. D: AGE440; Color Scale: Min = 6,43e3 / Max = 6,43e3.*

II. Analysis

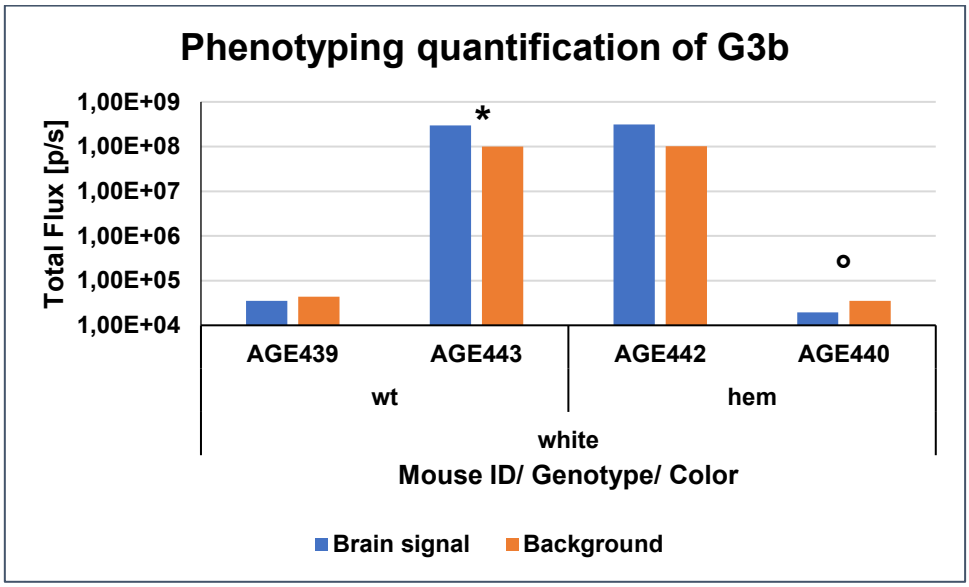

Figure 28. 2D BLI signal quantification of image of Figure 27. *AGE443 and AGE440 marked as outliers. Genotypically positive mouse AGE440 with negative phenotypic status marked with a circle (°). Genotypically negative mouse AGE443 with positive phenotypic status marked with an asterisk (*).wt = wildtype.*

III. Organ validation

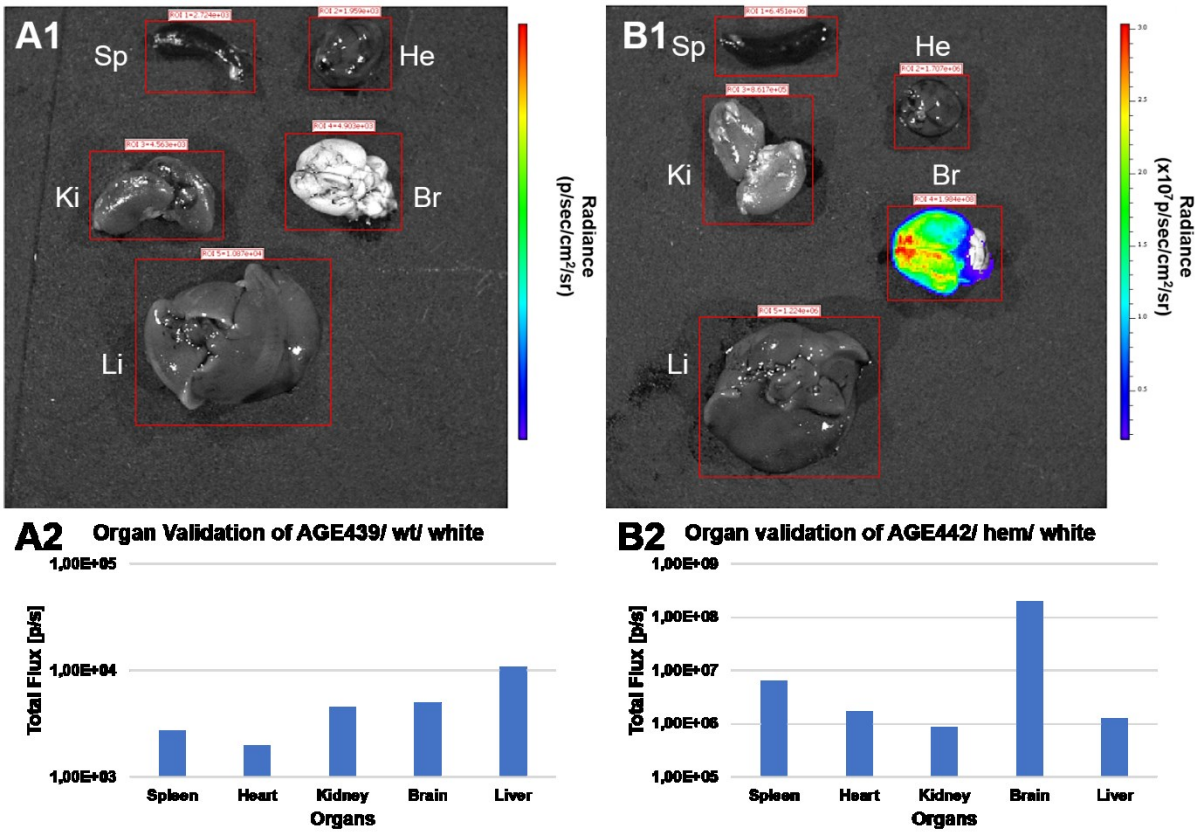

Figure 29. 2D Bioluminescence images and signal quantification of the organs of G3b mice. *A1: 2D BL images of the organs from AGE439; Color Scale: Min = 1,21e4 / Max = 1,21e4. A2: Signal quantification of organ images from A1. B1: 2D BLI of organs from AGE442; Color Scale: Min = 1,65e6 / Max = 3,04e7. B2: Signal quantification of organ images from B2. Br = Brain, He = Heart, Ki = Kidneys, Li = Liver, Sp = Spleen, wt = wildtype.*

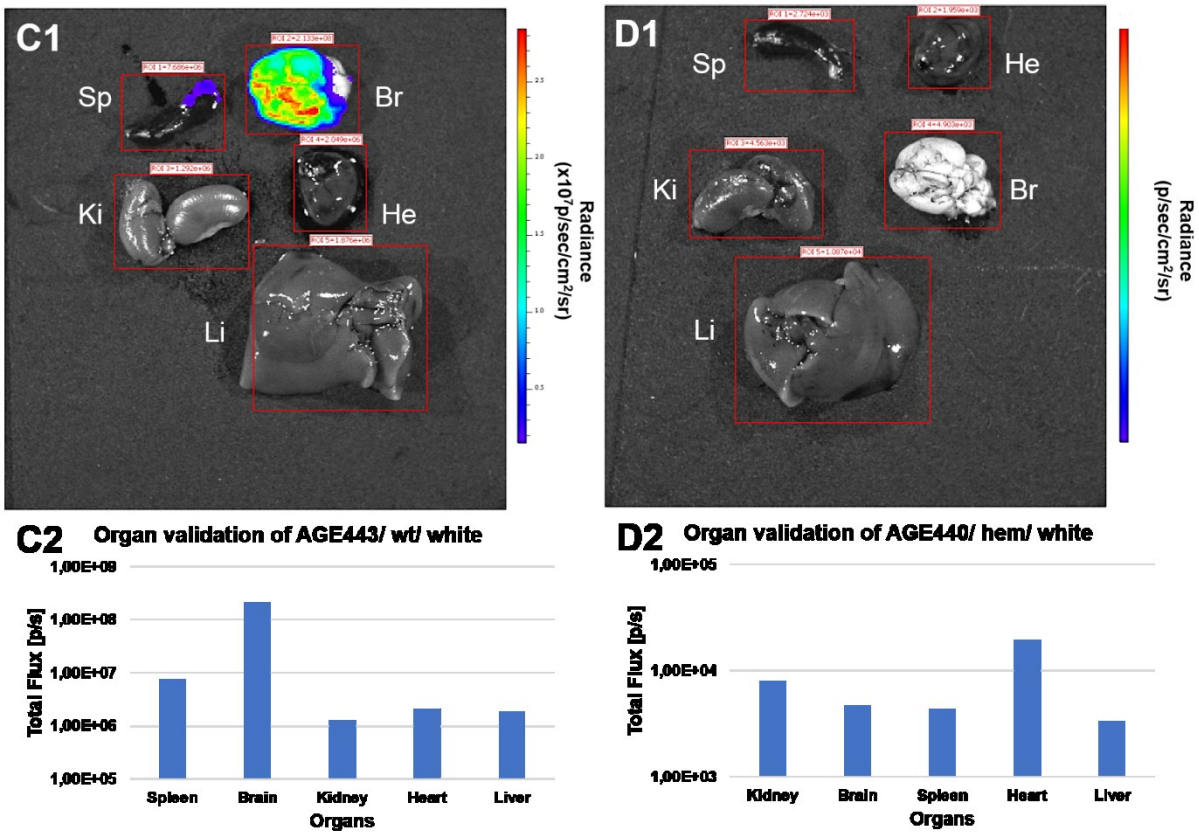

Figure 30. 2D Bioluminescence images and signal quantification of the organs of G3b mice. *C1: 2D BL images of the organs from AGE443; Color Scale: Min = 1,52e6 / Max = 2,85e. C2: Signal quantification of organ images from C1. D1: 2D BLI of organs from AGE440; Color Scale: Min = 1,21e4 / Max = 1,21e4. D2: Signal quantification of organ images from D2. Br = Brain, He = Heart, Ki = Kidneys, Li = Liver, Sp = Spleen, wt = wildtype.*

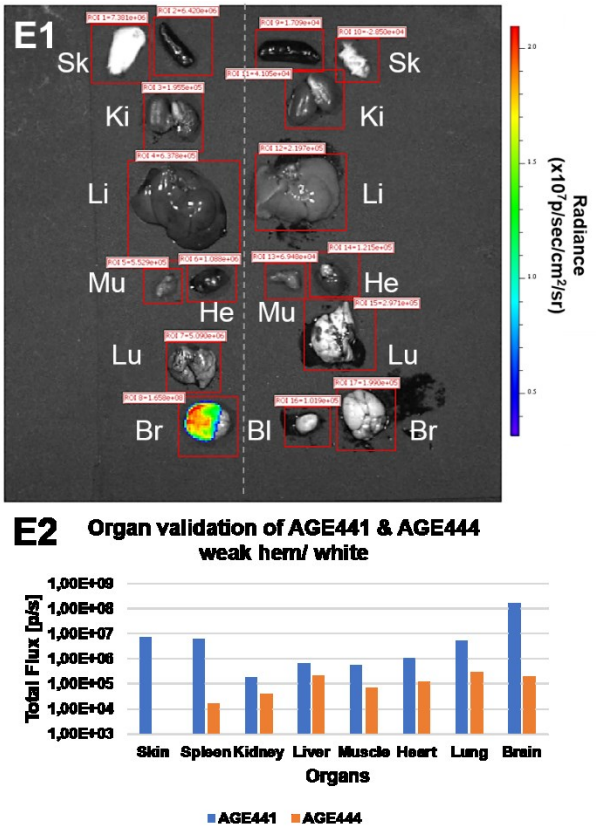

Figure 31. 2D Bioluminescence images and signal quantification of the organs of G3b mice. *E1: 2D BLI of organs from AGE441 (left) and AGE444 (right); Color Scale: Min = 3,17e6 / Max = 2,10e7. E2: Signal quantification of organ images from E2. Bl = Bladder, Br = Brain, He = Heart, Ki = Kidneys, Lu = Lung, Li = Liver, Mu = Muscle, Sk = Skin, Sp = Spleen.*

4.1.8 Generation G4a

One mouse from the generation G4a was phenotyped (Figure 32, 33) and, because of a neck injury, immediately euthanized and selected for organ imaging. This was a white wildtype mouse that, as expected, did not had a significant BLI signal (Figure 34 – A1, A2). Furthermore, two other wildtype, one weak hem, and two hem mice were taken for organ imaging. As the 2D BLI pictures and signal quantifications show (Figure 34, 35), all mice of this generation were phenotypically in agreement with their genotype.

I. 2D BLI

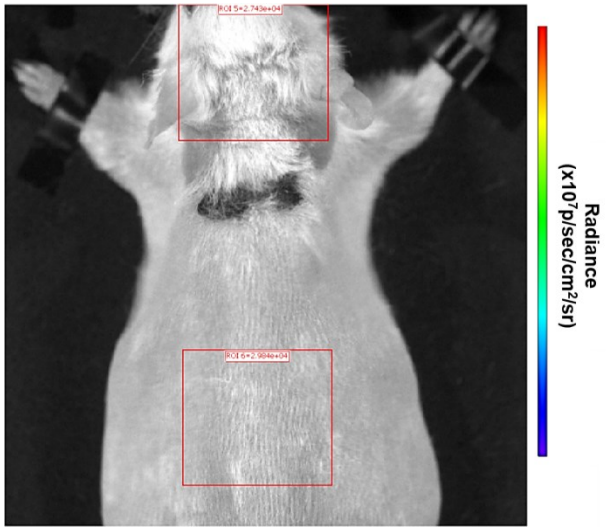

Figure 32. 2D bioluminescence image of G4a mouse AGE453 after s.c. injection of D-luciferin. *AGE453 was genotypically wildtype and had a white coat. Imaging position: prone; Color Scale: Min = 8,52e3 / Max = 8,52e3.*

II. Analysis

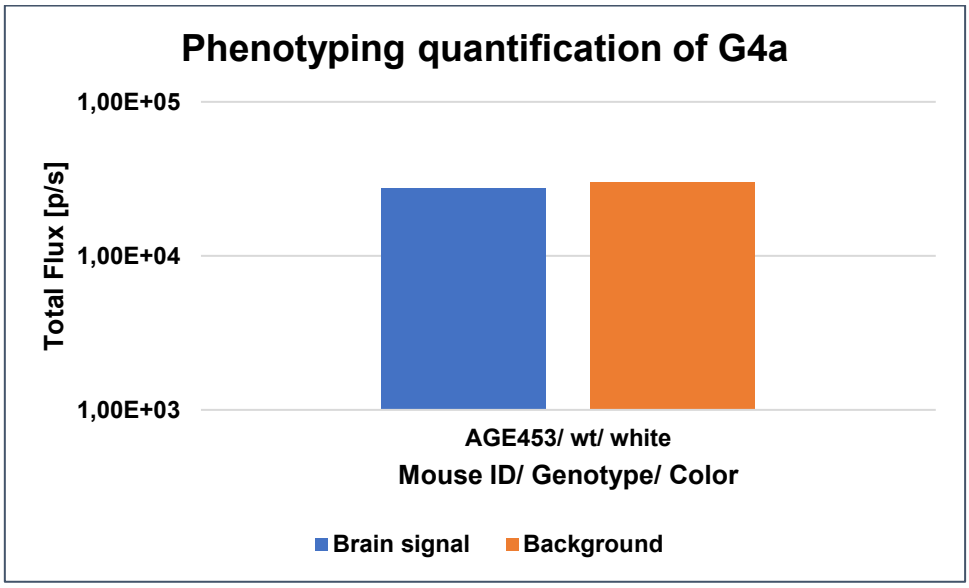

Figure 33. 2D BLI signal quantification of image of Figure 32. *wt = wildtype.*

III. Organ validation

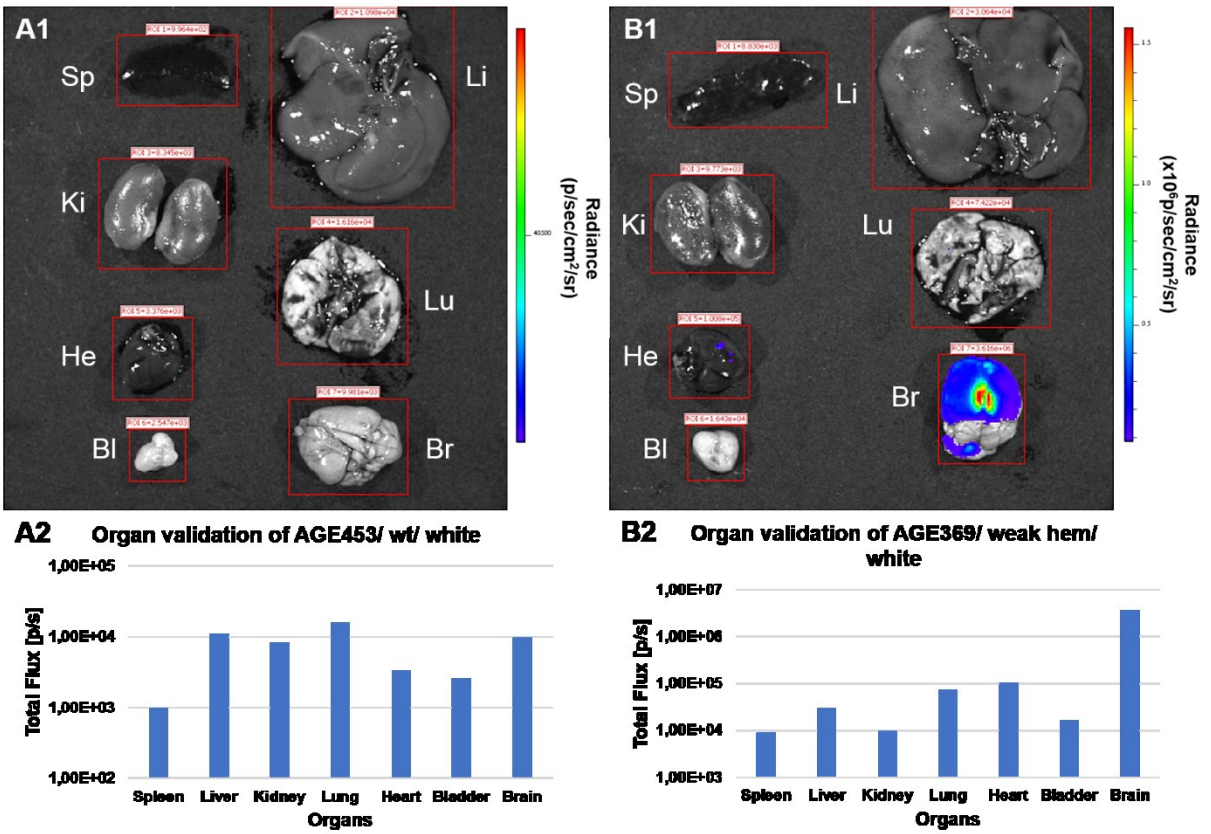

Figure 34. 2D Bioluminescence images and signal quantification of the organs of G4a mice. *A1: 2D BL images of the organs from AGE453; Color Scale: Min = 4,05e4 / Max = 4,05e4. A2: Signal quantification of organ images from A1. B1: 2D BLI of organs from AGE369; Color Scale: Min = 8,67e4 / Max = 1,56e6. B2: Signal quantification of organ images from B2. Bl = Bladder, Br = Brain, He = Heart, Ki = Kidneys, Lu = Lung, Li = Liver, Sp = Spleen, wt = wildtype.*

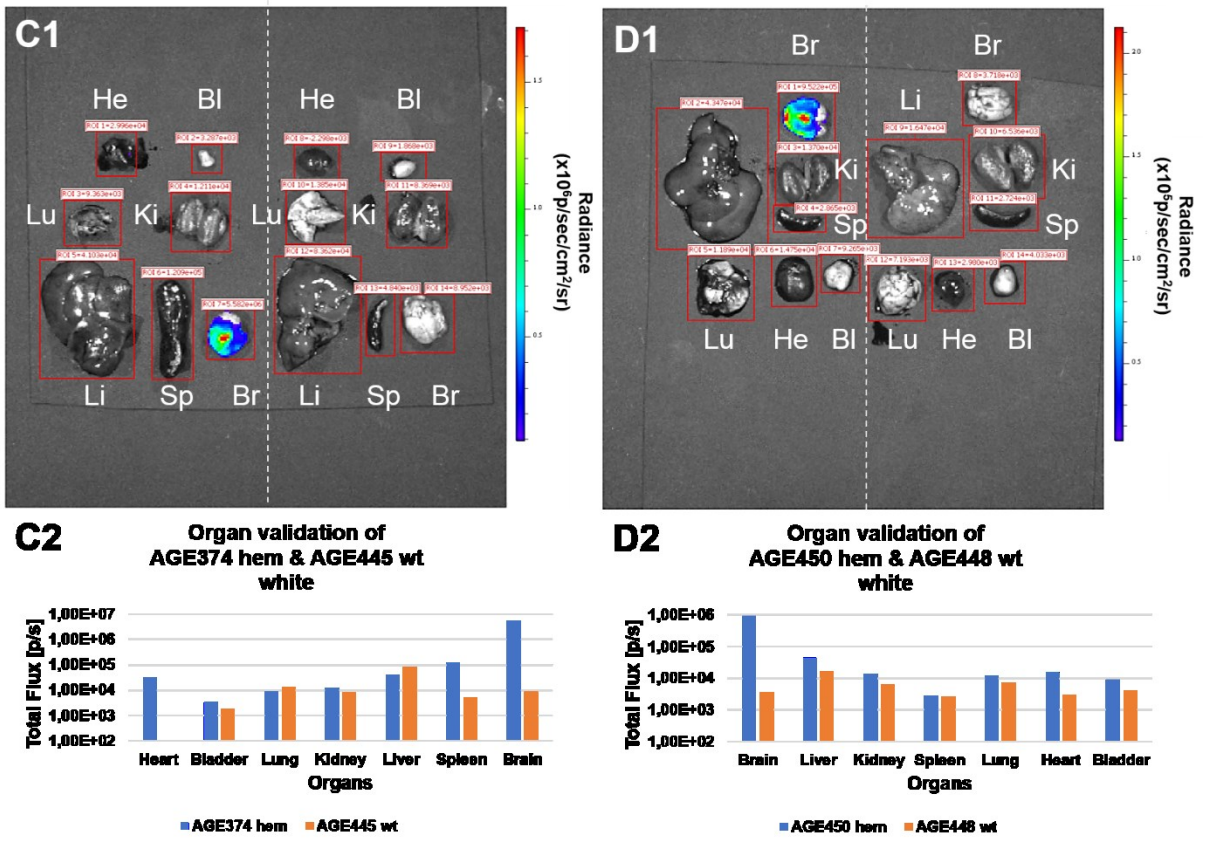

Figure 35. 2D Bioluminescence images and signal quantification of the organs of G4a mice. *C1: 2D BL images of the organs from AGE374 (left) and AGE445 (right); Color Scale: Min = 9,43e4 / Max = 1,72e6. C2: Signal quantification of organ images from C1. D1: 2D BLI of organs from AGE450 (left) and AGE448 (right); Color Scale: Min = 1,28e4 / Max = 2,13e5. D2: Signal quantification of organ images from D2. Bl = Bladder, Br = Brain, He = Heart, Ki = Kidneys, Lu = Lung, Li = Liver, Sp = Spleen, wt = wildtype.*

4.1.9 Generation G5a

No phenotyping of generation G5a was carried out.

One white wildtype mouse of this was chosen for organ validation. As expected, no significant signal in brain or the other organs was found (Figure 36).

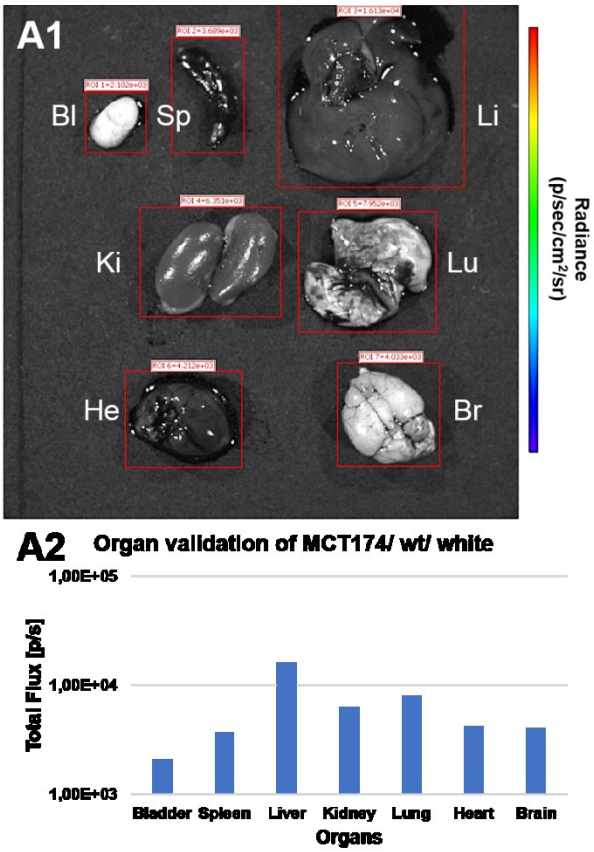

Figure 36. 2D Bioluminescence image and signal quantification of the organs of one G5a mouse. *A1: 2D BL images of the organs from MCT174; Color Scale: Min = 5,36e3 / Max = 5,36e3. A2: Signal quantification of organ images from A1. Bl = Bladder, Br = Brain, He = Heart, Ki = Kidneys, Lu = Lung, Li = Liver, Sp = Spleen, wt = wildtype.*

4.1.10 Summary of all Tg Thy 1.2-Luc results

In Figure 37 a summary of the phenotyping results of all 29 Tg Thy 1.2-Luc mice is shown. 20 out of 24 genotypically positive mice had a BLI signal in brain and 2 out of 5 wildtype mice had no significant brain signals as expected. So in summary the phenotype of 22 out of 29 mice matched with their genotypic status.

The 4 hem mice AGE256, AGE265, AGE293 and AGE440 showed no significant BLI signal in the brain region and were marked with a circle as outliers.

The 3 wildtype mice AGE266, AGE261 and AGE443 had high brain signals and were declared as phenotypically positive, which therefore did not match with their genotype and were labeled as outliers with an asterisk.

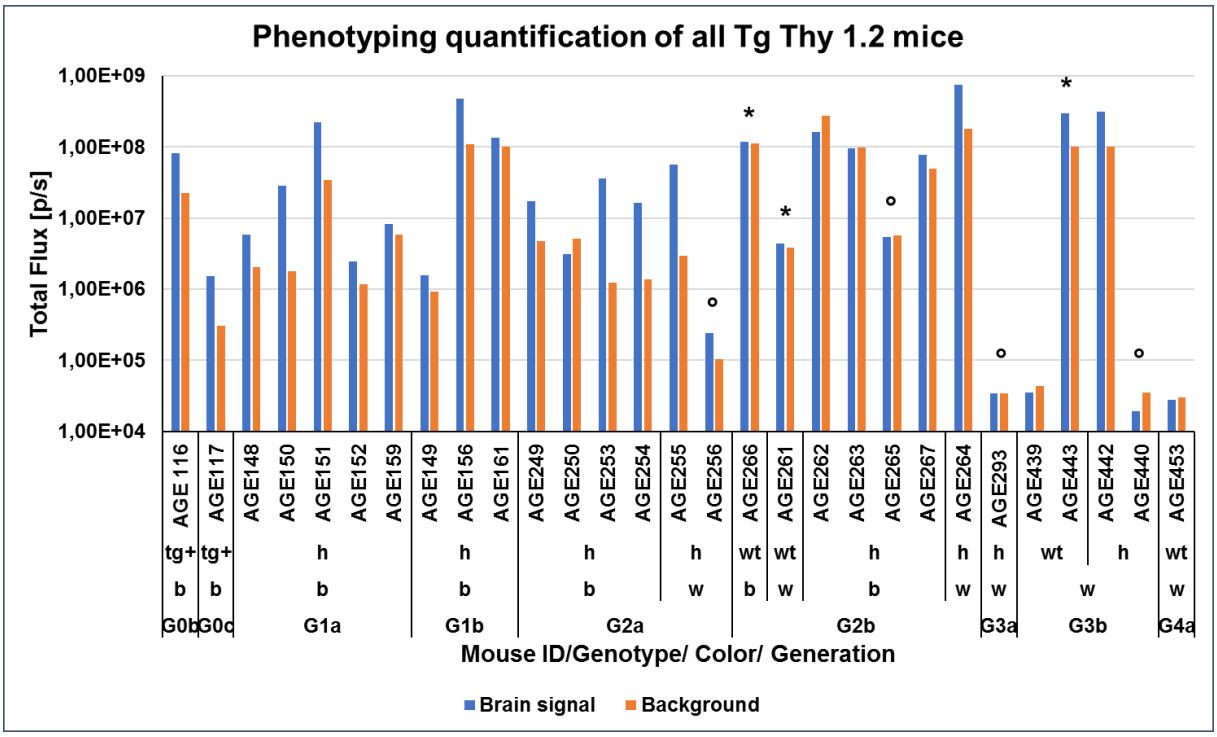

Figure 37. Signal quantification results of all imaged Tg Thy 1.2-Luc mice. *Genotypically positive mice with negative phenotypic status marked with a circle (°). Genotypically negative mice with positive phenotypic status marked with an asterisk (*). h = hem, wt = wildtype, b = black, w = white.*

In Figure 38 and 39 the organ imaging results of all 22 Tg Thy 1.2-Luc mice are presented graphically. 15 out of 19 mice genotypically positive mice had a visible BLI signal in brain and one two of three wildtype mice had no significant brain signals as expected. So, in summary the genotypic status of 17 mice was approved by organ imaging.

The 4 hem mice AGE263, AGE265, AGE293 and AGE440 showed no significant visible BLI signals wheras the wildtype mouse AGE443 a brain signal had. These mice were marked in Figure 38 as outliers.

Therefore, the rather unexpected phenotypic results of the 4 mice AGE293, AGE265, AGE440 and AGE443 was confirmed by organ imaging (Figure 37, 38).

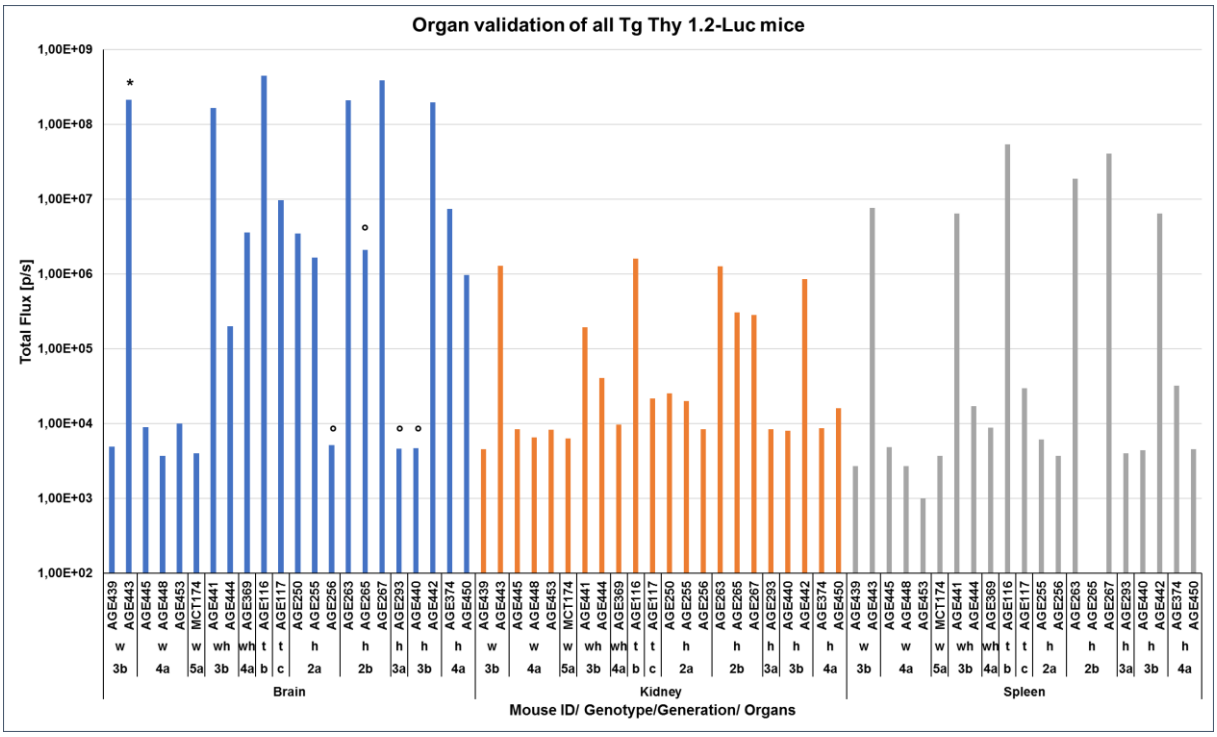

Figure 38. Signal quantification results of all organ images of Tg Thy 1.2-Luc mice Part 1. *Genotypically positive mice with negative phenotypic status marked with a circle (°) above brain signal. Genotypically negative mice with positive phenotypic status marked with an asterisk (*) above brain signal. w = wildtype, wh = weak hem, t = tg+, h = hem, 0b = G0b, 0c = G0c, 2a= G2a, 2b = G2b, 3a = G3a, 3b = G3b, 4a = G4a, 5a = G5a.*

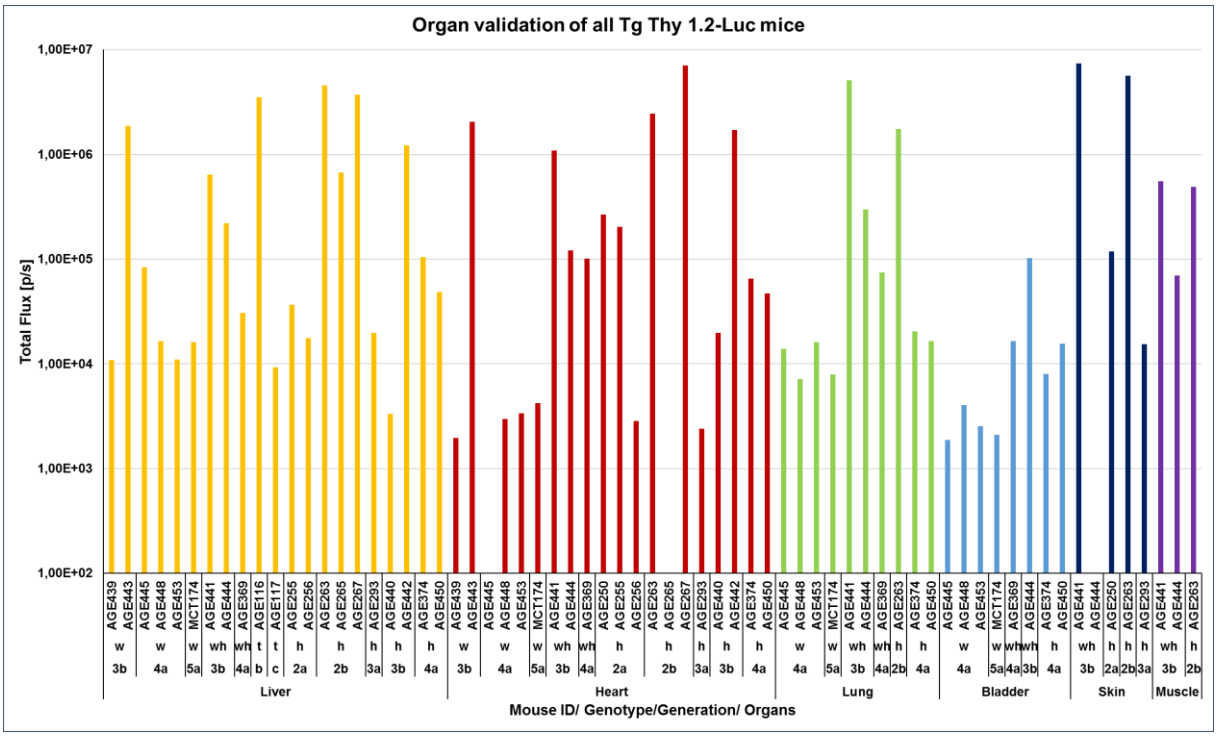

Figure 39. Signal quantification results of all organ images of Tg Thy 1.2-Luc mice Part 2. *w = wildtype, wh = weak hem, t = tg+, h = hem, 0b = G0b, 0c = G0c, 2a= G2a, 2b = G2b, 3a = G3a, 3b = G3b, 4a = G4a, 5a = G5a.*

Phenotyping result summary of Tg Thy 1.2-Luc mice				
	Mouse IDs	**Genotype**	**Generation**	**Color**
Mice with signals as expected as per genotype	AGE116	tg +	G0b	black
	AGE117	tg +	G0c	black
	AGE148 AGE150 AGE151 AGE152 AGE159	hem	G1a	black
	AGE149 AGE156 AGE161	hem	G1b	black
	AGE249 AGE253 AGE250 AGE254	hem	G2a	black
	AGE255	hem	G2a	white
	AGE262 AGE263 AGE267	hem	G2b	black
	AGE264	hem	G2b	white
	AGE439 AGE443	wildtype	G3b	white
	AGE442	hem	G3b	
	AGE453	wildtype	G4a	white
Outlier hem mice with low signals	AGE256	hem	G2a	white
	AGE265	hem	G2b	black
	AGE293	hem	G3a	white
	AGE440	hem	G3b	white
Outlier wildtype mice with high signals	AGE266	wildtype	G2b	black
	AGE261	wildtype	G2a	white

Table 10. Phenotyping result summary of Tg Thy 1.2-Luc mice.

Organ validation result summary of Tg Thy 1.2-Luc mice				
	Mouse IDs	**Genotype**	**Generation**	**Color**
Mice with signals as expected as per genotype	AGE116	tg+	G0b	black
	AGE117	tg+	G0c	black
	AGE250	hem	G2a	black
	AGE255	hem	G2a	white
	AGE263 AGE267	hem	G2b	black
	AGE293	hem	G3a	white
	AGE439	wildtype	G3b	white
	AGE441 AGE444	weak hem	G3b	white
	AGE445 AGE448 AGE453	wildtype	G4a	white
	AGE369	weak hem	G4a	white
	AGE374 AGE450	hem	G4a	white
	MCT174	wildtype	G5a	white
Outlier hem mice with low signals	AGE256	hem	G2a	white
	AGE265	hem	G2b	black
	AGE440 AGE442	hem	G3b	white
Outlier wildtype mice with high signals	AGE443	wildtype	G3b	white

Table 11. Organ validation result summary of Tg Thy 1.2-Luc mice.

4.2 Phenotyping and organ validation results of Tg SpC-Luc

For phenotyping of Tg SpC-Luc mice one to three animals were taken per imaging session. The anesthetized mice were placed in supine position in the imaging chamber and the 2D BLI pictures were acquired right after subcutaneous injection of D-luciferin in the right abdominal side. The picture with the highest bioluminescence signal of each session was selected for the analysis. By using the Living Image software one ROI was applied over the lung region and a second one over the whole body, because it was found out that the skin also expresses the luciferase enzyme. Mo et al. [40] reported the expression of surfactant proteins, like SpC, in human skin, which would also explain the BLI signal in the skin of the animals of this study. Mice of the generations G1 and G2 with whole body ROIs that provided values of over log 6 in the signal quantification were assessed as phenotypically positive and the values below log 6 were evaluated with a negative phenotype. For the generations G2a, G3 and G4 mice with whole body values over log 8 were determined as phenotypically positive and below as negative. Higher limits were used for these three generations as it seemed that in the signal quantification results the very high values of the phenotypically positive mice covered the low values of the wildtype animals.

The phenotyping data includes wildtype, weak hem and hem mice of the generations G1, G2, G2a, G3 and G4 (Table 6).

For validation by organ imaging nine mice were sacrificed by cervical dislocation 20 minutes after subcutaneous injection of D-Luciferin. After euthanasia lung, skin and different other organs such as spleen, heart, kidney and liver were directly removed and imaged. Also here ROIs were placed around each organ and were quantified. To determine a positive phenotype, a visibly detected BLI signal of the skin and after its removal and reimaging a signal of the lung in the organ images was expected. For this experiments wildtype, weak hem and hem mice from generation G2, G2a and G3 were used (Table 7).

4.2.1 Generation G1

Two hem Tg SpC-Luc mice with black coat were imaged by 2D BLI. Both show in Figure 40 a significant BLI signal over the whole body. The signal quantification of Figure 41 shows values over log 8 over the lung region and over log 9 over the whole

body. These two results confirm that both mice are phenotypically positive. No organ validation was carried out.

I. 2D BLI

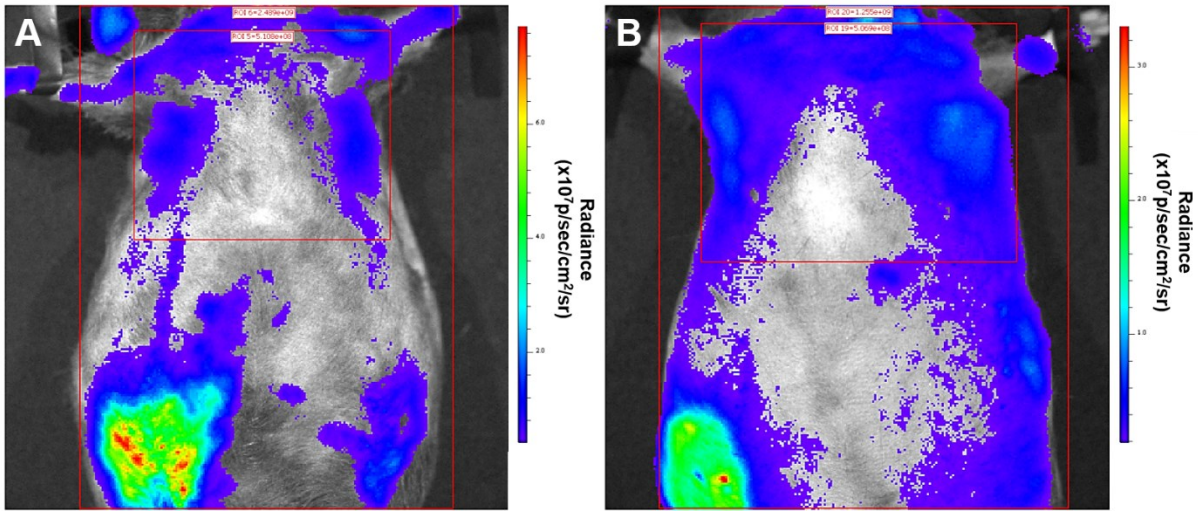

Figure 40. 2D bioluminescence images of G1 mice after s.c. injection of D-luciferin. *Both were genotypically hem and had a black coat. Imaging position: supine. A: AGE312; Color Scale: Min = 4,16e6 / Max = 7,74e7. B: AGE316; Color Scale: Min = 1,93e6 / Max = 3,35e7.*

II. Analysis

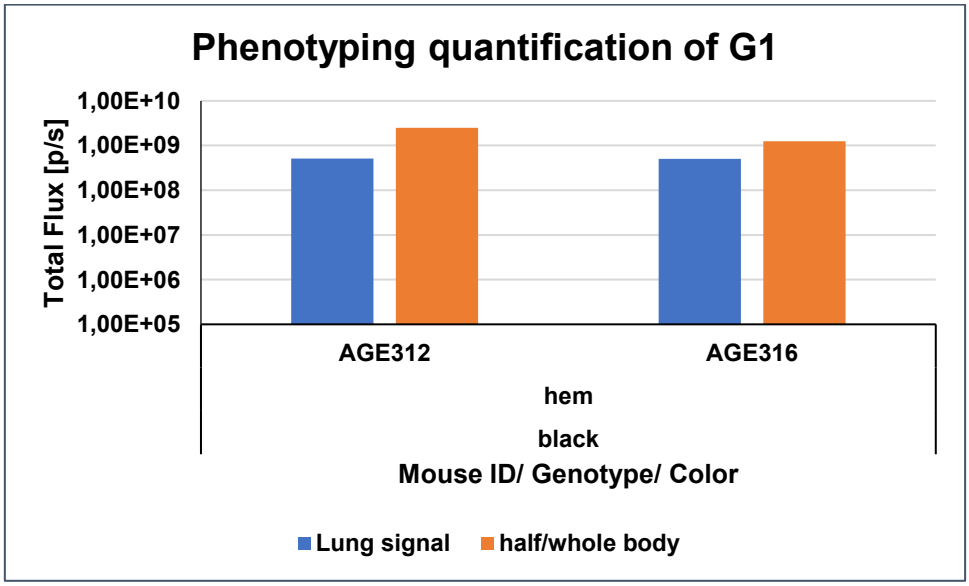

Figure 41. 2D BLI signal quantification of image of Figure 40.

4.2.2 Generation G2

The phenotype was determined for 17 mice of generation G2. Nine mice were genotypically weak hem, eight of them had a black and one a white fur. The eight other G2 animals were genotypically weak hem, of which three had a black and five a white coat. All three mice of Figure 42 - E showed no significant BLI signal and were therefore considered as phenotypically negative, which therefore does not agree with their specific genotype. Another mouse that was classified phenotypically negative was AGE342 (M8) from Figure 42 - C. The assumption why these four mice showed a negative signal was that possibly the black coat attenuates the signal. Therefore, two of these animals were also used for organ validation, but again, the quantification of organs showed no significant values, confirming the negative phenotypes (Figure 44).

The signal quantification of Figure 43 showed that the rest of the 17 mice had all high values lying between log 6 and log 9 and were therefore determined as phenotypically positive. Many of them also showed a strong visible signal in the BLI pictures (Figure 42), which extends over the entire body.

I. 2D BLI

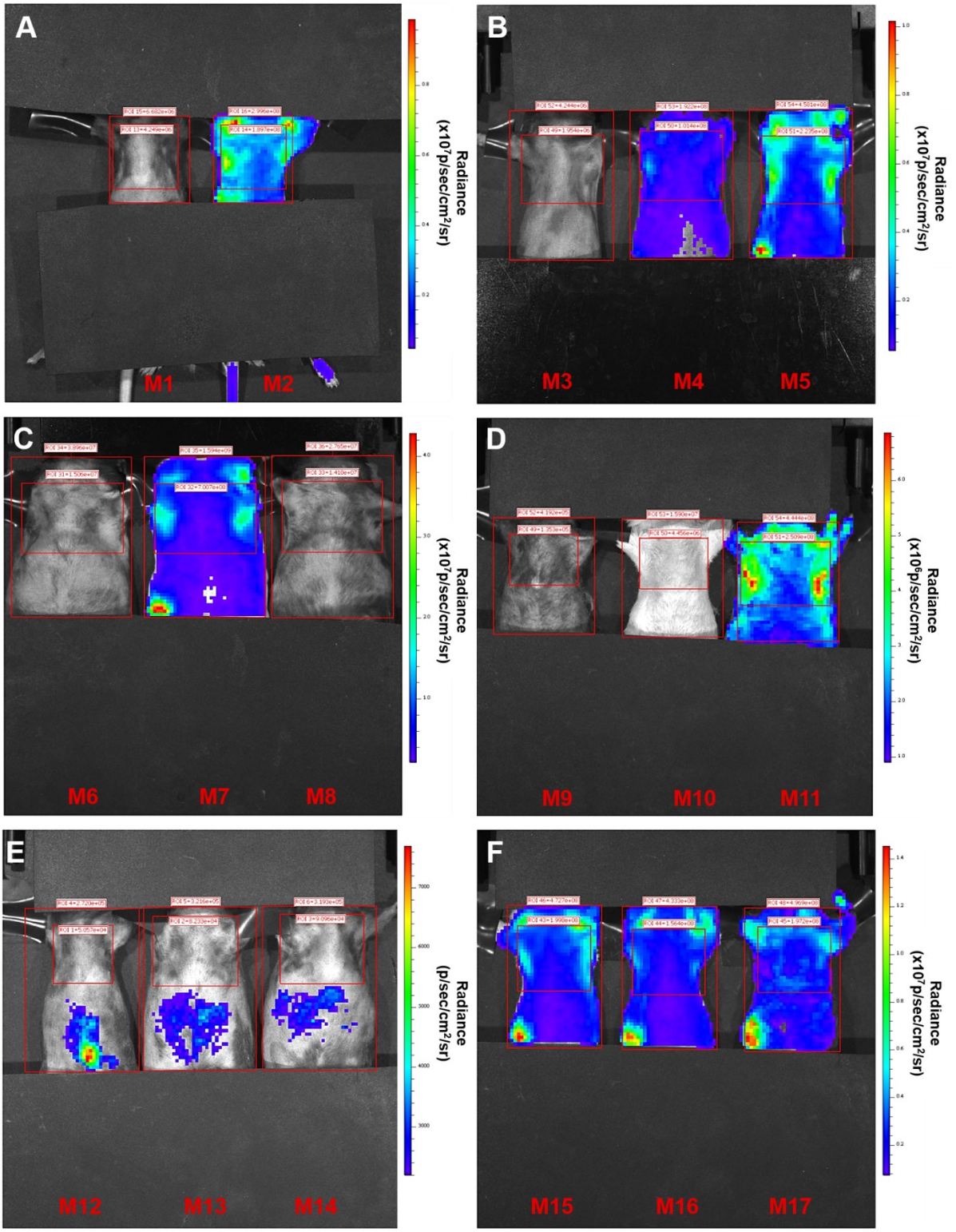

Figure 42. 2D bioluminescence images of G2 mice after s.c. injection of D-luciferin. *Eight weak hem mice had a black coat and one a white coat. Three hem mice had a black coat and five a white coat. Imaging position: supine. A: M1 = AGE348, M2 = AGE347; Color Scale: Min = 5,05e5 / Max = 9,90e6. B: M3 = AGE359, M4 = AGE350, M5 = AGE346; Color Scale: Min = 5,57e5 / Max = 1,02e7. C: M6 = AGE343, M7 = AGE345, M8 = AGE342; Color Scale: Min = 2,17e6 / Max = 4,29e7. D: M9 = AGE357, M10 = AGE355, M11 = AGE344; Color Scale: Min = 9,09e5 / Max = 6,87e6. E: M12 = AGE362, M13 = AGE363, M14 = AGE364; Color Scale: Min = 2,20e3 / Max = 7,70e3. F: M15 = AGE361, M16 = AGE360, M17 = AGE359; Color Scale: Min = 7,55e5 / Max = 1,46e7.*

II. Analysis

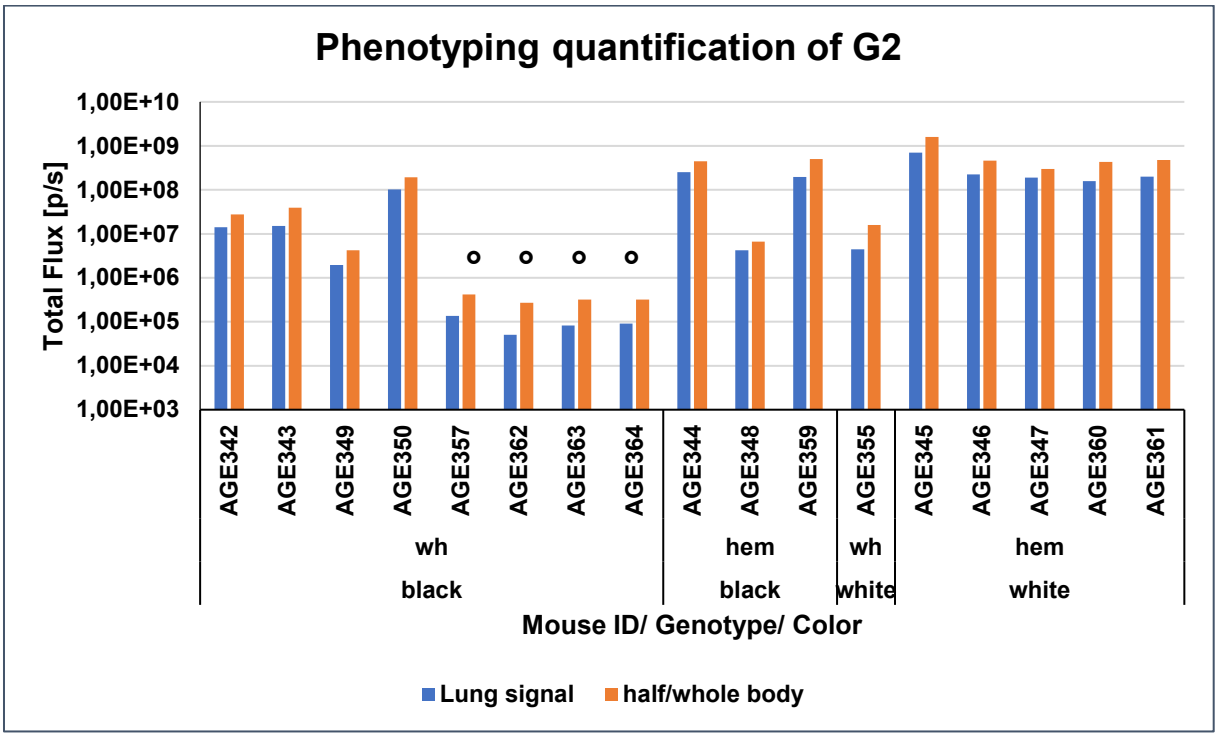

Figure 43. 2D BLI signal quantification of image of Figure 42. *Genotypically positive mice AGE357, AGE362, AGE363 and AGE364 with negative phenotypic status marked with a circle (°) marked as outliers. wh = weak hem.*

III. Organ validation

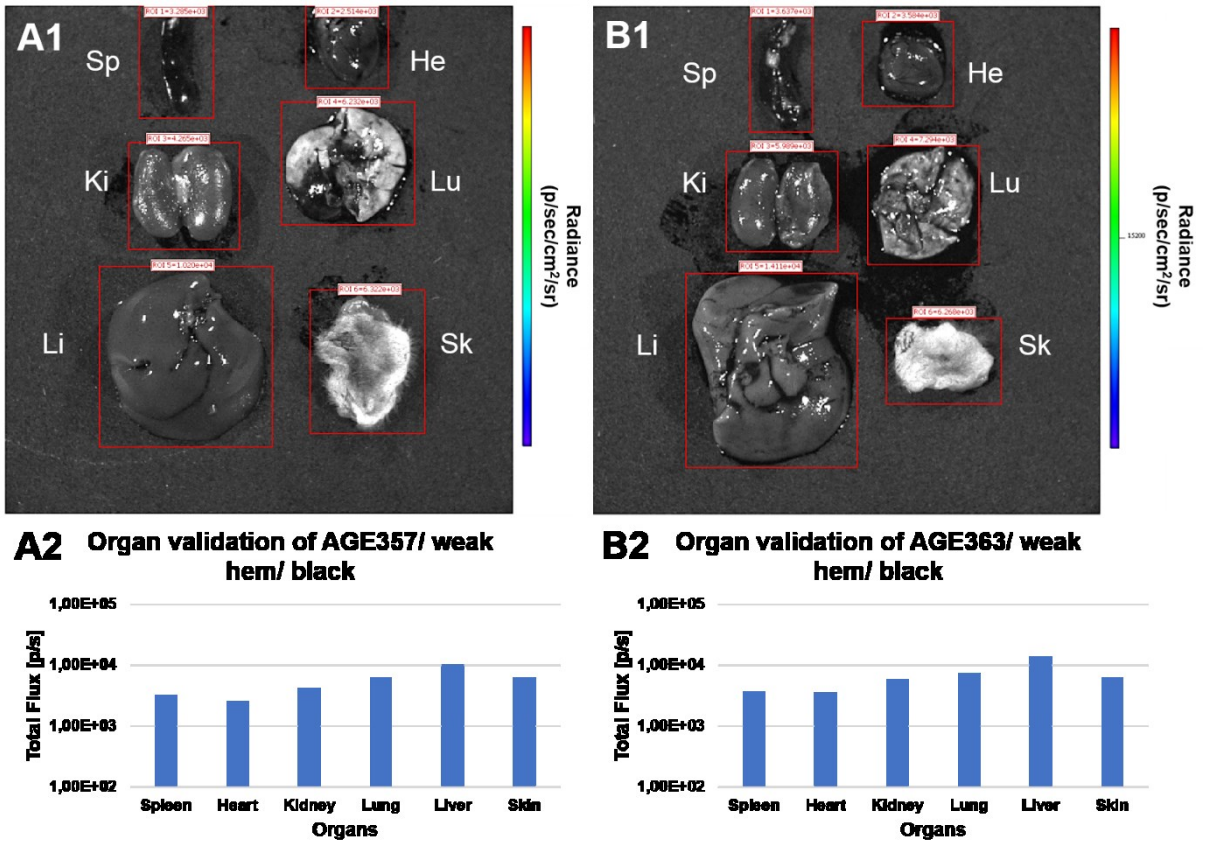

Figure 44. 2D Bioluminescence images and signal quantification of the organs of G2 mice. *A1: 2D BL images of the organs from AGE357; Color Scale: Min = 7,04e3 / Max = 7,04e3. A2: Signal quantification of organ images from A1. B1: 2D BLI of organs from AGE363; Color Scale: Min = 1,52e4 / Max = 1,52e4. B2: Signal quantification of organ images from B2. He = Heart, Ki = Kidneys, Li = Liver, Lu = Lung, Sk = Skin, Sp = Spleen.*

4.2.3 Generation G2a

One weak hem and one wildtype mouse from the G2a generation, which had a black coat, were imaged and phenotyped. A strong light signal over the whole body of the mouse M1 was detected (Figure 45 – A), which was also confirmed with a value of over log 9 in the signal quantification (Figure 46). The wildtype mouse M2 showed no detectable light signal in the image (Figure 45 – B) and the quantification yields a 2 log lower value compared to the weak hem mouse and was therefore determined as phenotypically negative (Figure 46).

One black hem mouse from generation G2a was sacrificed for validation of the genotype by organ imaging. In Figure 47 – A1 a strong signal in lung and skin is visible. Since it was recognized that the skin covers the signal of the lung, another image was

taken after removal of the skin. In the image afterwards (Figure 47 – A2), the signal of the lung increased minimally as the quantification showed (Figure 47 – A3).

I. 2D BLI

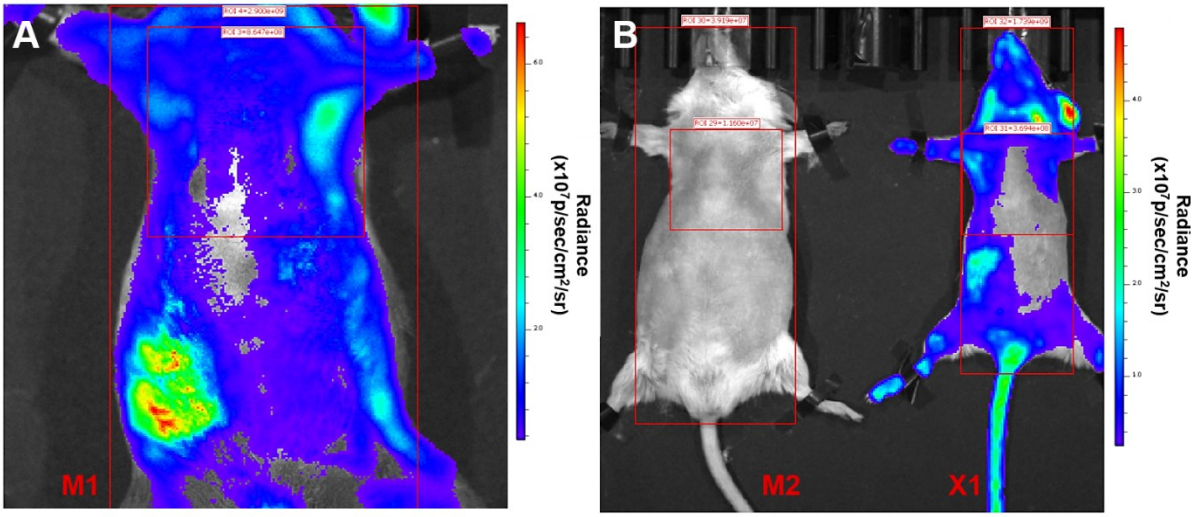

Figure 45. 2D bioluminescence images of two G2a mice after s.c. injection of D-luciferin. *M1 was weak hem and M2 was wildtype. Both mice had a black coat. Imaging position: supine. A: M1 = AGE416; Color Scale: Min = 3,45e6 / Max = 6,63e7. B: M2 = AGE413, X1 = G4 mouse; Color Scale: Min = 2,48e6 / Max = 4,80e7.*

II. Analysis

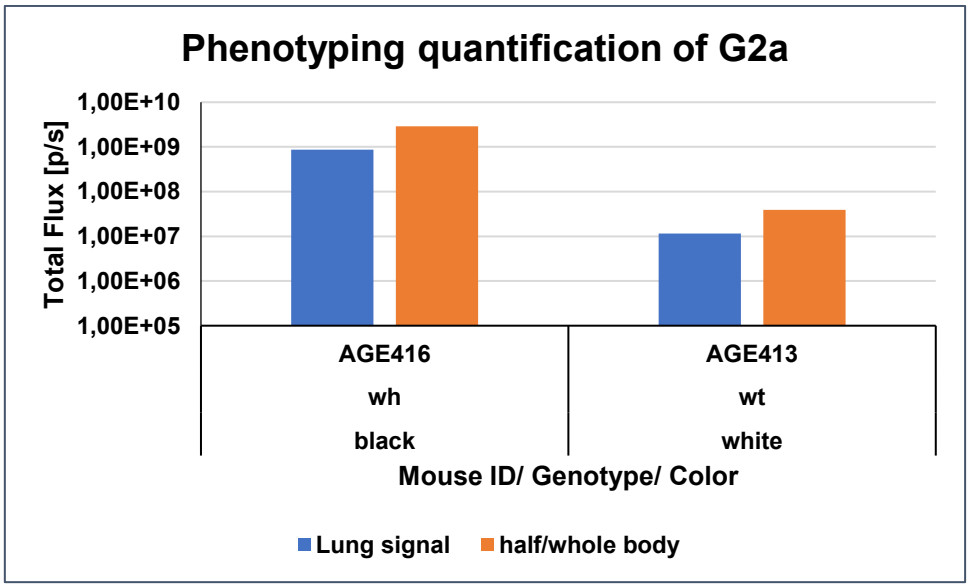

Figure 46. 2D BLI signal quantification of image of Figure 45. *wh = weak hem, wt = wildtype.*

III. Organ validation

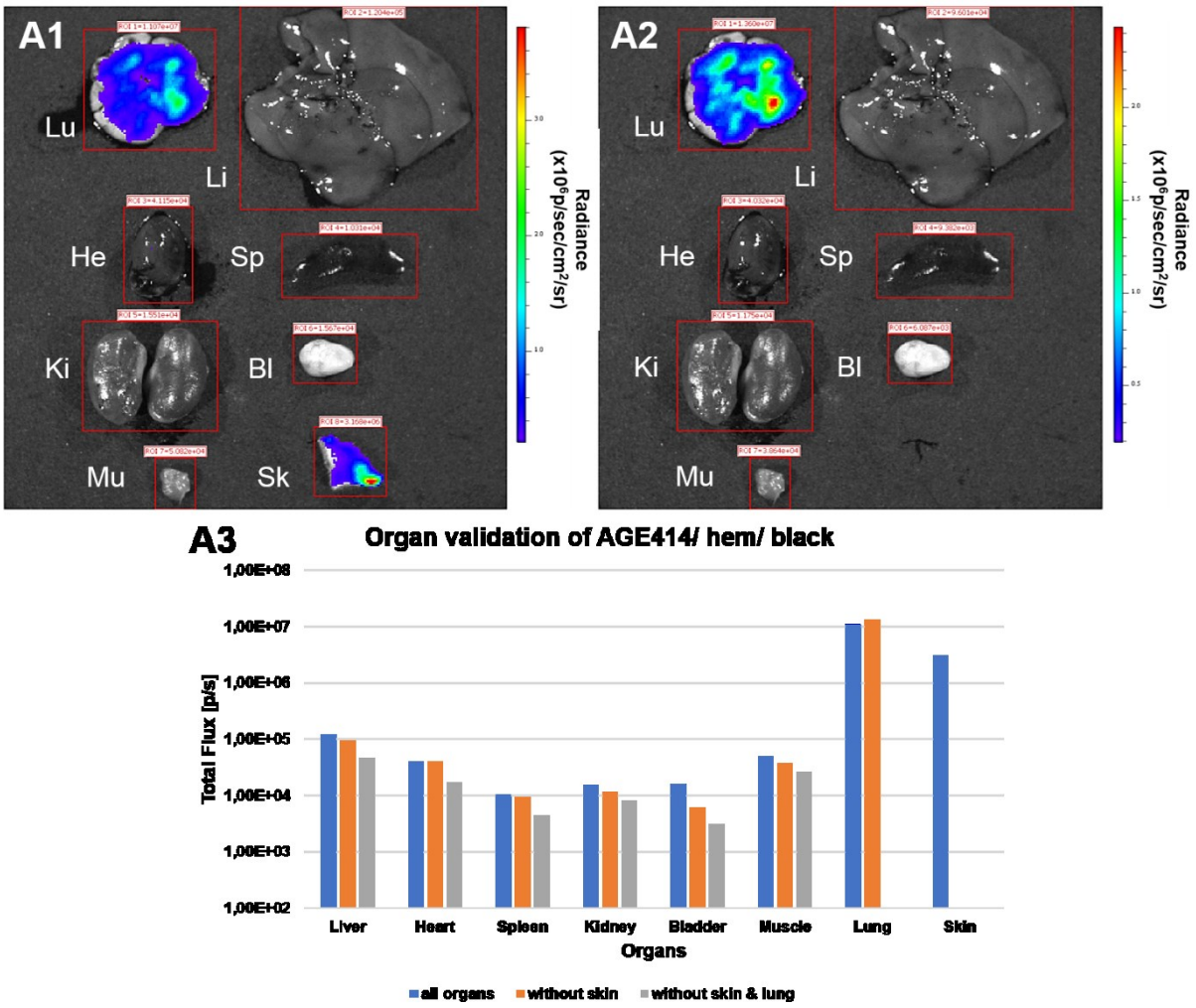

Figure 47. 2D Bioluminescence images and signal quantification of the organs of the G2a mouse AGE414*. A1: 2D BL images of the organs; Color Scale: Min = 2,16e5 / Max = 3,81e6. A2: 2D BL images of the organs without skin; Color Scale: Min = 1,96e5 / Max = 2,44e6. A3: Signal quantification of organ images. Bl = Bladder, He = Heart, Ki = Kidneys, Li = Liver, Lu = Lung, Mu = Muscle, Sk = Skin, Sp = Spleen.*

4.2.4 Generation G3

Twelve mice of generation G3 were imaged. One mouse of them was hem, two mice were weak hem and the remaining wildtypes. The weak hem mouse M9 had a black coat and the rest a white coat.

The two hem mice MCT236 (M1) and MCT239 (M4), as well as the weak hem mouse MCT241 (M9), showed a visible light signal over the entire body (Figure 48, 49), which is also confirmed in the signal quantification with a value over log 8 (Figure 50). The two wildtype mice MCT238 (M3) and AGE476 (M7) from Figure 48 showed comparable

signals and were therefore also assessed as phenotypically positive, which did not agree with their genotype. In the images from Figure 48 and 49, the remaining wildtype mice did not show any visible BLI signal. Their signal quantification values were below log 8 and were determined as phenotypically negative (Figure 50).

Furthermore, three wildtype mice were selected for organ imaging. In Figure 47 and 48 is shown that none of these mice had a significant signal and were determined as phenotypically negative.

As shown in Figure 53, 54 and 55 three weak hem mice were taken additionally for organ imaging. In all three figures a significant signal was detected in the skin (Figure 53 – D1, Figure 54 – E1, Figure 55 – F1). After removing skin another image was acquired and a strong signal in the lung was visible (Figure 53 – D2, Figure 54 – E2, Figure 55 – F2). The signal quantifications (Figure 53 – D3, Figure 54 – E3, Figure 55 – F3) confirmed that the skin of each mouse had the highest value and showed that after removing of that organ the lung signal increased minimally.

I. 2D BLI

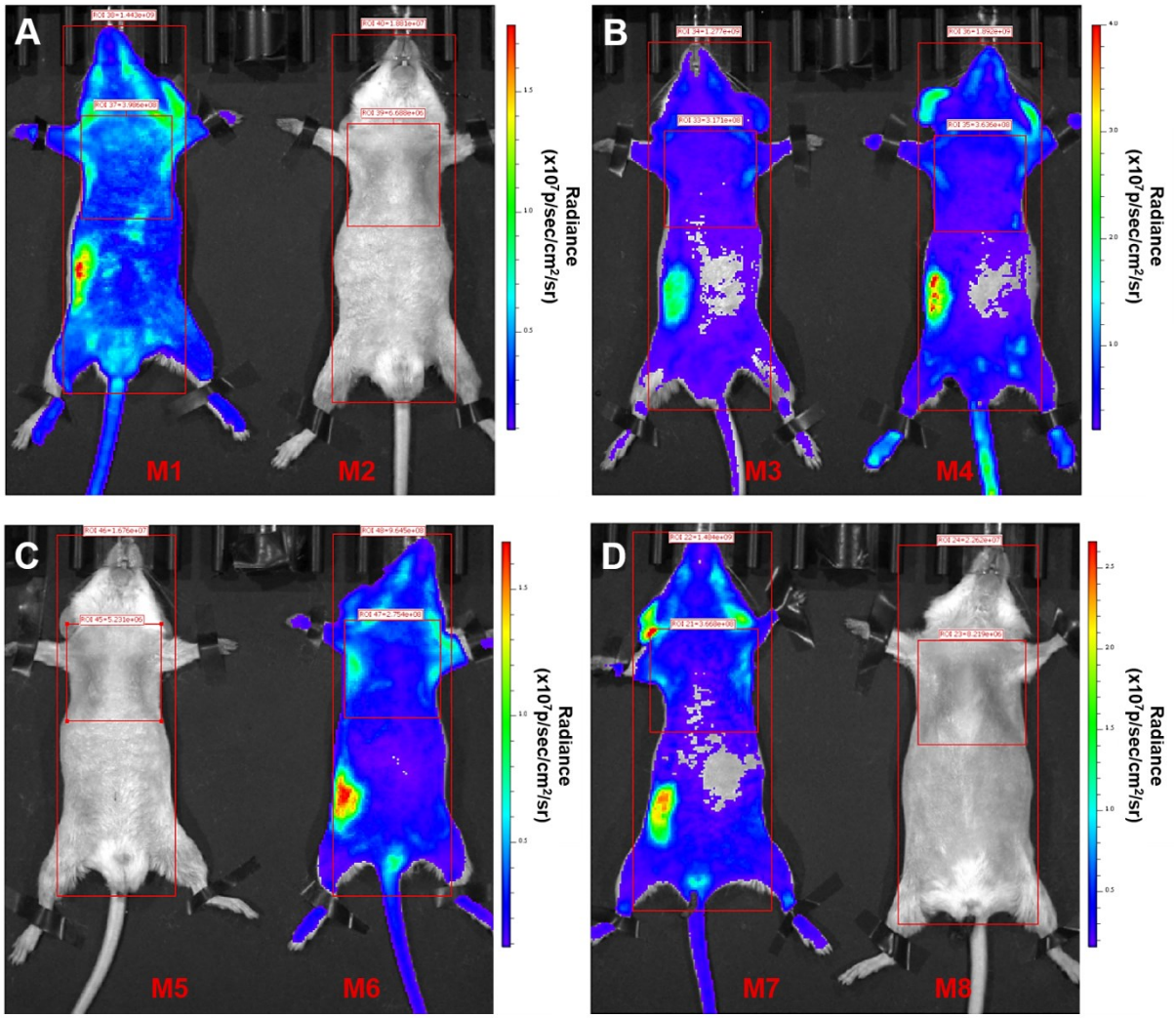

Figure 48. 2D bioluminescence images of G3 mice after s.c. injection of D-luciferin. *M1 was hem, M4 was weak hem and all the others were wildtype. All mice had a white coat. Imaging position: supine. A: M1= MCT236, M2 = MCT237; Color Scale: Min = 9,33e5 / Max = 1,78e7. B: M3 = MCT238, M4 = MCT239; Color Scale: Min = 2,17e6 / Max = 4,00e7. C: M5 = MCT240, M6 = MCT242; Color Scale: Min = 8,70e5 / Max = 1,69e7. D: M7 = AGE476, M8 = AGE477; Color Scale: Min = 1,59e6 / Max = 2,67e7.*

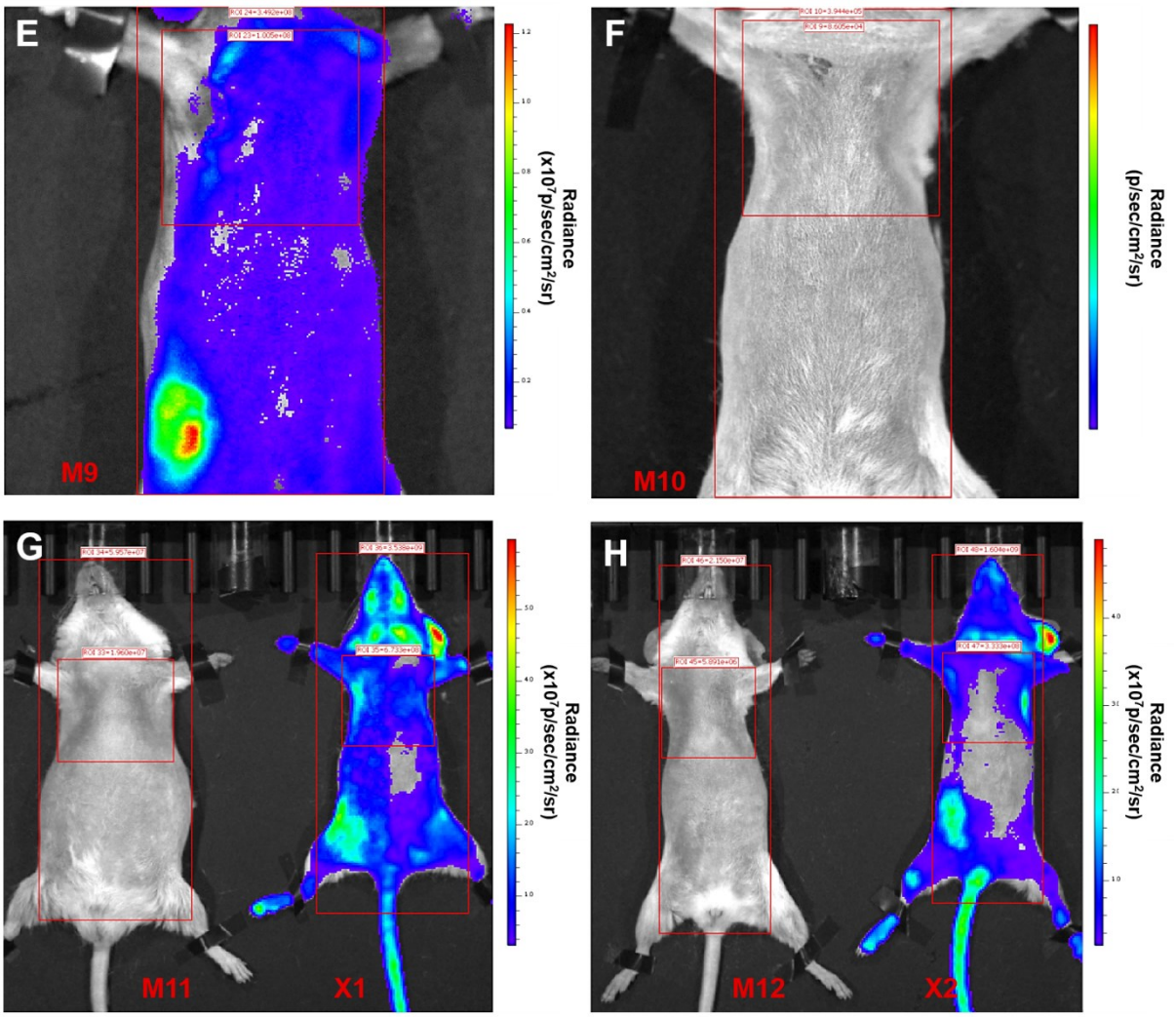

Figure 49. 2D bioluminescence images of G3 mice after s.c. injection of D-luciferin. *M9 was weak hem and had a black coat. All the other mice were wildtype and had a white coat. Imaging position: supine. E: M9= MCT241; Color Scale: Min = 6,88e5 / Max = 1,23e7. F: M10 = AGE45; Color Scale: Min = 1,35e4 / Max = 1,35e4. G: M11 = AGE467, X1: G4 mouse; Color Scale: Min = 3,18e6 / Max = 5,98e7. H: M12 = AGE478, X2: G4 mouse; Color Scale: Min = 2,61e6 / Max = 4,91e7.*

II. Analysis

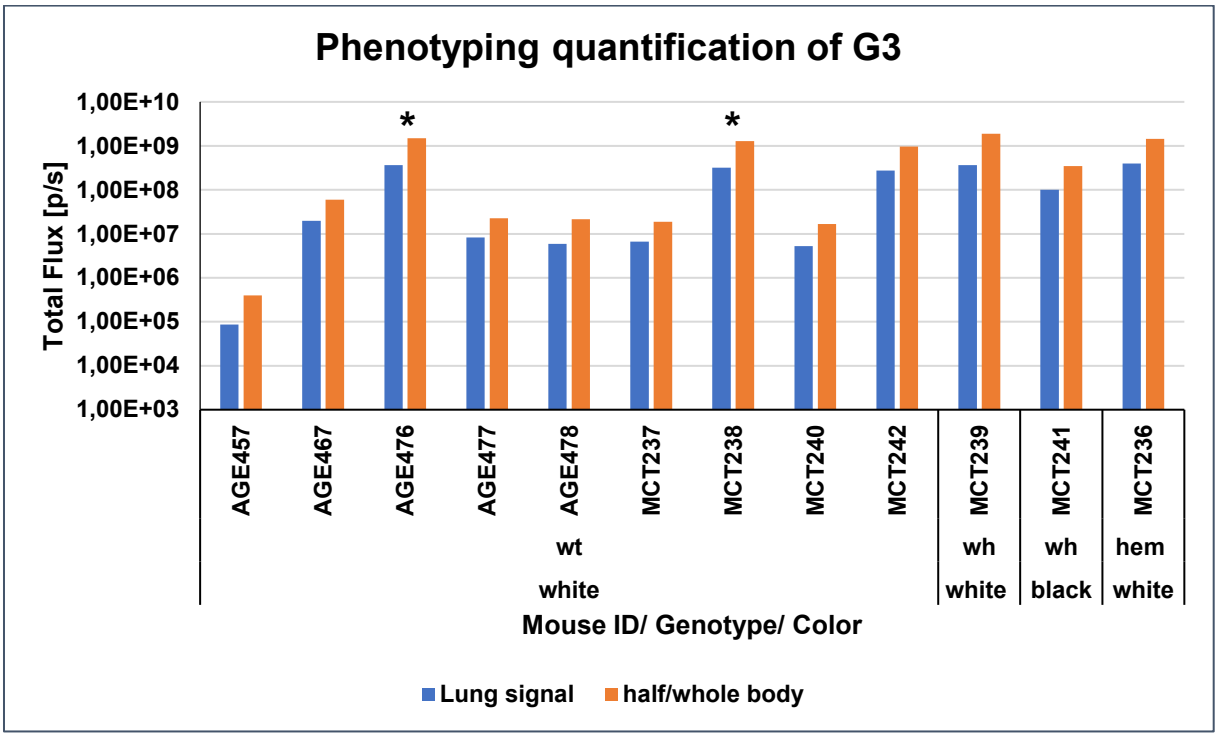

Figure 50. 2D BLI signal quantification of image of Figure 49. *Genotypically negative mice AGE476 and MCT238 with positive phenotypic status marked with an asterisk (*) as outliers. wh = weak hem, wt = wildtype.*

III. Organ validation

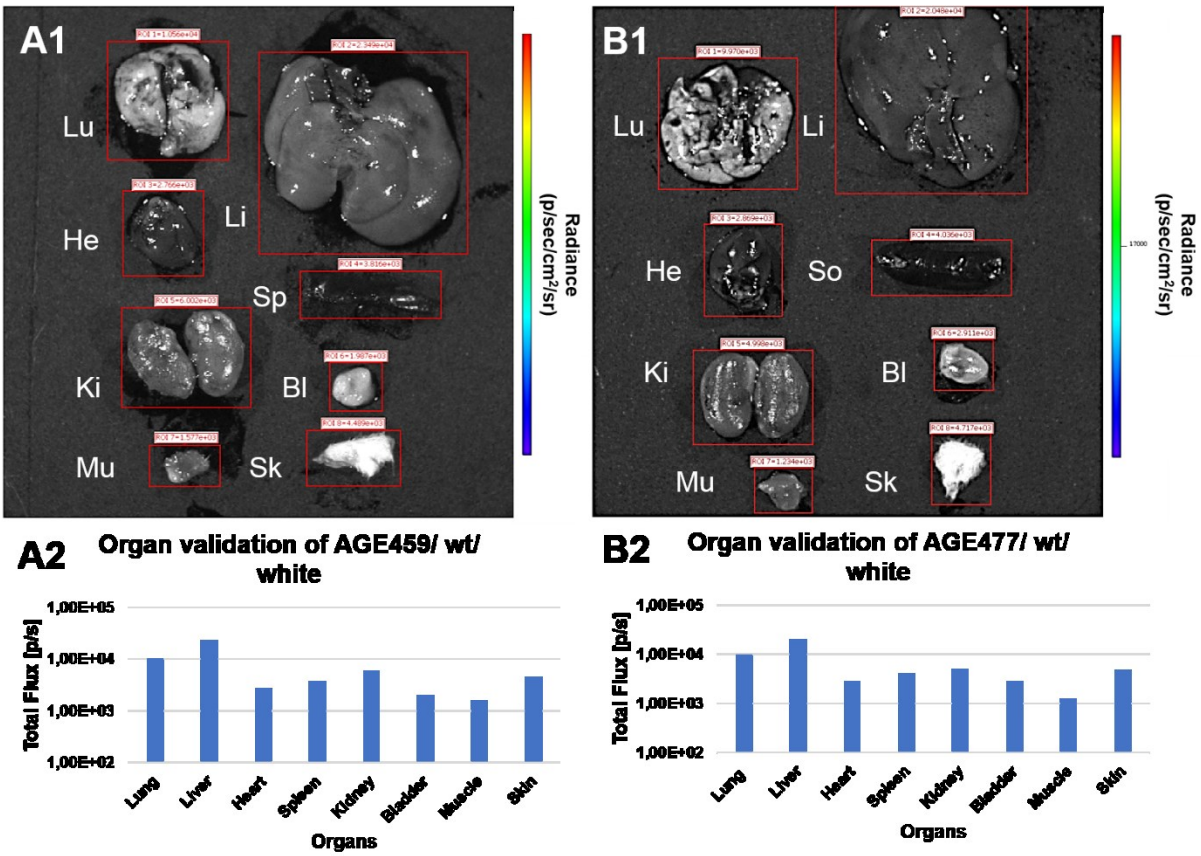

Figure 51. 2D Bioluminescence images and signal quantification of the organs of G3 mice. *A1: 2D BL images of the organs from AGE459; Color Scale: Min = 1,21e4 / Max = 1,21e4. A2: Signal quantification of organ images from A1. B1: 2D BLI of organs from AGE477; Color Scale: Min = 1,70e4 / Max = 1,70e4. B2: Signal quantification of organ images from B2. Bl = Bladder, He = Heart, Ki = Kidneys, Li = Liver, Lu = Lung, Mu = Muscle, Sk = Skin, Sp = Spleen, wt = wildtype.*

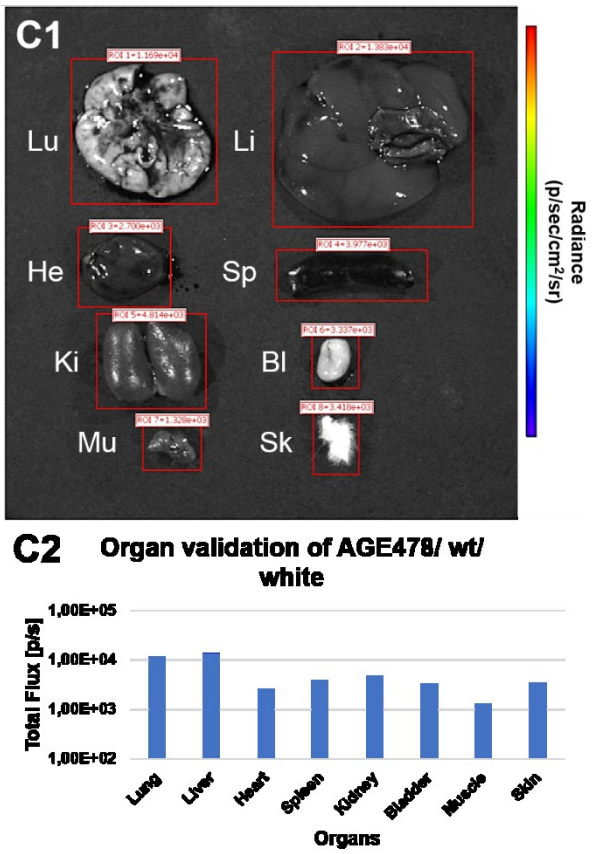

Figure 52. 2D Bioluminescence image and signal quantification of the organs of the G3 mouse AGE478. *C1: 2D BL images of the organs from AGE478; Color Scale: Min = 1,23e4 / Max = 1,23e4. C2: Signal quantification of organ images from C1. Bl = Bladder, He = Heart, Ki = Kidneys, Li = Liver, Lu = Lung, Mu = Muscle, Sk = Skin, Sp = Spleen, wt = wildtype.*

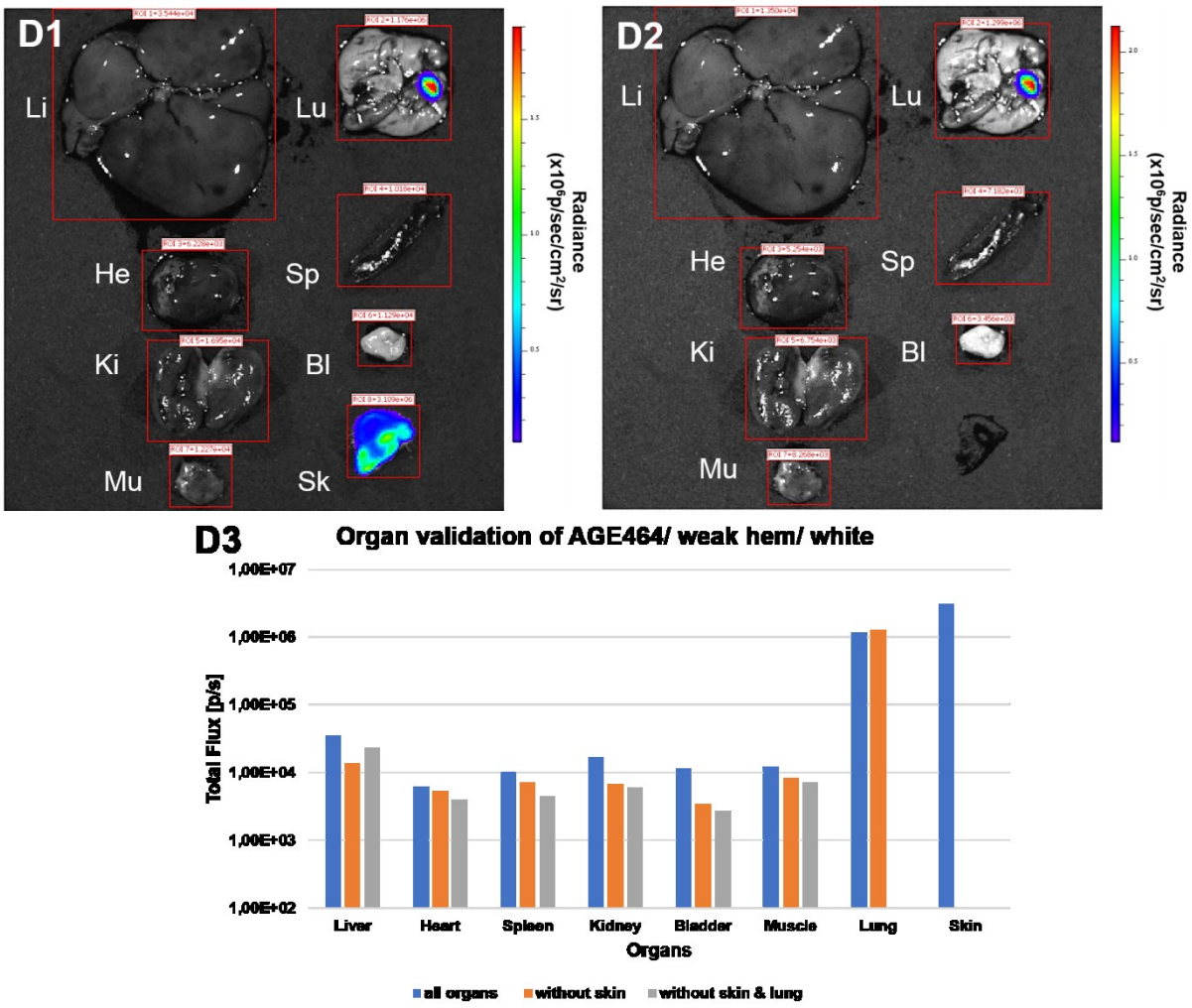

Figure 53. 2D Bioluminescence images and signal quantification of the organs of the G3 mouse AGE464. *D1: 2D BL images of the organs; Color Scale: Min = 1,07e5 / Max = 1,90e6. D2: 2D BL images of the organs without skin; Color Scale: Min = 1,20e5 / Max = 2,13e6. D3: Signal quantification of organ images. Bl = Bladder, He = Heart, Ki = Kidneys, Li = Liver, Lu = Lung, Mu = Muscle, Sk = Skin, Sp = Spleen.*

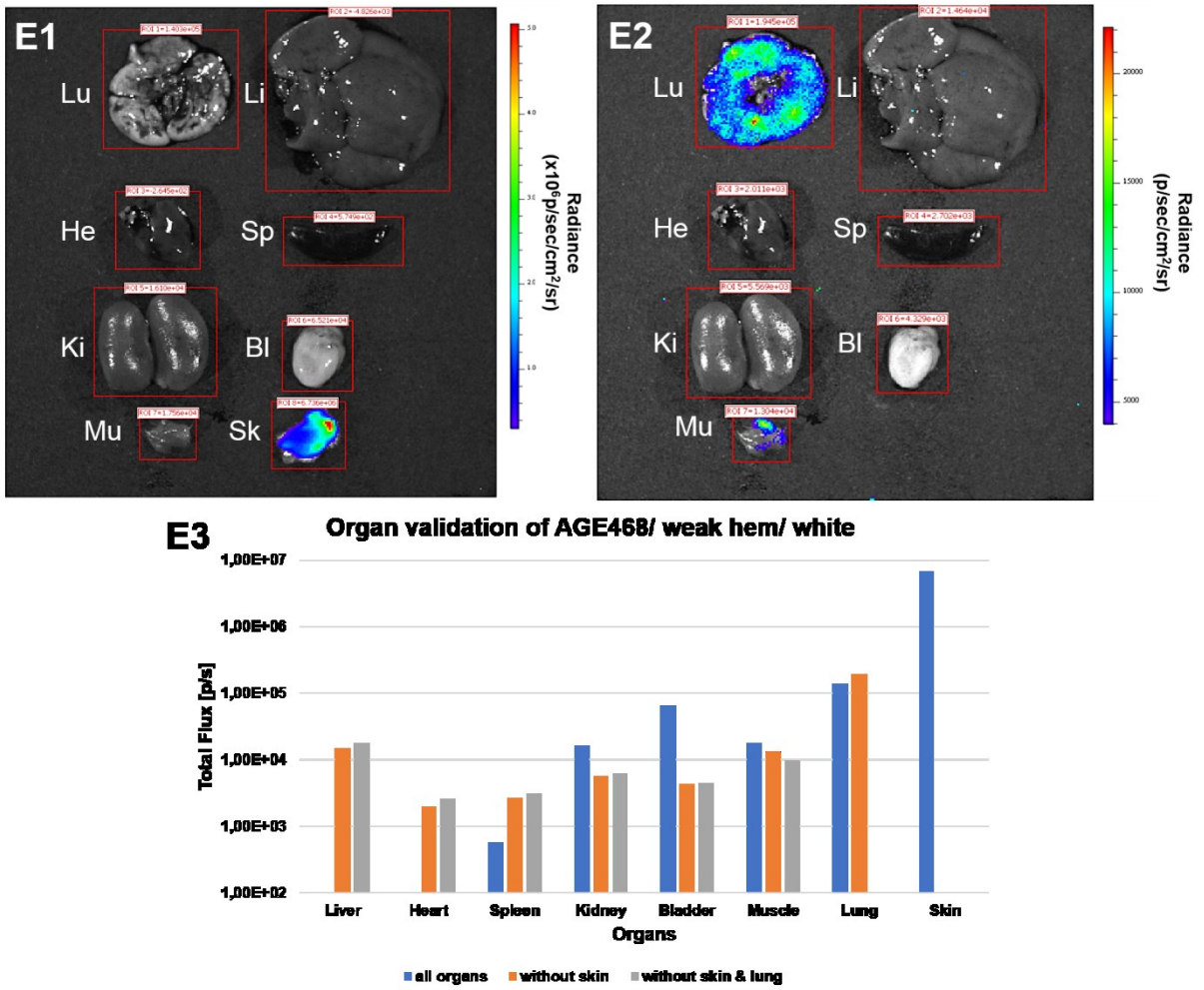

Figure 54. 2D Bioluminescence images and signal quantification of the organs of the G3 mouse AGE468. *E1: 2D BL images of the organs; Color Scale: Min = 3,01e5 / Max = 5,07e6. E2: 2D BL images of the organs without skin; Color Scale: Min = 3,98e3 / Max = 2,21e4. E3: Signal quantification of organ images. Bl = Bladder, He = Heart, Ki = Kidneys, Li = Liver, Lu = Lung, Mu = Muscle, Sk = Skin, Sp = Spleen.*

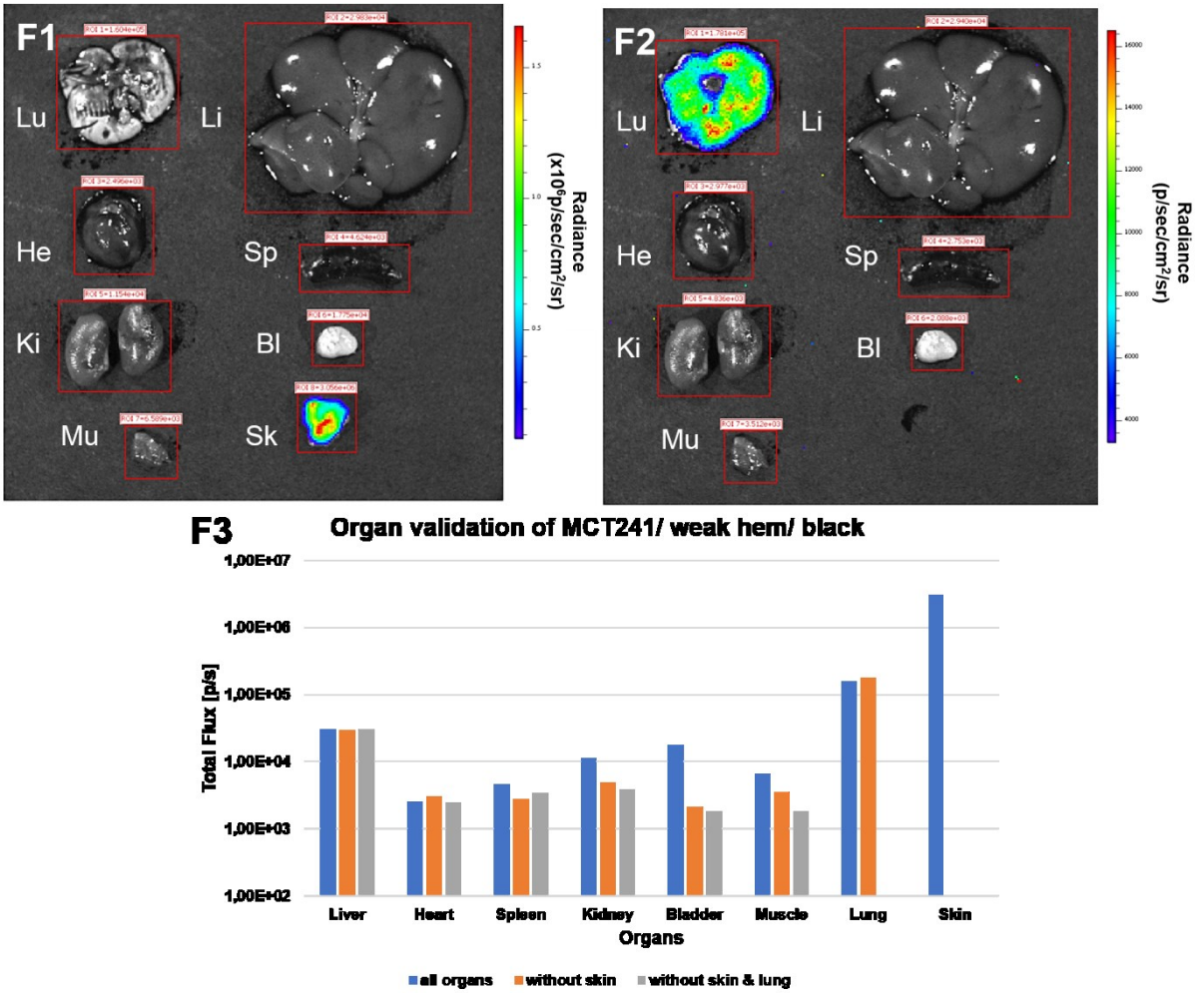

Figure 55. 2D Bioluminescence images and signal quantification of the organs of the G3 mouse MCT241. *E1: 2D BL images of the organs; Color Scale: Min = 8,65e4 / Max = 1,66e6. E2: 2D BL images of the organs without skin; Color Scale: Min = 3,30e3 / Max = 1,65e4. E3: Signal quantification of organ images. Bl = Bladder, He = Heart, Ki = Kidneys, Li = Liver, Lu = Lung, Mu = Muscle, Sk = Skin, Sp = Spleen.*

4.2.5 Generation G4

One wildtype, four weak hem and three hem mice with white coat of generation G4 were imaged. All genotypically positive mice had significant BLI signals over the whole body, as shown in Figure 56. Also, the signal quantification showed (Figure 57) whole body values over log 9, which can be considered as positive phenotype. In the wildtype mouse MCT196 (M5) no signal was detected, and the quantification showed a log 2 lower value compared to the others. So, this mouse was determined as phenotypically negative. No organ validation was carried out.

I. 2D BLI

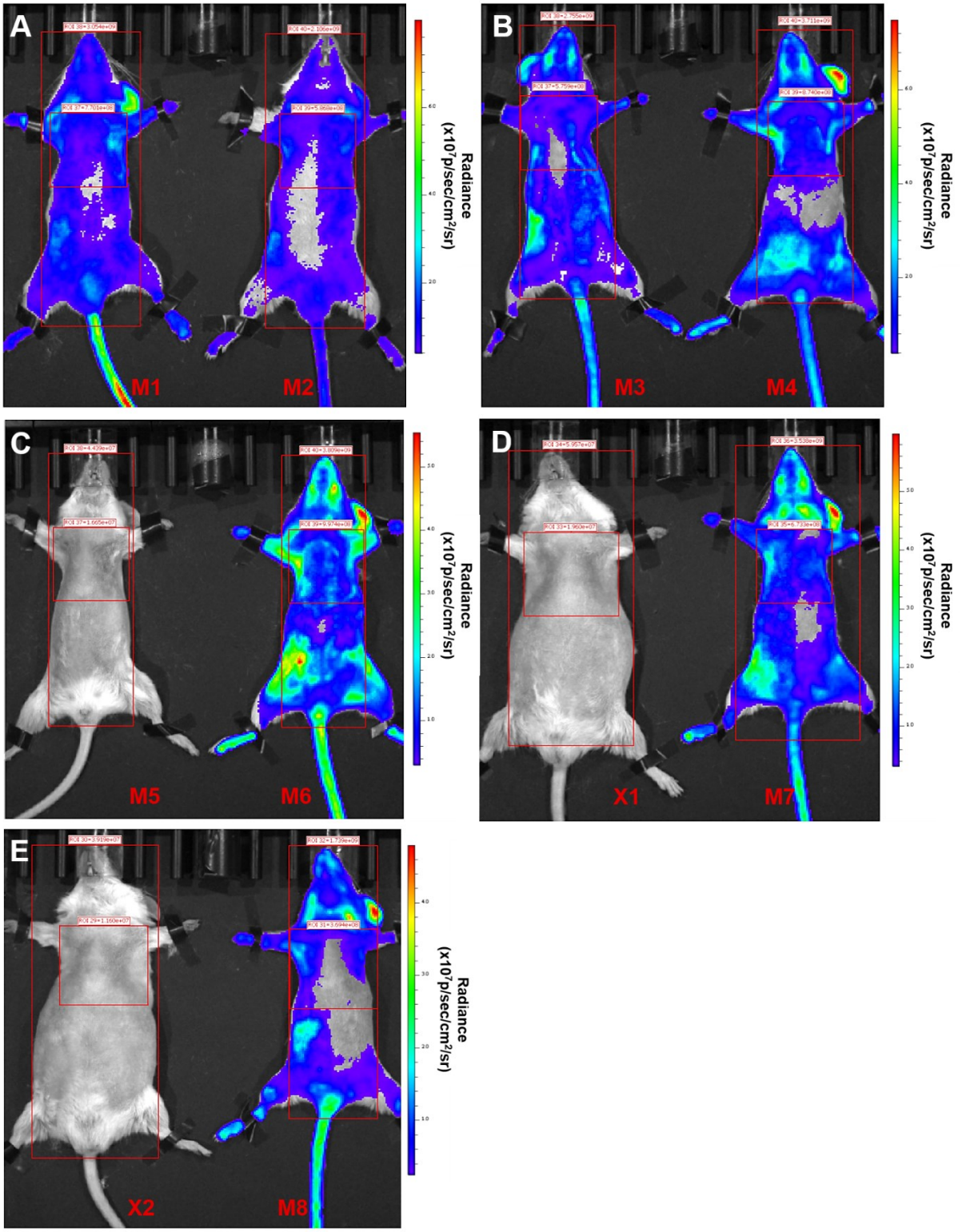

Figure 56. 2D bioluminescence images of G3 mice after s.c. injection of D-luciferin. *M5 was wildtype, M4, M7 and M8 were hem and all the others were weak hem. All mice had a white coat. Imaging position: supine. A: M1= MCT192, M2 = MCT191; Color Scale: Min = 4,00e6 / Max = 8,00e7. B: M3 = MCT194, M4 = MCT193; Color Scale: Min = 3,90e6 / Max = 7,50e7. C: M5 = MCT196, M6 = MCT195; Color Scale: Min = 3,04e6 / Max = 5,54e7. D: X1 = G3 mouse, M7 = MCT197; Color Scale: Min = 3,18e6 / Max = 5,98e7. E: X2 = G2a mouse, M8 = MCT198; Color Scale: Min = 2,48e6 / Max = 4,80e7.*

II. Analysis

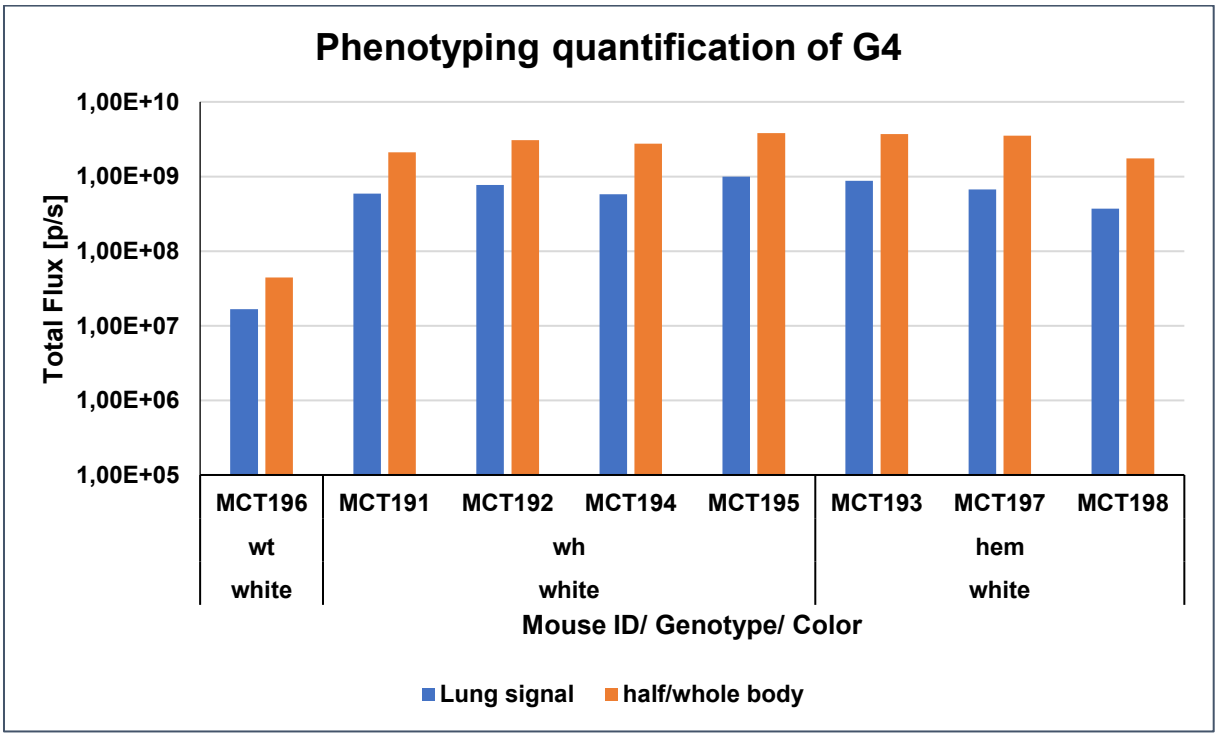

Figure 57. 2D BLI signal quantification of image of Figure 56.

4.2.6 Summary of all Tg SpC-Luc results

In Figure 58 a summary of the phenotyping results of all 41 Tg SpC-Luc mice is shown. 26 out of 30 genotypically positive mice had a BLI signal over the whole body and nine out of eleven wildtype mice had no significant light signal as expected. So in summary the phenotype of 35 out of 41 mice matched with their genotypic status.

The 4 weak hem mice AGE357, AGE362, AGE363 and AGE364 showed no significant BLI signal and were marked with a circle as outliers.

The 2 wildtype mice AGE476 and MCT238 had high whole body signals and were declared as phenotypically positive, which therefore did not match with their genotype and were labeled as outliers with an asterisk.

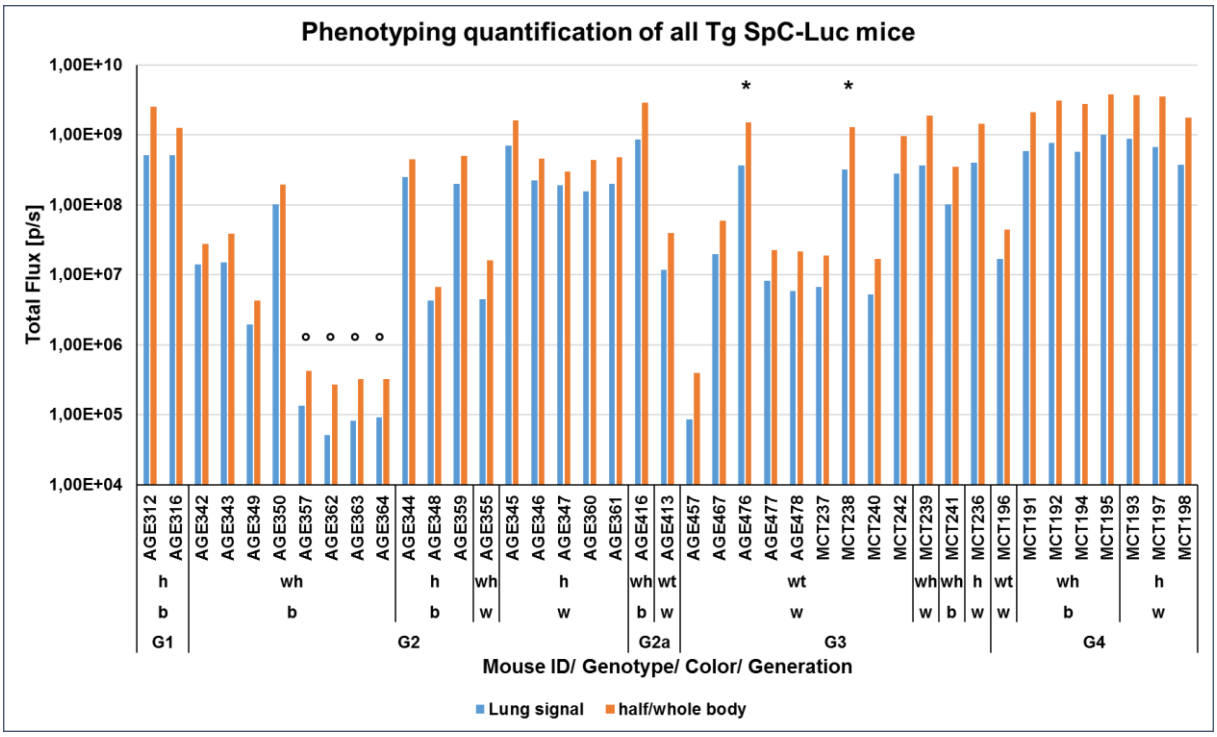

Figure 58. Signal quantification results of all imaged Tg SpC-Luc mice.*Genotypically positive mice with negative phenotypic status marked with a circle (°). Genotypically negative mice with positive phenotypic status marked with an asterisk (*). h = hem, wh = weak hem, wt = wildtype, b = black, w = white.*

In Figure 59 the organ imaging results of all 8 Tg SpC-Luc mice are presented graphically. 4 out of 6 mice genotypically positive mice had a BLI signal in lung and skin and all wildtype mice had no significant light signals as expected. So, in summary the genotypic status of 6 mice was approved by organ imaging.

The 2 weak hem mice AGE357 and AGE363 showed no significant BLI signals and were marked in Figure 59 as outliers.Therefore, the not expected phenotypic results of these two mice was confirmed by organ imaging (Figure 59, 60).

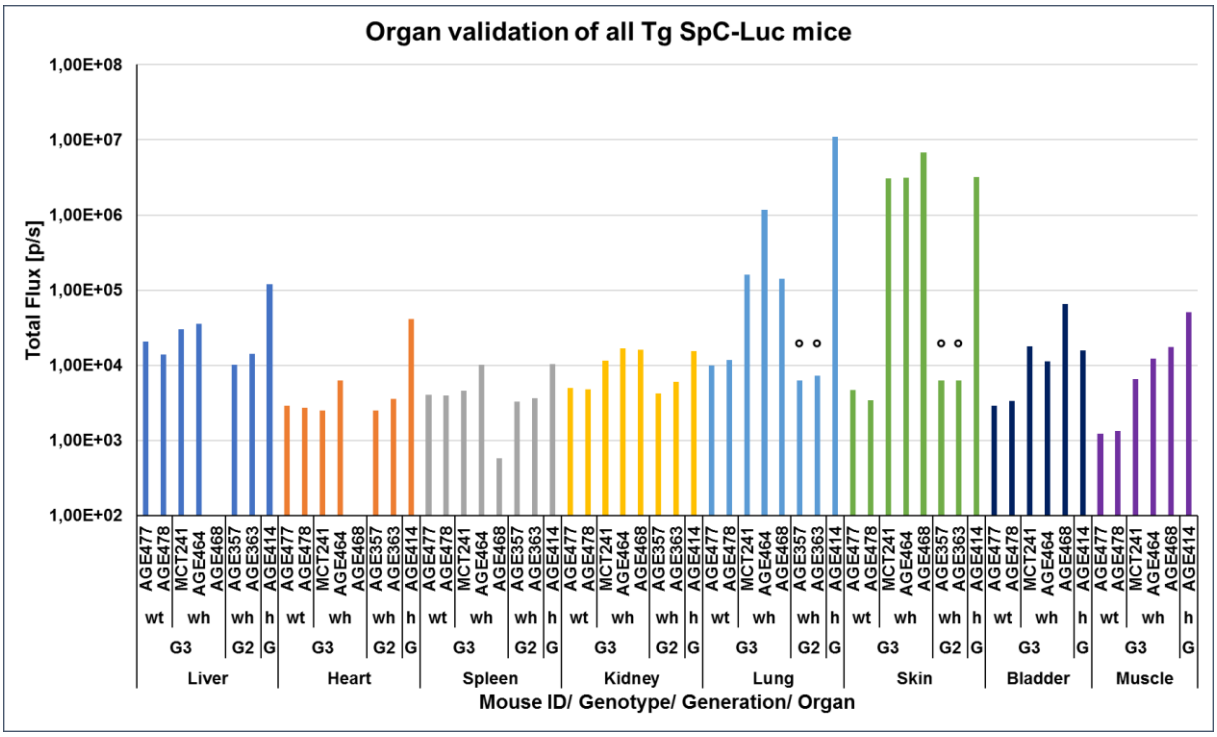

Figure 59. Signal quantification results of all organ images of Tg SpC-Luc mice. *Genotypically positive mice with negative phenotypic status marked with a circle (°) above lung signal. wt = wildtype, wh = weak hem, h = hem, G = G2a.*

Phenotyping result summary of Tg SpC-Luc mice					
	Mouse IDs		**Genotype**	**Generation**	**Color**
Mice with signals as expected as per genotype	AGE312	AGE316	hem	G1	black
	AGE342 AGE349	AGE343 AGE350	weak hem	G2	black
	AGE344 AGE359	AGE348	hem	G2	black
	AGE355		weak hem	G2	white
	AGE345 AGE347 AGE361	AGE346 AGE360	hem	G2	white
	AGE416		weak hem	G2a	black
	AGE413		wildtype	G2a	white
	AGE457 AGE477 MCT237 MCT242	AGE467 AGE478 MCT240	wildtype	G3	white
	MCT239		weak hem	G3	white
	MCT241		weak hem	G3	black
	MCT236		hem	G3	white
	MCT196		wildtype	G4	white
	MCT191 MCT192	MCT194 MCT195	weak hem	G4	white
	MCT193 MCT198	MCT197	hem	G4	white
Outlier weak hem mice with low signals	AGE357 AGE363	AGE362 AGE364	weak hem	G2	black
Outlier wildtype mice with high signals	AGE476 MCT238		wildtype	G3	white

Table 12. Phenotyping result summary of Tg SpC-Luc mice.

Organ validation result summary of Tg SpC-Luc mice				
	Mouse IDs	**Genotype**	**Generation**	**Color**
Mice with signals as expected as per genotype	AGE414	hem	G2a	black
	AGE477 AGE478	wildtype	G3	white
	MCT241	weak hem	G3	black
	AGE464 AGE468	weak hem	G3	white
Outlier weak hem mice with low signals	AGE357 AGE363	weak hem	G2	black

Table 13. Organ validation result summary of Tg SpC-Luc mice.

4.3 Split Luc

For phenotyping of Tg (705) Split-Luc mice three animals were taken per imaging session. The anesthetized mice were placed in supine position in the imaging chamber and the 2D BLI pictures were acquired right after subcutaneous injection of D-luciferin in the right abdominal side. The picture with the highest bioluminescence signal of each session was selected for the analysis. By using the Living Image software one ROI was applied over the whole body, because no tissue specific luciferase expression was expected. Actually, no luciferase expression was expected in the mice of this strain since the luciferase gene should be disrupted, but some mice already showed partial enzyme activity without any treatment. One could speculate that spontaneous splice correction could have occurred, or by another mechanism we could not clarify yet. In any case, further studies are needed to investigate whether treatment with SSOs would change the signal intensity or not. Mice with ROIs that provided values of over log 6 in the signal quantification were assessed as outliers irrespective of their genotype and the values below log 6 were evaluated with an expected negative phenotype. The phenotyping data includes wildtype, weak hem and hem mice of the generations G2b, G2c and G3b (Table 8).

For validation by organ imaging 6 mice were sacrificed by cervical dislocation 20 minutes after subcutaneous injection of D-Luciferin. After euthanasia especially the organs skin, brain, liver, spleen, muscle, heart, kidneys, lung, bladder were removed

and imaged. Also here ROIs were placed around each organ and quantified. Mice with visibly detected signals of the organs, were evaluated as outliers. For this experiments wildtype, weak hem and hem mice from generation G2b, G2c and G3b were used (Table 9).

4.3.1 Generation G2b

Three white wildtype mice of generation G2b were imaged. As shown in Figure 60 no BLI signal was in AGE380 (M1) and AGE387 (M2) detected. AGE404 (M3) showed in comparison to them a signal in the area of the bladder. Additionally, the signal quantification showed a much higher value of the whole body ROI of AGE404 (Figure 61) compared to the other to mice. Due to that AGE404 was determined as outlier.

Furthermore, one wildtype, one weak hem and one hem mouse were sacrificed for organ imaging. As expected none of them showed a significant signal as shown in Figure 62 and 63.

I. 2D BLI

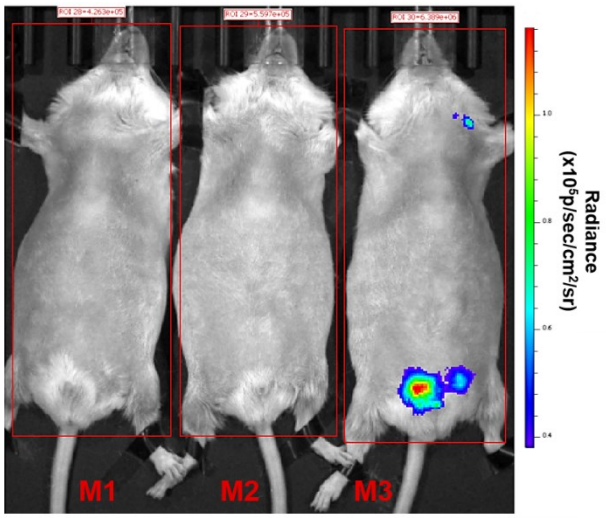

Figure 60. 2D bioluminescence image of G2b mice after s.c. injection of D-luciferin. *All three mice were wildtype and had a white coat. Imaging position: supine. M1= AGE380, M2 = AGE387, M3 = AGE404; Color Scale: Min = 3,81e4 / Max = 1,16e5.*

II. Analysis

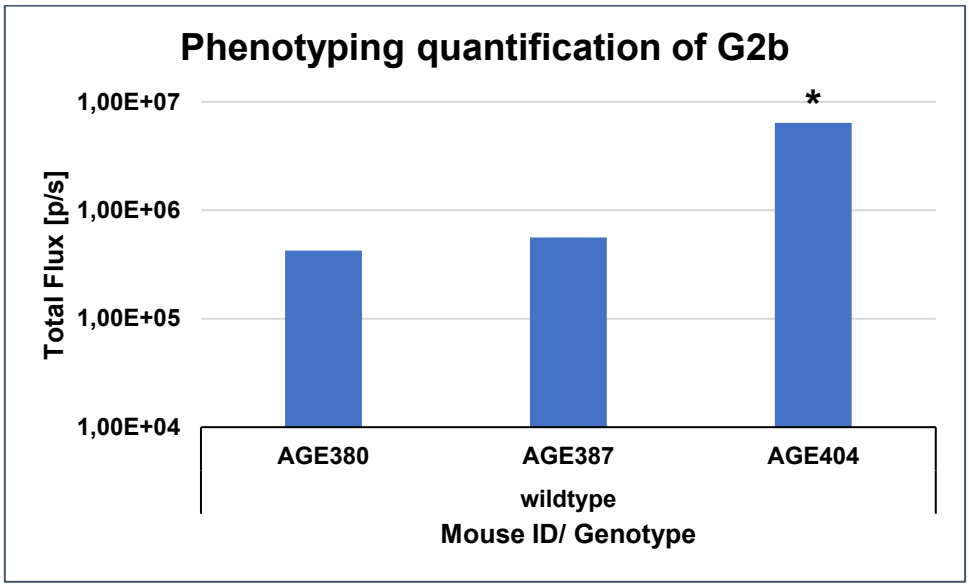

Figure 61. 2D BLI signal quantification of image of Figure 60. *AGE404 marked with an asterisk (*) as outlier.*

III. Organ validation

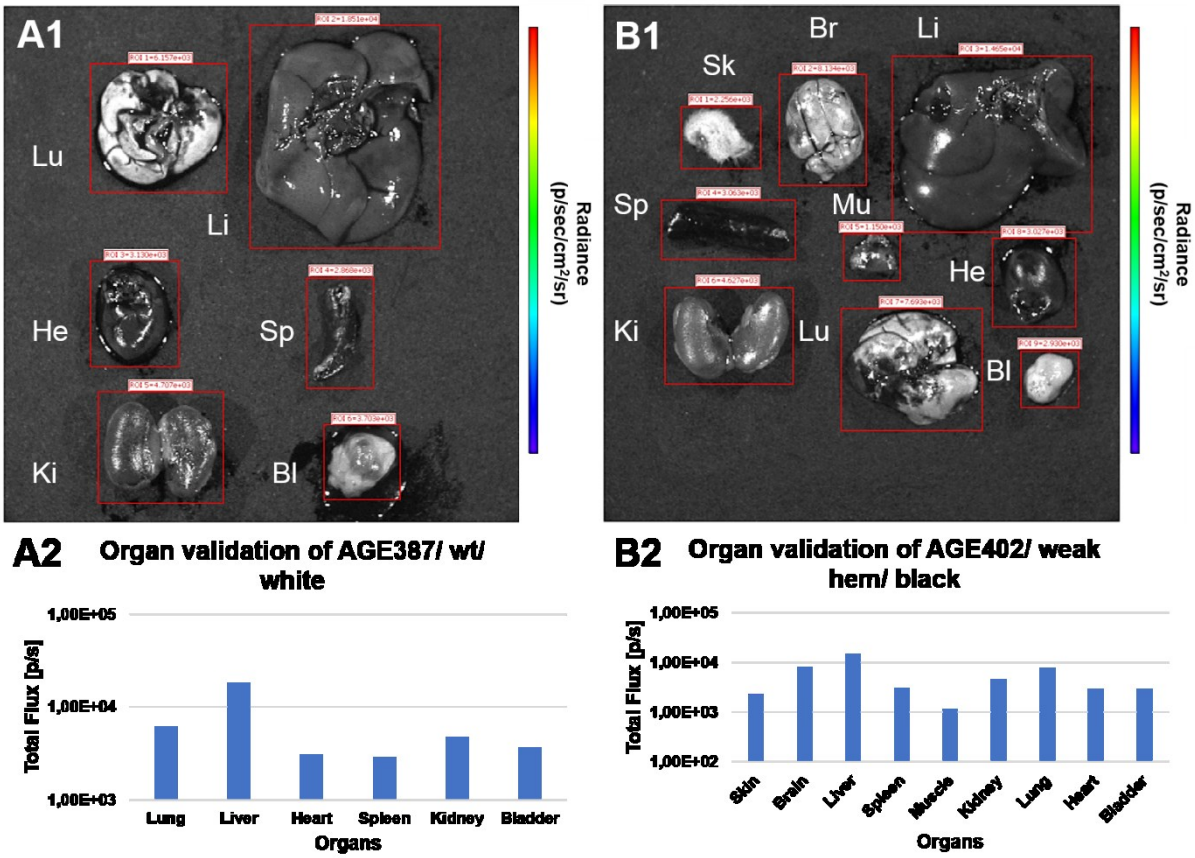

Figure 62. 2D Bioluminescence images and signal quantification of the organs of G2b mice. *A1: 2D BL images of the organs from AGE387; Color Scale: Min = 7,96e3 / Max = 7,96e3. A2: Signal quantification of organ images from A1. B1: 2D BLI of organs from AGE402; Color Scale: Min = 9,64e3 / Max = 9,64e3. B2: Signal quantification of organ images from B2. Bl = Bladder, Br = Brain, He = Heart, Ki = Kidneys, Li = Liver, Lu = Lung, Mu = Muscle, Sk = Skin, Sp = Spleen, wt = wildtype.*

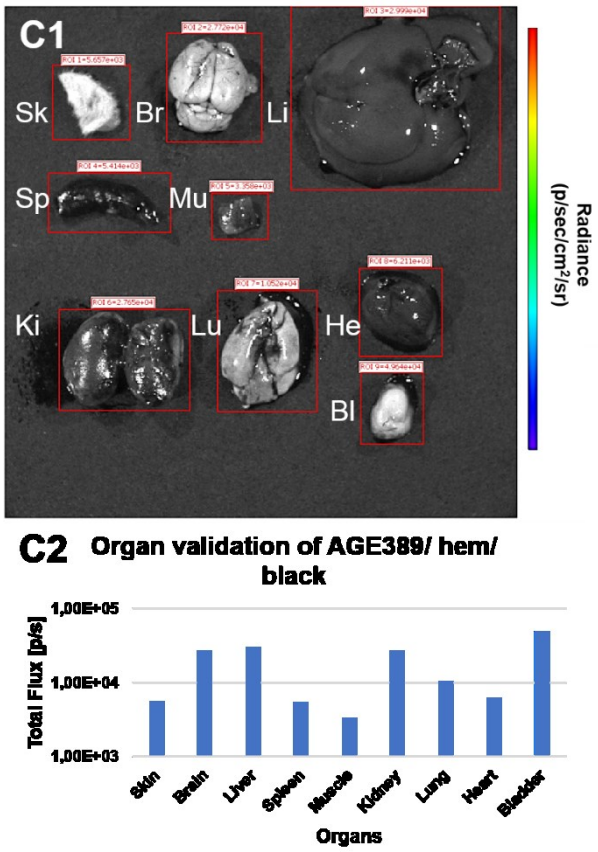

Figure 63. 2D Bioluminescence image and signal quantification of the organs of the G2b mouse AGE389. *C1: 2D BL images of the organs; Color Scale: Min = 2,94e4 / Max = 2,94e4. C2: Signal quantification of organ images from A1. Br = Brain, Bl = Bladder, He = Heart, Ki = Kidneys, Li = Liver, Lu = Lung, Mu = Muscle, Sk = Skin, Sp = Spleen.*

4.3.2 Generation G2c

One white hem mouse of generation G2c was phenotyped by 2D BLI. In the image of Figure 64 a BLI signal over the whole body was detected and the signal quantification of Figure 65 shows a value over log 8, which can be therefore determined as outlier.

Additionally, one wildtype and one weak hem mouse were chosen for organ imaging. The organs of the wildtype mouse AGE431 showed no significant signals (Figure 66 – A1, A2). In contrast to this, a unexpected high BLI signal was found in the lung, but also in the liver and kidney of the weak hem mouse AGE434, which is also confirmed by the signal quantification as outlier(Figure 66 – B1, B2).

I. 2D BLI

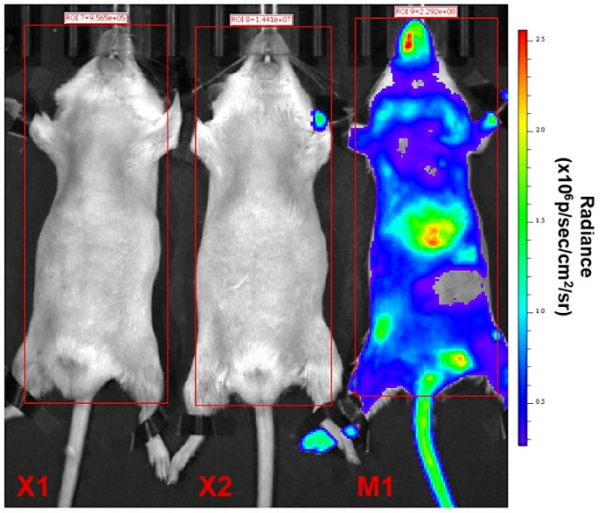

Figure 64. 2D bioluminescence image of one G2c mouse after s.c. injection of D-luciferin. *The mouse was hem and had a white coat. Imaging position: supine. X1, X2 = G3b mice, M1 = AGE435; Color Scale: Min = 2,67e5 / Max = 2,56e6.*

II. Analysis

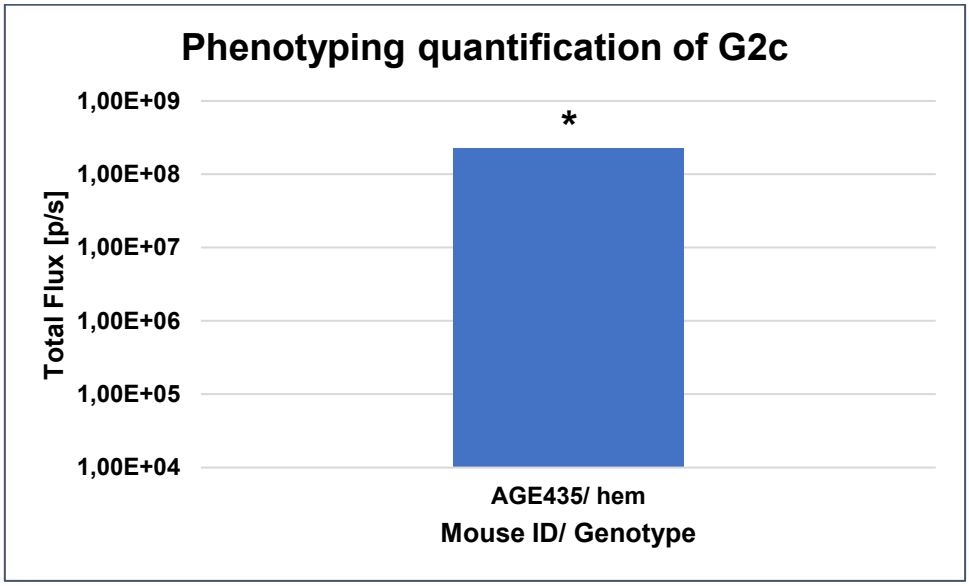

Figure 65. 2D BLI signal quantification of image of Figure 64. *AGE435 marked with an asterisk (*) as outlier.*

III. Organ validation

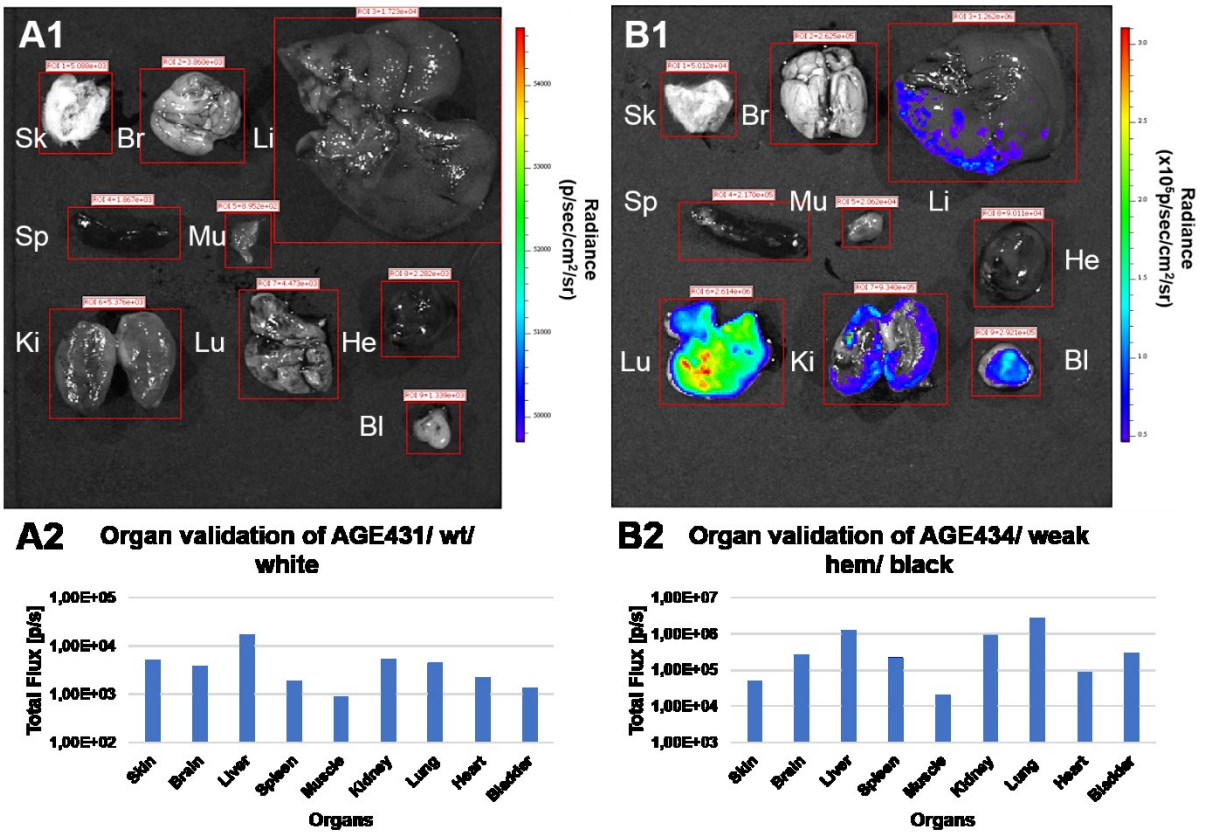

Figure 66. 2D Bioluminescence images and signal quantification of the organs of G2c mice. *A1: 2D BL images of the organs from AGE431; Color Scale: Min = 4,97e4 / Max = 5,47e4. A2: Signal quantification of organ images from A1. B1: 2D BLI of organs from AGE434; Color Scale: Min = 4,65e4 / Max = 3,11e5. B2: Signal quantification of organ images from B2. Br = Brain, Bl = Bladder, He = Heart, Ki = Kidneys, Li = Liver, Lu = Lung, Mu = Muscle, Sk = Skin, Sp = Spleen, wt = wildtype.*

4.3.3 Generation G3b

14 white mice of generation G3b were imaged. 5 of them were wildtype, 2 weak hem and 7 hem. Only the hem mouse MCT168 (M9) and the 2 wildtype miceMCT163 (M10) and MCT164 (M11) showed as expected no significant signal, which can be verified in the whole body images (Figure 67, Fig. 68). The wildtype mouse MCT183 (M13) displays in Figure 68 a value exactly at log 6 and shows no visible signal in Figure 67 - E and therefore requires a validation by organ imaging. Also MCT167 (M12) showed a comparable value (Figure 67), but had visible signals in the whole body image (Figure 68 - D) and was therefore determined as outlier. All the other mice were marked as outliers too, due of their significant values (Figure 67).

For organ imaging one wildtype mouse was sacrificed. This mouse showed no significant results and was therefore determined as phenotypically negative (Figure 69).

I. 2D BLI

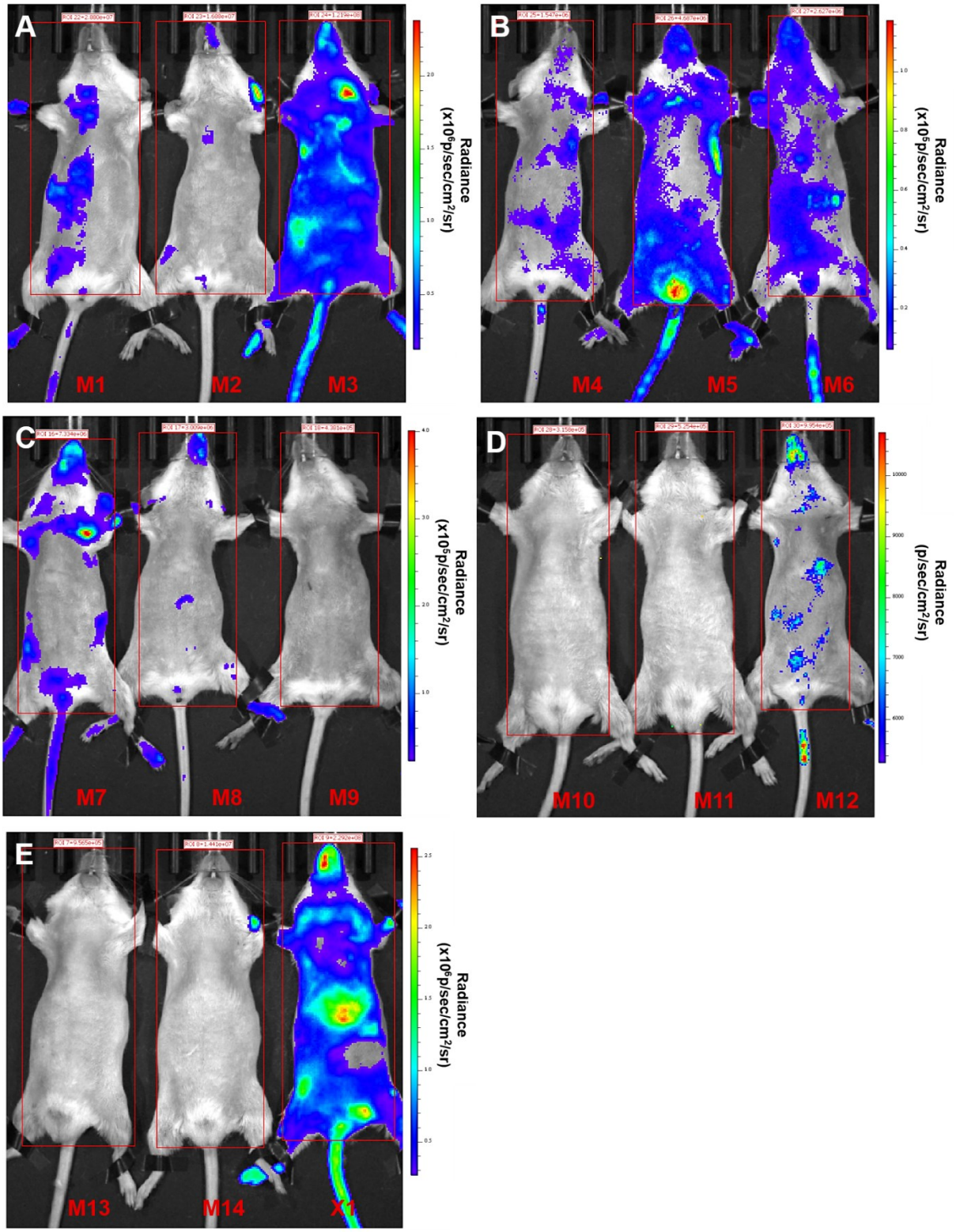

Figure 67. 2D bioluminescence images of G3b mice after s.c. injection of D-luciferin. *Five wildtype, two weak hem and seven hem mice. All had a white coat. Imaging position: supine. A: M1 = MCT185, M2 = MCT169, M3 = MCT186; Color Scale: Min = 1,26e5 / Max = 2,38e6. B: M4 = MCT165, M5 = MCT170, M6 = MCT166; Color Scale: Min = 6,45e3 / Max = 1,17e5. C: M7 =MCT187, M8 = MCT171, M9 = MCT168; Color Scale: Min = 2,30e4 / Max = 4,01e5. D: M10 = MCT163, M11 = MCT164, M12 = MCT167; Color Scale: Min = 5,29e3 / Max = 1,07e4. E: M13 = MCT183, M14 = MCT184, X1= G2c mouse; Color Scale: Min = 2,67e5 / Max = 2,56e6.*

II. Analysis

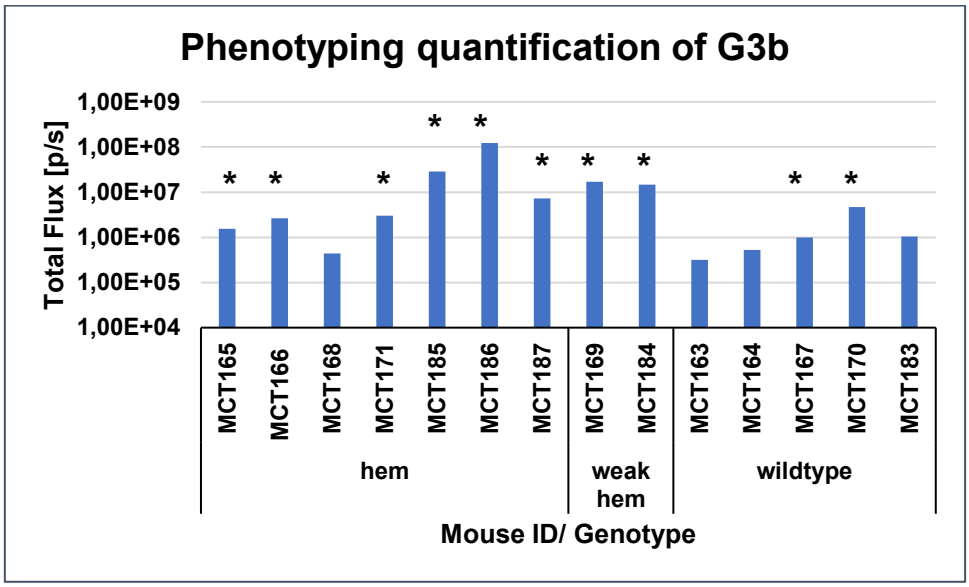

Figure 68. 2D BLI signal quantification of image of Figure 67. *All except MCT168, MCT163, MCT164 and MCT167 marked with an asterisk (*) as outlier.*

III. Organ validation

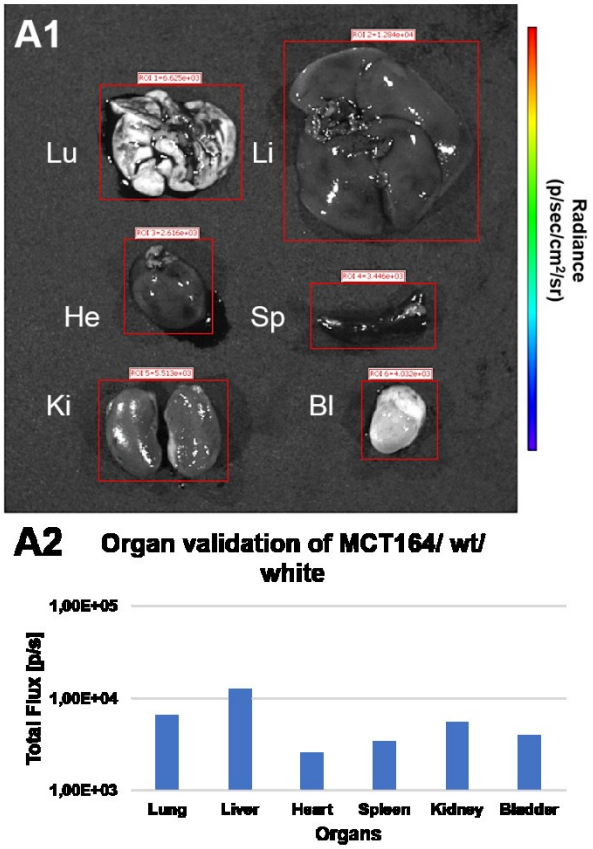

Figure 69. 2D Bioluminescence image and signal quantification of the organs of the G3b mouse MCT164. *A1: 2D BL images of the organs; Color Scale: Min = 6,89e3 / Max = 6,89e3. A2: Signal quantification of organ images from A1. Bl = Bladder, He = Heart, Ki = Kidneys, Li = Liver, Lu = Lung, Sp = Spleen, wt = wildtype.*

4.3.4 Summary of all Tg (705) Split-Luc results

In Figure 70 a summary of the phenotyping results of all 18 Tg (705) Split-Luc mice is shown. 9 out of 10 genotypically positive mice and 3 out of 8 wildtype had a BLI signal over the body. In summary, 12 outliers were determined.

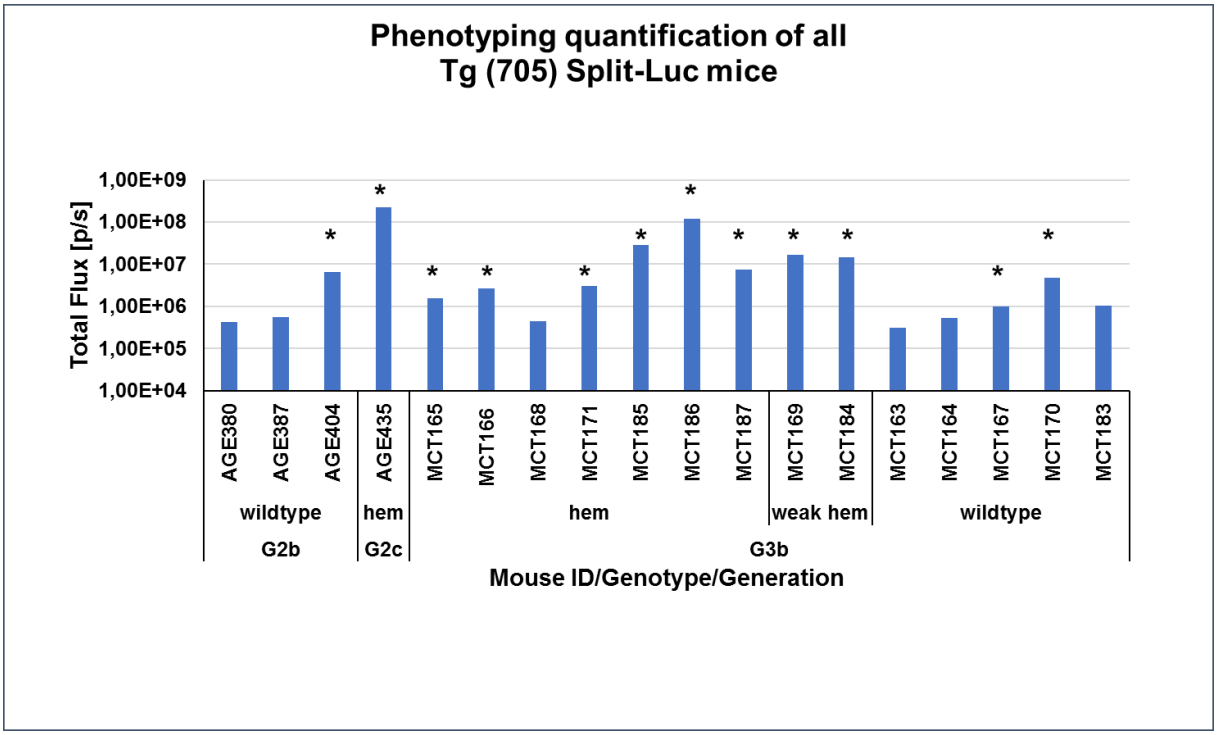

Figure 70. Signal quantification results of all imaged Tg (705) Split-Luc mice. *Outliers marked with an asterisk (*)*

In Figure 71 the organ imaging results of all six Tg (705) Split-Luc mice are presented graphically. One hem, two weak hem and three wildtype were taken for organ imaging. The weak hem mouse AGE434 showed high signals in lung, liver and kindeys and was marked with an asterix above the lung signal.

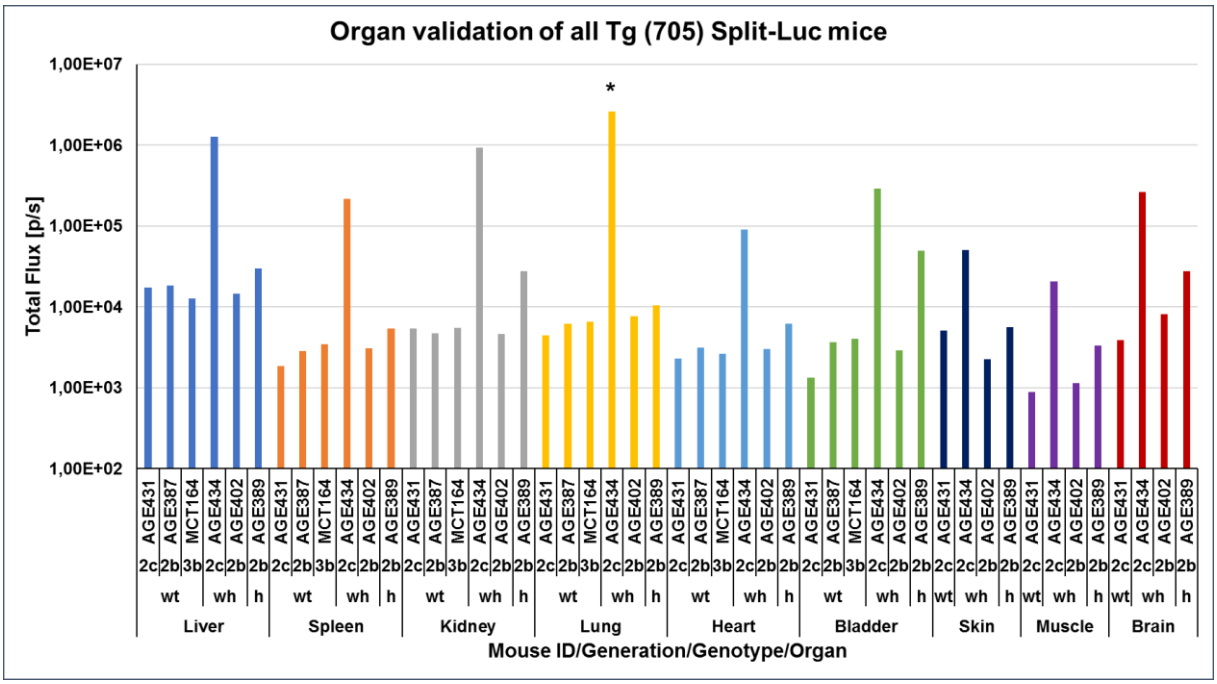

Figure 71. Signal quantification results of all organ images of Tg (705) Split-Luc mice. *wt = wildtype, wh = weak hem, h = hem. AGE434 marked as outlier with an asterisk above lung signal (*).*

Phenotyping result summary of Tg (705) Split-Luc mice				
	Mouse IDs	**Genotype**	**Generation**	**Color**
Mice with no signal as expected	AGE380 AGE387	wildtype	G2b	white
	MCT163 MCT164 MCT183	wildtype	G3b	white
	MCT168	hem	G3b	white
Outlier weak hem and hem mice with unexpected signals	MCT169 MCT184	weak hem	G3b	white
	MCT165 MCT166 MCT171 MCT185 MCT186 MCT187	hem	G3b	white
	AGE435	hem	G2c	white
Outlier wildtype mice with unexpected signals	AGE404	wildtype	G2b	white
	MCT167 MCT170	wildtype	G3b	white

Table 14. Phenotyping result summary of Tg (705) Split-Luc mice.

Organ validation result summary of Tg (705) Split-Luc mice				
	Mouse IDs	**Genotype**	**Generation**	**Color**
Mice with no signals as expected	AGE402	weak hem	G2b	black
	AGE389	hem	G2b	black
	AGE387	wildtype	G2b	white
	MCT164	wildtype	G3b	white
	AGE431	wildtype	G2c	white
Outlier mouse with unexpected signals	AGE434	weak hem	G2c	black

Table 15. Organ validation result summary of Tg (705) Split-Luc mice.

5 Conclusion

In this study the phenotypes of three transgenic mouse lines, named Tg Thy 1.2-Luc, Tg SpC-Luc and Tg (705) Split-Luc, were determined using the BLI technology. For this purpose, the mice were injected subcutaneously with D-luciferin and were directly afterwards imaged, in dependence of their strain, in prone or supine position. Some mice were also chosen for organ imaging to validate their phenotypic status.

29 Tg Thy 1.2-Luc mice were investigated, of which 5 were genotypically wildtype and 24 hem animals. 20 out of 24 hem mice showed clear signals as expected in the brain region and agreed therefore with their genotype. Only in 2 of the 5 wildtypes no significant signals and corresponded to their genotypic status. So, the phenotypes of 6 (AGE256, AGE293, AGE440, AGE265, AGE266, AGE261, AGE443) of the Tg Thy 1.2-Luc mice did not match their genotypes and were determined as outliers. In the mice that were also used for organ imaging and showed positive BLI signals already in the whole-body images, clearly visible BLI signals could be detected in the brain, which confirmed the phenotyping results.

41 Tg SpC-Luc mice were imaged, of which 11 had a negative and 30 a positive genotype. 9 wildtype mice showed no significant signals and 26 transgenic mice showed signals over the whole body. The results showed altogether 6 outliers, which were AGE357, AGE362, AGE363, AGE364, AGE476, MCT238. In this strain, it has been found that in the positive mice, luciferase is not only expressed in the lung but also in the skin, which was showed by the pictures from the organ imaging sessions. Also, here we were able to confirm the phenotypic determination by significant lung and skin signals in the organ images.

In the last strain Tg (705) Split-Luc 18 mice were phenotyped. 8 of them were wildtype and 10 genotypically positive mice. Normally we did not expect in none of these mice any signals, because even in the transgenic animals the luciferase gene should have been disrupted. However, the whole-body images and signal quantifications of 9 hem/weak hem (MCT169, MCT184, MCT165, MCT166, MCT171, MCT185, MCT186, MCT187, AGE435) and 3 wildtype (AGE404, MCT157, MCT170) mice have shown positive unambiguous values over log 6, which were assessed with a positive phenotype. Here further investigation would be needed to find out if the phenotyping results would reach higher values after splice correction. Furthermore, 3 wildtype and 3 genotypically positive mice were also selected for organ imaging. Here, one weak

hem mouse, AGE434, showed a clear signal in the lung, but also in the liver and kidneys.

In summary, we were able to employ bioluminescence based imaging to determine the phenotypic status in all three mice strains. Sometimes the location of the BLI signals was not clearly visible in the whole body images. However, we were able to detect tissue or organ specific signals and to confirm the phenotypes with the help of organ images.

6 List of Abbreviations

ATI	Alveolar type I
ATII	Alveolar type II
ATP	Adenosine triphosphate
Black 6	C57BL/6
BLI	Bioluminescence imaging
cAMP	Cyclic adenosine monophosphate
CBR	Click beetle luciferase
CDD	charge coupled device
cDNA	complementary DNA
CT	Computed tomography
EGFP	Enhanced green fluorescent protein
FLI	Fluorescence imaging
Fluc	Firefly luciferase
Gluc	Gaussia luciferase
GPCR	G protein-coupled receptors
GPI	Glycosylphosphatidylinositol
hem	hemizygous
iRFP	Near-infrared fluorescent protein
NIR	Near infrared
Rluc	Renilla luciferase
ROI	Region of interest
SFTPC	Surfactant protein C gene
SP	Surfactant protein
SPECT	Single-photon emission computed tomography
SSO	splice switching oligonucleotides
TF	Transcription factor
tg+	transgenic positive

7 List of Figures

8 List of Tables

9 References

1. Hickman-Davis JM, Davis IC. Transgenic mice. *Paediatric Respiratory Reviews*. 2006;7(1):49-53.

2. Dunn DA, Pinkert CA, Kooyman DL. Foundation Review: Transgenic animals and their impact on the drug discovery industry. *Drug Discovery Today*. 2005;10(11):757-767.

3. Gordon J, Ruddle F. Integration and stable germ line transmission of genes injected into mouse pronuclei. *Science*. 1981;214(4526):1244-1246.

4. Caroni P. Overexpression of growth-associated proteins in the neurons of adult transgenic mice. *Journal of Neuroscience Methods*. 1997;71:3-9.

5. Pinczolits S. Optimising genotyping protocols in three novel transgenic reporter mouse strains. 2017. Diplomarbeit, Universität Wien. Fakultät für Lebenswissenschaften.

6. Feng G, Mellor RH, Bernstein M, et al. Imaging neuronal subsets in transgenic mice expressing multiple spectral variants of GFP. *Neuron*. 2000;28(1):41-51.

7. Livet J, Weissman TA, Kang H, et al. Transgenic strategies for combinatorial expression of fluorescent proteins in the nervous system. *Nature*. 2007;450(7166):56-62.

8. Evans GA, Ingraham HA, Lewis K, et al. Expression of the Thy-1 glycoprotein gene by DNA-mediated gene transfer. *Proceedings of the National Academy of Sciences of the United States of America*. 1984;81(17):5532-5536.

9. Seki T, Spurr N, Obata F, Goyert S, Goodfellow P, Silver J. The human Thy-1 gene: structure and chromosomal location. *Proceedings of the National Academy of Sciences of the United States of America*. 1985;82(19):6657-6661.

10. Vidal M, Morris R, Grosveld F, Spanopoulou E. Tissue-specific control elements of the Thy-1. *The EMBO Journal*. 1990;9(3):833-840.

11. Rawlins EL, Perl A-K. The a“MAZE”ing World of Lung-Specific Transgenic Mice. *American journal of respiratory cell and molecular biology*. 2012;46(3):269-282.

12. Glasser SW, Eszterhas SK, Detmer EA, Maxfield MD, Korfhagen TR. The murine SP-C promoter directs type II cell-specific expression in transgenic mice.

American Journal of Physiology-Lung Cellular and Molecular Physiology. 2005;288(4):L625-L632.

13. Roper JM, Staversky RJ, Finkelstein JN, Keng PC, O'Reilly MA. Identification and isolation of mouse type II cells on the basis of intrinsic expression of enhanced green fluorescent protein. *American Journal of Physiology-Lung Cellular and Molecular Physiology*. 2003;285(3):L691-L700.

14. Hong D, Qi Y, Liu J, Wang H, Wang L, Qian L. A novel surfactant protein C mutation resulting in aberrant protein processing and altered subcellular localization causes infantile interstitial lung disease. *Pediatric Research*. 2017;81(6):891-897.

15. Mulugeta S, Maguire JA, Newitt JL, Russo SJ, Kotorashvili A, Beers MF. Misfolded BRICHOS SP-C mutant proteins induce apoptosis via caspase-4- and cytochrome c -related mechanisms. *American Journal of Physiology-Lung Cellular and Molecular Physiology*. 2007;293(3):L720-L729.

16. Bridges JP, Wert SE, Nogee LM, Weaver TE. Expression of a human surfactant protein C mutation associated with interstitial lung disease disrupts lung development in transgenic mice. *The Journal of biological chemistry*. 2003;278(52):52739-52746.

17. Glasser SW, Burhans MS, Korfhagen TR, et al. Altered stability of pulmonary surfactant in SP-C-deficient mice. *Proceedings of the National Academy of Sciences of the United States of America*. 2001;98(11):6366-6371.

18. Lopez-Rodriguez E, Pérez-Gil J. Structure-function relationships in pulmonary surfactant membranes: From biophysics to therapy. *Biochimica et Biophysica Acta (BBA) - Biomembranes*. 2014;1838(6):1568-1585.

19. Roldan N, Nyholm TKM, Slotte JP, Pérez-Gil J, García-Álvarez B. Effect of Lung Surfactant Protein SP-C and SP-C-Promoted Membrane Fragmentation on Cholesterol Dynamics. *Biophysical Journal*. 2016;111(8):1703-1713.

20. Resina S, Abes S, Turner JJ, et al. Lipoplex and peptide-based strategies for the delivery of steric-block oligonucleotides. *International Journal of Pharmaceutics*. 2007;344(1-2):96-102.

21. Sazani P, Gemignani F, Kang S, et al. Systemically delivered antisense

oligomers upregulate gene expression in mouse tissues. *Nature Biotechnology*. 2002;20:1228-1233.

22. Keyaerts M, Caveliers V, Lahoutte T. Bioluminescence imaging: looking beyond the light. *Trends in Molecular Medicine*. 2012;18(3):164-172.

23. Ray P. Multimodality molecular imaging of disease progression in living subjects. *Journal of Biosciences*. 2011;36(3):499-504.

24. Tseng J-C, Vasquez K, Peterson JD. Optical Imaging on the IVIS SpectrumCT System: General and Technical Considerations for 2D and 3D Imaging. 2015;(1):1-18.

25. Choy G, Choyke P, Libutti SK. Current Advances in Molecular Imaging: Noninvasive in Vivo Bioluminescent and Fluorescent Optical Imaging in Cancer Research. *Molecular Imaging*. 2003;2(4):303-312.

26. Luciferase Reporters. https://www.thermofisher.com/at/en/home/life-science/protein-biology/protein-biology-learning-center/protein-biology-resource-library/pierce-protein-methods/luciferase-reporters.html. Accessed July 28, 2019.

27. McKinnon E, Moore A, Dixit S, Zhu Y, Broome AM. Fluorescence and bioluminescence imaging of orthotopic brain tumors in mice. In: *Methods in Molecular Biology*. Vol 1530. ; 2017:283-305.

28. Martelli C, Lo Dico A, Diceglie C, Lucignani G, Ottobrini L. Optical imaging probes in oncology. *Oncotarget*. 2016;7(30):48753-48787.

29. Filonov GS, Piatkevich KD, Ting L-M, Zhang J, Kim K, Verkhusha V V. Bright and stable near-infrared fluorescent protein for in vivo imaging. *Nature Biotechnology*. 2011;29(8):757-761.

30. Tran MTN, Tanaka J, Hamada M, et al. In vivo image analysis using iRFP transgenic mice. *Experimental animals*. 2014;63(3):311-319.

31. Kulathunga K, Hamada M, Hiraishi Y, et al. A Novel iRFP-Incorporated in vivo Murine Atherosclerosis Imaging System. *Scientific Reports*. 2018;8(1):14515.

32. Sadikot RT, Blackwell TS. Bioluminescence: Imaging Modality for In Vitro and In Vivo Gene Expression. In: ; 2008:383-394.

33. Dressler H, Economides K, Favara S, Wu NN, Pang Z, Polites HG. The CRE luc Bioluminescence Transgenic Mouse Model for Detecting Ligand Activation of GPCRs. *Journal of Biomolecular Screening*. 2014;19(2):232-241.

34. Manni I, de Latouliere L, Gurtner A, Piaggio G. Transgenic Animal Models to Visualize Cancer-Related Cellular Processes by Bioluminescence Imaging. *Frontiers in pharmacology*. 2019;10:235.

35. Buckley SMK, Delhove JMKM, Perocheau DP, et al. In vivo bioimaging with tissue-specific transcription factor activated luciferase reporters. *Scientific Reports*. 2015;5(1):11842.

36. Szyska M, Herda S, Althoff S, et al. A Transgenic Dual-Luciferase Reporter Mouse for Longitudinal and Functional Monitoring of T Cells In Vivo. *Cancer Immunology Research*. 2018;6(1):110-120.

37. Chewning JH, Dugger KJ, Chaudhuri TR, Zinn KR, Weaver CT. Bioluminescence-based visualization of CD4 T cell dynamics using a T lineage-specific luciferase transgenic model. *BMC immunology*. 2009;10:44.

38. Lyons SK, Meuwissen R, Krimpenfort P, Berns A. The generation of a conditional reporter that enables bioluminescence imaging of Cre/loxP-dependent tumorigenesis in mice. *Cancer research*. 2003;63(21):7042-7046.

39. Jósvay K, Winter Z, Katona RL, et al. Besides neuro-imaging, the Thy1-YFP mouse could serve for visualizing experimental tumours, inflammation and wound-healing. *Scientific Reports*. 2015;4(1):6776.

40. Mo Y, Kankavi O, Masci PP, et al. Surfactant Protein Expression in Human Skin : Evidence and Implications. *Journal of Investigative Dermatology*. 2007;127(2):381-386.